Stefan Kirnstötter, BSc

Investigation of photo reactive interfacial layers and application of TIPS-pentacene as active layer material

MASTER THESIS

for obtaining the academic degree
Diplom-Ingenieur

Master Programme of
Technical Physics

Graz University of Technology

Supervisor:
Ao.Univ.-Prof. Dipl.-Ing. Dr.techn. Zojer Egbert
Institute of Solid State Physics

Graz, January 2011

Acknowledgements

Five years ago it was unbelievable for me, but now it's done. A lot of people supported and helped me during the time of my studies, this diploma thesis and apart from it as well. First of all I want to thank my supervisor Ao. Univ. Prof. DI. Dr. Egbert Zojer for giving me the opportunity to work in his great team, for his scientific support and for guiding me through the last year of my studies.

This work would not exist without so many people from the Institute of Solid State Physics at the Graz University of Technology. First of all I want to thank my workgroup, especially DI. Marco Marchl. He taught me everything I know about assembling OTFTs and working conscientiously in the laboratory.

I have to express my gratitude to Mag. Simon Ausserlechner, Lukas Ladinig, DI. Thomas Obermüller, Reinhold Hetzel, Hannes Brandner, DI. David Egger, DI. Ferdinand Rissner and DI. Lukas Witwer for fruitful scientific discussions as well as for amusing coffee breaks during the last year.

Apart from our group I want to thank Ao. Univ. Prof. DI. Dr. Roland Resel and DI. Dr. Heinz Georg Flesch for supporting me with the x-ray diffraction and x-ray reflectivity measurements.

Additionally I want to thank DI. Dr. Thomas Griesser, DI. Matthias Edler from the Institute of Chemistry of Polymeric Materials, University of Leoben and DI. Lucas Hauser, Assoc. Prof. DI. Dr. Gregor Trimmel from the Institute for Chemistry and Technology of Materials, University of Technology Graz for the great cooperation during my thesis.

Another gratitude goes to DI. Alexander Fian, DI. Dr. Anja Haase, DI. Dr. Barbara Stadelober and DI. Sebastian Dunst from the Institute of Nanostructured Materials and Photonics, Joanneum Research, Weiz for the AFM measurements and some important hints during my thesis.

Special thanks go to my friends from Graz and Upper Austria. Thank you guys for the awesome moments we had during and apart from studies and for always being there when I needed it. Moreover I want to thank my family: my Mum, my Dad and my sister for their support in every moment of my life. And finally I want to thank a very special person in my live, my girlfriend Stephanie Hocheneder, you always reminded me of the important things in life. You kept your faith in me and supported me during the whole time.

Abstract

The present work deals with the investigation of organic thin film transistors either with photo reactive interfacial layers or with TIPS-pentacene as organic semiconductor material.

First, pentacene based organic thin film transistors (OTFTs) with photo-reactive interfacial layers were investigated. These functional polymer interfacial layers are used to control the OTFT performance by irradiation of the OTFTs with ultraviolet or visible light. To optimize the growth process of the organic semiconductor layer on top of the interfacial layer or to shift the threshold voltage of the OTFTs by illumination.

For the second type of investigated OTFTs, TIPS-pentacene as organic semiconducting material has been used. It has been used because of its promising mobilities and unlike regular pentacene it is soluble and thus it is possible to produce OTFTs by spin coating or drop casting. Here, the focus is on the optimization of the manufacturing process and the device performance of the TIPS-pentacene OTFTs.

Minor parts of this work deal illumination experiments with ultraviolet and visible light.

Kurzfassung

Die hier vorliegende Arbeit beschäftigt sich mit der Untersuchung von organischen Dünnfilmtransistoren, die einerseits funktionelle Zwischenschichten enthalten und andererseits aus dem neuartigen organischen Halbleitermaterial TIPS-Pentacen hergestellt wurden.

Zuerst werden auf Pentacen basierende organische Dünnfilmtransistoren mit photoreaktiven Zwischenschichten beschrieben. Diese funktionellen Polymer Zwischenschichten werden verwendet um kontrolliert die Transistoreigenschaften durch Bestrahlung des OTFTs mit UV Licht zu verändern. Dies geschieht einerseits um den Wachstumsprozess des organischen Halbleiters über der Zwischenschicht zu optimieren und andererseits um die Schwellspannung der OTFTs durch Belichtung kontrolliert zu verschieben.

Die zweite Art der untersuchten Bauteile sind mit TIPS-Pentacen als organischem Halbleitermaterial hergestellte OTFTs. TIPS-Pentacen wird wegen seiner hohen Mobilität und guten Löslichkeit verwendet. Da es im Gegensatz zu regulärem Pentacen leicht löslich ist, können damit OTFTs mittels Rotationsbeschichtung oder Auftropfens hergestellt werden. Hierbei liegt der Fokus auf der Optimierung des Herstellungsprozesses und der OTFT Eigenschaften.

Kleinere Teile dieser Arbeit beschäftigen sich mit Belichtungsversuchen mit ultraviolettem und sichtbarem Licht.

Deutsche Fassung:
Beschluss der Curricula-Kommission für Bachelor-, Master- und Diplomstudien vom 10.11.2008
Genehmigung des Senates am 1.12.2008

EIDESSTATTLICHE ERKLÄRUNG

Ich erkläre an Eides statt, dass ich die vorliegende Arbeit selbstständig verfasst, andere als die angegebenen Quellen/Hilfsmittel nicht benutzt, und die den benutzten Quellen wörtlich und inhaltlich entnommene Stellen als solche kenntlich gemacht habe.

Graz, am ……. ……..
(Unterschrift)

Englische Fassung:

STATUTORY DECLARATION

I declare that I have authored this thesis independently, that I have not used other than the declared sources / resources, and that I have explicitly marked all material which has been quoted either literally or by content from the used sources.

……. ……..
date (signature)

Contents

Introduction and Overview

The field-effect transistor (FET) was first proposed by J.E. Lilienfeld [1], who received a patent for his idea in 1930. He proposed that a field-effect transistor behaves as a capacitor with a conducting channel between a source and a drain electrode. Applied voltage on the gate electrode controls the amount of charge carriers flowing through the system.

The first field-effect transistor was designed and prepared in 1960 by Kahng and Atalla [2] using a metal-oxide-semiconductor. However, rising costs of materials and manufacturing, as well as public interest in more environmentally friendly materials supported development of organic based electronics in more recent years. In 1987, Koezuka and co-workers reported the first organic field-effect transistor based on poly(thiophene) [3]. Poly(thiophene) is a type of conjugated polymer that is able to conduct charge. Additionally, other conjugated polymers have been shown to have semiconducting properties. OFET design also improved in the past decades. Many OFETs are now designed based on the thin film transistor (TFT) model. In the past few years, the field-effect mobility and on-off current ratio have improved significantly.

In recent years, the number of publications on organic transistors has increased substantially. Organic FETs are technologically interesting as they could serve as the main component in cheap and flexible electronic circuits. Major possible applications are radio frequency identification (RF-ID) tags, flexible displays, and many others. Prototypes of these products have already been demonstrated, and some are already on the market. For example the non flexible AMOLED-display(active matix organic light emitting display) is a common display for modern smartphones [4].

Certainly my investigations were focused on a small part of this big field of research, so the next few lines will give a rough overview what this thesis is about.

In the first chapter, some organic semiconducting materials as well as the setup and functionality of organic thin film transistors are presented. Additionally the electrical characteristics, charge transport models and data extraction methods for the most important quantities are introduced.

In the second chapter the measurement methods for the investigation of OTFTs are explained. The electrical measurements with the parametric analyzer and the Keithley source meter enable the extraction of significant device parameters(mobility, threshold voltage, on/off-ratio). To analyze and to fully understand the OTFT behaviour, contact angle measurements, atomic force microscope measurements, X-ray reflectivity and diffraction measurements, UV-VIS, respectively, IR spectroscopy, and

temperature dependent measurements were important methods of investigation.

In the third chapter, the device fabrication and pretreatment is explained after that the results of the measurements are presented and discussed. In the beginning of this chapter photo-reactive interfacial layers in pentacene based OTFTs were investigated. Here the focus lies on shifts of the threshold voltage, changes of the mobility and the surface energy. Another subject is the production of transistors with TIPS-pentacene (6,13-bis (triisopropylsilylethynyl) pentacene) as active layer material. With this organic semiconductor it should be possible to produce solution processed OTFTs with very high mobilities [5]. The goal here was to optimize the production process to achieve high mobilities, on/off ratios and a reliable production process.

In the end the conclusion and outlook and the bibliography complete this thesis.

Chapter 1

Fundamentals

In the beginning of this chapter some organic semiconductors, their properties as well as the setup and functionality of organic thin film transistors are introduced. Additionally, the electrical characteristics, data extraction methods for the most important device quantities, and charge transport models are presented.

1.1 Organic Semiconductors

The following pages are referred to [6], [7], and [8]. An organic semiconductor is an organic material with semiconducting properties. This means a material that has an electrical conductivity due to flowing electrons or holes, which is intermediate in magnitude between that of a conductor and an insulator. This means roughly in the range 10^3 to 10^{-8} siemens per centimetre. Typical examples for organic semiconductors used for organic thin film transistors are pentacene or poly(3-hexylthiophene) as can be seen in Fig. 1.1.

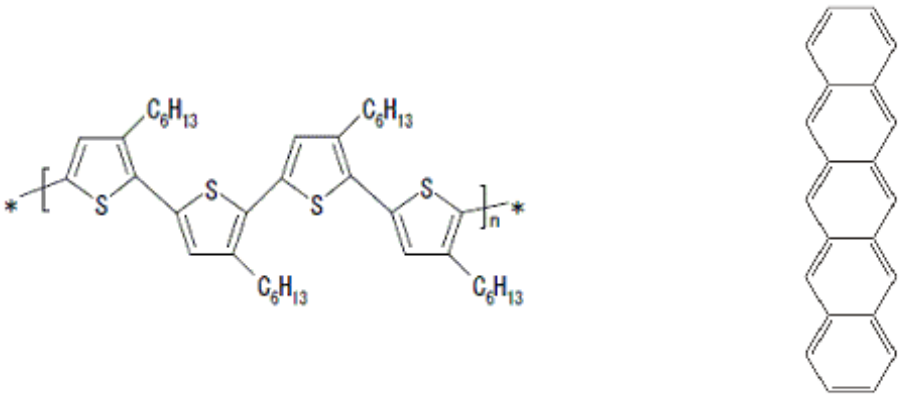

Figure 1.1: Molecular structure of poly(3-hexylthiophene) (left) and pentacene (right)

As can be seen in Fig. 1.1 poly(3-hexylthiophene) is a polymer and pentacene a so called small molecule. A big difference between small molecules and polymers beyond their chemical structure, is the way they are used to form thin films. Polymers are processed from solution via spin–coating, drop-casting or printing techniques, whereas small molecules may be deposited from the gas phase by sublimation or evaporation(with a few notable exceptions like TIPS-pentacene). TIPS-pentacene is also a small molecule but because of it's side chains it is soluble in common solvents. Further differences between conjugated polymers and small molecules lie in their charge transport.

Nearly all organic solids are insulators. But when their constituent molecules have π-conjugated systems, electrons can move via π-electron cloud overlap. They can move by hopping, tunnelling, and related mechanisms. To take a little closer look on the semiconductor behaviour of organic compounds, like pentacene or poly(3-hexylthiophene), the delocalized π-electron system, molecule orbital theory, and the different bondings between the atoms and orbitals have to be understood.

There are two common types of bondings in organic chemistry, σ– bonds and π–bonds. σ– bonds show rotational symmetry with respect to the bond axis and can be formed between s - orbitals, a s – orbital and a p – orbital or between two axially aligned p – orbitals. A π– bond is formed between two parallel neighbouring p – orbitals and shows maximum electron density above and below the nodal plane. The strength of the bond depends on the bond angle of the molecule and the number of participating pairs of valence electrons. Due to the higher bonding strength of double bonds the atoms show a closer arrangement [9], [6].

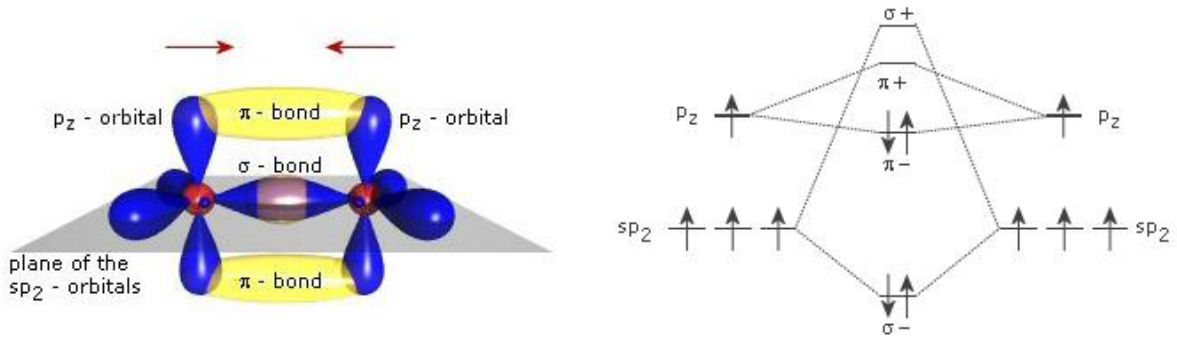

Figure 1.2: Different schemes of the chemical bonding between the orbitals of two carbon atoms in sp^2 – hybridisation. Left: 3 dimensional illustration of the bondings parallel to the plane of the sp^2-orbitals, right: schematic illustration of the sp^2 hybridisation levels and bondings (taken from [7])

The ground state configuration of carbon is $1s^2\ 2s^2\ 2p^2$. Atoms like carbon or nitrogen are able to mix their atomic orbitals to so called hybrid orbitals [8]. The for us

significant hybridisation of carbon is the sp^2 – hybridisation: here two carbon atoms form a molecule with a double bond in between. This possibility of hybridisation is very important for organic conducting polymers. One s orbital and two p orbitals (e.g. p_x and p_y) are mixed to form three equivalent sp^2 hybrid orbitals. The third p_z state remains unchanged (Figure 1.2 right), lies perpendicular to the plane of the sp^2 orbitals and forms the π – bond by overlapping. This overlap prevents axial rotation of the atoms around the bonding axis [9], [6].

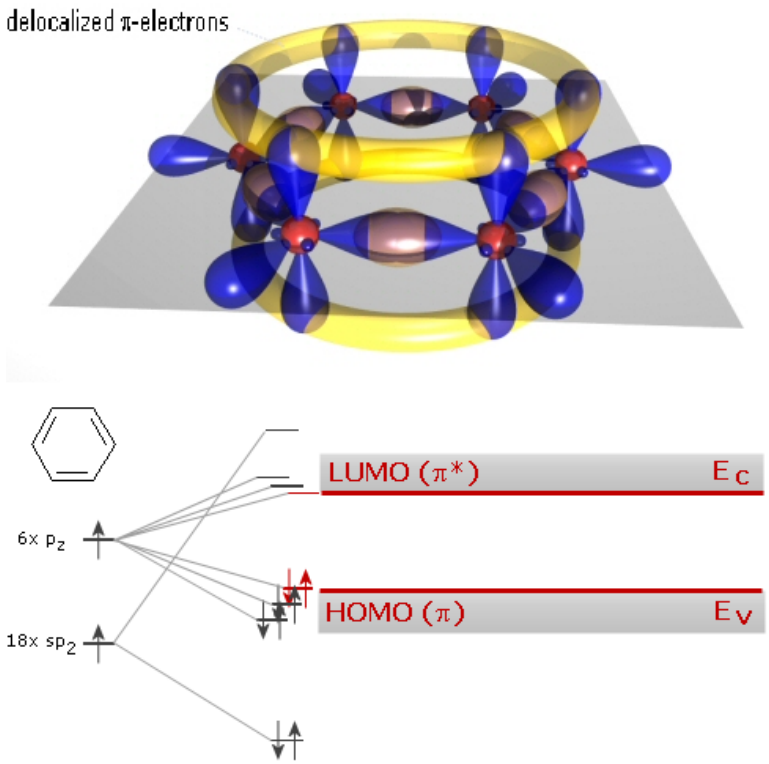

Figure 1.3: Top: 3 dimensional scheme of a benzene ring with the delocalized π-electrons. Bottom: band arrangement of small-molecule organics with the sp_2 and p_z orbitals that form the HOMO and LUMO of the organic semiconductor (taken from [7])

The most basic building block in many small molecules is the benzene ring, consisting of six carbon atoms in sp^2 – hybridised states plus six hydrogen atoms. Polymers and oligomers are molecules consisting of 10^2 - 10^5 respectively approximately 10 units of repeating monomers which are linked via covalent bonds. Polymers as well as oligomers can have a conjugated π – electron system. The term "conjugated" stands for alternating single and double bonds. The π – electron system consists of electrons from the p_z – orbital of the sp^2 – hybridisation. From Molecular Orbital Theory we know that there are additive or subtractive overlaps of the atomic orbitals.

The bonding molecular orbitals (σ and π) and the antibonding molecular orbitals (σ* and π*). The σ – bonds form the backbone of the molecule. The π – electrons from the weaker π – bonds are delocalized within the molecule or along the chain in the case of polymers. The HOMO(highest occupied molecular orbital) is formed by the bonding π – bonds and the LUMO is formed by the antibonding π* – bonds. The π – electron system accounts for the π – π* - transition between the so called HOMO and the LUMO that is a very important factor for the electronic properties of the system [6] (Fig. 1.3 and 1.4).

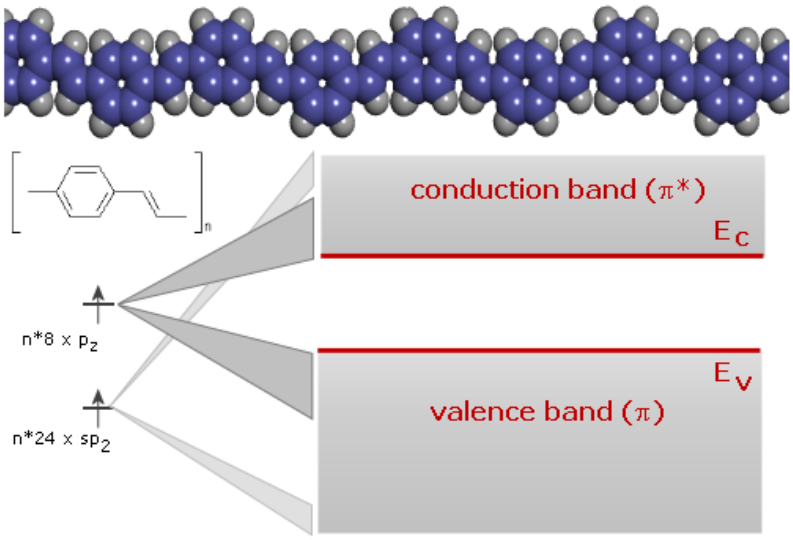

Figure 1.4: Top: scheme of poly-para-phenylene-vinylene (PPV). Bottom: band arrangement of PPV of the sp_2 and p_z orbitals that form the HOMO and LUMO of the organic semiconductor (taken from [7])

As can be seen in Fig. 1.3 and 1.4 all orbitals together generate the HOMO and LUMO of the organic semiconductors but the p_z orbitals and thus the delocalized π-electron overlap(π and π*) are the crucial factors for the semiconducting properties of the material. In the benzene molecule or in conjugated polymers where the π-orbitals become delocalized the HOMO-LUMO gab becomes smaller with increasing delocalization. In the case of a long chain of carbon atoms the π-electron cloud can delocalize over the whole chain.

1.2 Organic Thin Film Transistors: Setup and Functionality

In this subsection, the schematic structure and working principle of OTFTs are shown. Additionally different device geometries and operating regimes are explained. Figure 1.5 shows a bottom-contact bottom-gate organic thin-film transistor. An OTFT consists of a substrate, an insulating layer, the gate-, source- and drain-electrodes and an organic semiconductor as active layer. It depends on the semiconductor, whether the semiconducting layer is vacuum evaporated, spin-coated or drop-cast. The gate electrode can be a conducting polymer, a metal, or a highly doped silicon serves as substrate and gate electrode at once. As gate dielectric, inorganic insulators such for example SiO_2(thermally grown on Si or sputtered), Al_2O_3 or polymeric insulators such as, for example, poly(methyl methacrylate) (PMMA) are used [10], [11], [12]. For p-channel devices the source and drain electrodes, which inject charges into the semiconductor, are usually high work function metals like gold [13], but conductive polymers e.g. PEDOT:PSS [14] are used as well.

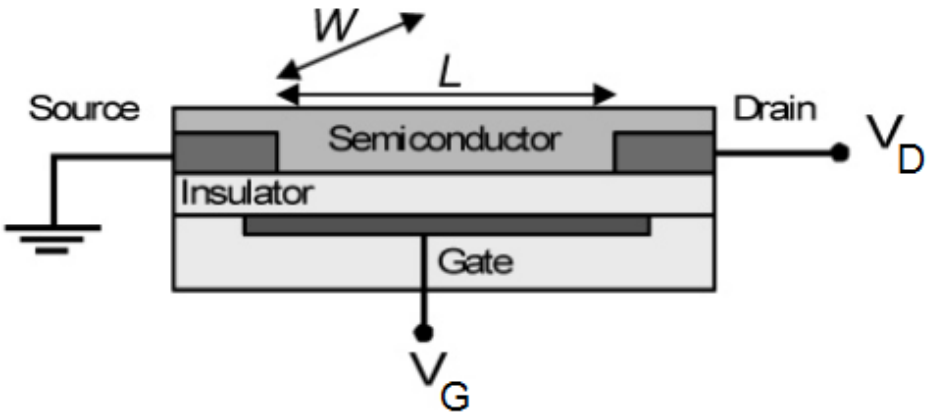

Figure 1.5: Schematic structure of a bottom-contact bottom-gate organic thin-film transistor and for the applied voltages: L=channel length, W=channel width, V_D = drain voltage, V_G = gate voltage (taken from [15])

The distance between the source and the drain electrode is called the channel length, and the transverse dimension of the structure is the channel width. The gate electrode is electrically isolated from the semiconductor film by a thin isolating layer, hence forming a metal-insulator-semiconductor(MIS) structure.

To get current flow in the channel of the thin film transistor, charges have to be injected from the gold electrodes into the semiconductor. For the injection of electrons or holes, metals with a work function similar to the electron affinity E_a respectively to

the ionisation energy E_i of the semiconductor are suitable. For materials with a work function between the electron affinity and the ionisation energy electrons as well as holes have to overcome an injection barrier, to come into the OSC. In Fig. 1.6 several different device geometries of organic thin film transistors can be seen. There are a lot of other possibilities to produce OTFTs, but during this thesis only bottom gate ,bottom(a) or top-contact(b) devices were produced.

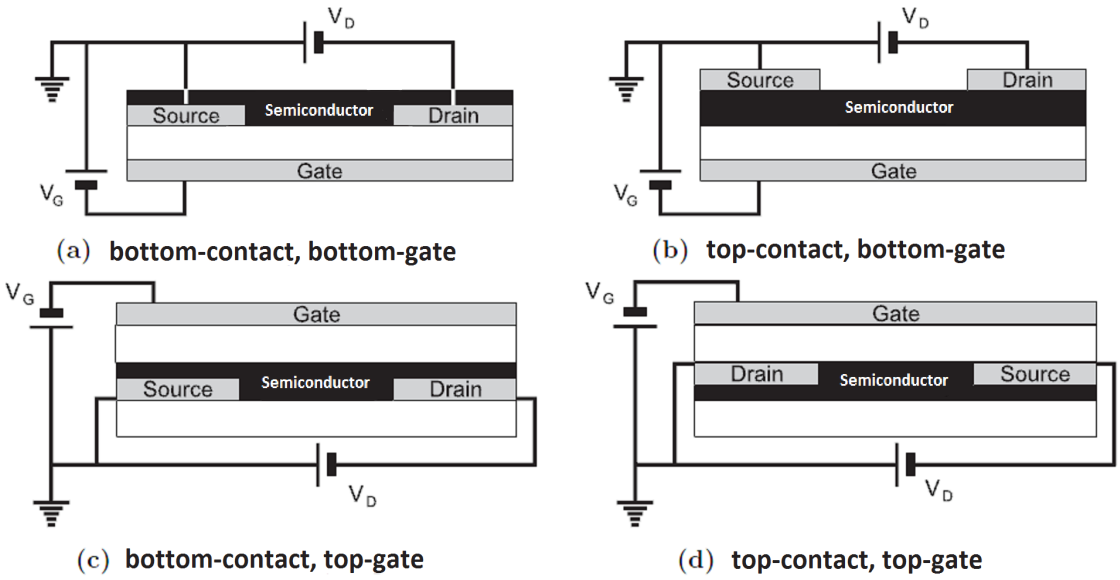

Figure 1.6: Different device geometries of organic thin-film transistors (taken from [16])

Normally voltage is applied to the gate and the drain electrode, the source electrode is grounded. The source is the charge carrier injecting electrode, because it is always more negative than the gate electrode. When a positive gate voltage V_G is applied(electrons are injected), and more positive when a negative gate voltage V_G is applied(holes are injected). For a simple MIS-structure(no potential difference between source and drain) with a positive gate bias V_G, negative charge carriers(electrons) are accumulated at the insulator/semiconductor interface that were injected from the grounded electrodes(source, drain). For a negative gate bias V_G, positive charges(holes) are accumulated at the interface. The number of accumulated charges is proportional to V_G and the capacitance C_i of the insulator. However, not all induced charges are mobile and will thus contribute to the current in a field effect transistor. Deep traps have to be filled first before the additionally induced charges flow as the mobile charge carrier current in the channel. So a gate voltage that is higher than the threshold voltage V_{th} has to be applied, so the effective gate voltage is $V_G - V_{th}$ [15],[17]

When no source-drain voltage is applied, the charge carrier concentration over the channel is uniform as can be seen in figure 1.7 a). When a small source-drain voltage

is applied($V_{DS} << V_g$), a constant gradient of charge carrier density from the carrier injecting source to the extracting drain is formed. This is called the linear regime, here the current flowing through the channel is directly proportional to V_{DS}. In the linear regime the potential V(x) within the channel linearly increases from the source (V(x)=0) to V_{DS} at the drain electrode (V(x)=V_{DS}). When the source-drain voltage V_{DS} is further increased, a point $|V_{DS}| = |V_G - V_{th}|$ is reached, at which the channel is "pinched off" (Fig. 1.7 b). Now a depletion region forms next to the drain electrode because the difference between the local potential V(x) and the gate voltage is now below the threshold voltage. Now just a space-charge-limited saturation current $I_{DS,sat}$ can flow across this narrow depletion zone. Here carriers are swept from the pinch-off point to the drain by the comparatively high electric field in the depletion region. Further increasing the source-drain voltage will not substantially increase the current but leads to an expansion of the depletion region and thus a slight shortening of the channel. Since the potential at the pinch-off remains $V_G - V_{th}$ and, thus, the potential drop between that point and the source electrode stays approximately the same, the current will saturate at $I_{DS,sat}$ (Fig. 1.7 c).

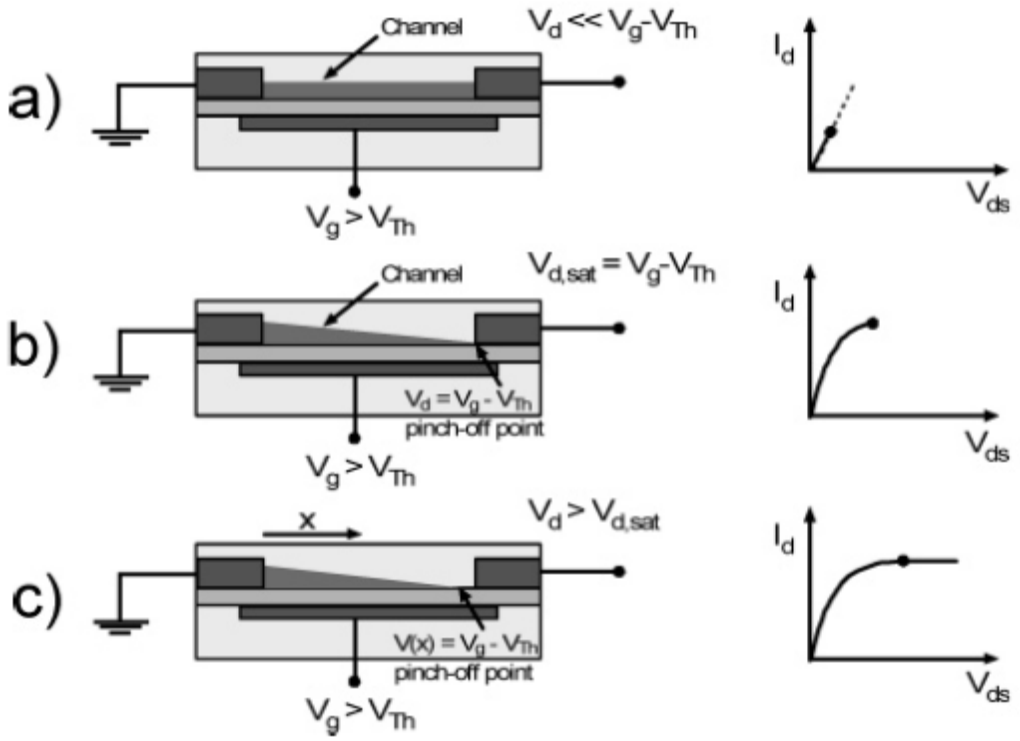

Figure 1.7: Illustration of operating regimes(left) of an organic thin-film transistors: a) linear regime, b) start of saturation regime at pinch off, c) saturation regime and corresponding current-voltage characteristic(right) (taken from [15]).

In short, I-V characteristics(Fig. 1.8) can be given either for varying the gate voltage at a constant drain voltage(transfer characteristics) or for changing the drain voltage at constant gate voltage(output characteristics). In the output characteristics the curves are divided in the linear regime at low V_D and in the saturation regime when $V_D > V_G$.

The most popular equations to describe the current-voltage curves of an OTFT are very simple, but this simplicity hides several assumptions that are usually not fulfilled in organic devices. These are that (1) the transverse electric field induced by the drain voltage is largely higher than the longitudinal field induced by the gate voltage and (2) the mobility is constant all over the channel. So it is important that transistors with short channel lengths require thin gate dielectrics, typically $L > 10\ d_{dielectric}$, in order to ensure that the field created by the gate voltage determines the charge distribution in the channel(gradual channel approximation) and is not dominated by the lateral field due to the source-drain voltage. Otherwise the gate voltage cannot determine the on- or off-state of the transistor. The reason why the mobility is not constant all over the channel is explained in the sub chapter charge transport

The current in both regimes is given by the equations 1.1 and 1.2.

$$I_{Dlin} = \frac{Z}{L} C_i \mu [(V_G - V_{th}) V_D - \frac{V_D^2}{2}] \tag{1.1}$$

$$I_{Dsat} = \frac{Z}{2L} C_i \mu (V_G - V_{th})^2 \tag{1.2}$$

Here, C_i is the capacitance of the insulator, μ the mobility in the semiconductor and V_{th} the threshold voltage. In short the threshold voltage is the gate voltage beyond which the conducting channel forms.

From the output characteristic one can learn whether the device has 1) a good saturation behaviour and 2) it gives information about the contact resistance. For devices with a high contact resistance the output curve is not linear for small V_D. The transfer characteristic gives much more direct information about the device and some important device parameters but this will be explained in the following section.

Most of the electric characteristics are measured by a forward and a backward sweep. So the first curve is measured from, e.g., V_G = +20V to V_G = -20V for a constant V_D and the second curve from V_G = -20 V to V_G = +20 V. For a perfect transistor, both curves should look exactly the same, but for real devices a hysteresis occurs. This can have many different reasons: charge carrier trapping or impurities are just a few of them. So the origin of the hysteresis is still a not fully understood topic [18].

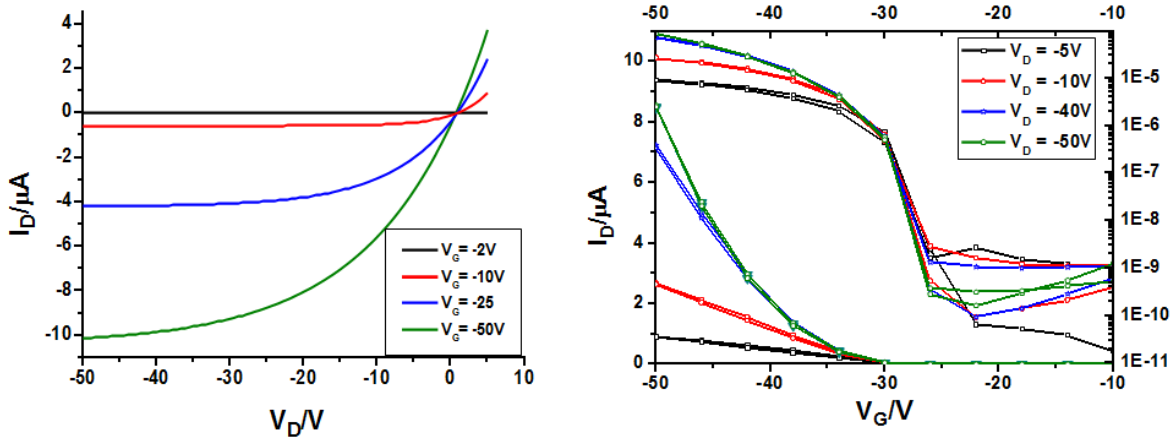

Figure 1.8: Output(left) and transfer(right) characteristic of an organic thin-film transistors. In the output characteristic the linear and the saturation regime of a thin-film transistor can be seen clearly

1.3 Data Extraction of Important Quantities of Organic Thin Film Transistors

In this subsection it is shown how the most important parameters of an OTFT can be extracted from the electrical characteristics: the mobility, the turn-on and threshold voltage, the on-off ratio, the contact resistance as well as the subthreshold swing. Additionally the extraction of the surface energy by contact angle measurements is explained. This sub chapter is based in [15] and [19].

1.3.1 Mobility

The mobility can be extracted either from the linear or from the saturation regime of the transistor. μ is not the intrinsic mobility of a charge carrier (which would be the quotient of the velocity v of a charge carrier and an applied electric field E: $\mu = \frac{v}{E}$), but instead an effective quantity that characterizes the device performance.

A widely used method for the extraction of the mobility consists of plotting the square root of the drain current as a function of the gate voltage in the saturation regime. As seen in equation 1.2, this is supposed to give a straight line. From the slope of this line it is possible to calculate μ.

The calculation of this equation assumes that the mobility is constant over the entire channel, but this is not always true. For the extraction of the gate voltage dependent mobility, the transconductance has to be calculated. This quantity is the first derivative of the drain current with respect to the gate voltage(in the linear regime):

$$g_m = \frac{\delta I_D}{\delta V_{GS}}|_{V_{DS}=const} = - \frac{W \cdot C_i \cdot \mu}{L} \cdot V_{DS} \tag{1.3}$$

Here g_m is the transconductance, I_D is the drain current, V_{GS} is the gate-source voltage, V_{DS} is the drain-source voltage, W is the width of the channel, C_i is the capacitance per area of the dielectric and L is the length of the channel. The mobility can then be calculated from the ratio $\frac{g_m}{V_{DS}}$ for each of the applied gate voltages. Because of the gate and drain voltage dependency of the mobility it is very important to know how this value was extracted, when this it is compared with mobilities from literature.

1.3.2 Turn-on, Threshold Voltage and Subthreshold Swing

The threshold voltage can be extracted from the transfer characteristic for the linear as well as for the saturation regime. As already mentioned a widely used method for parameter extraction consists of plotting the square root of the saturation current as a function of the gate voltage. The extrapolation of the resulting straight line to the V_G axis corresponds to the threshold voltage(Fig. 1.9 right).

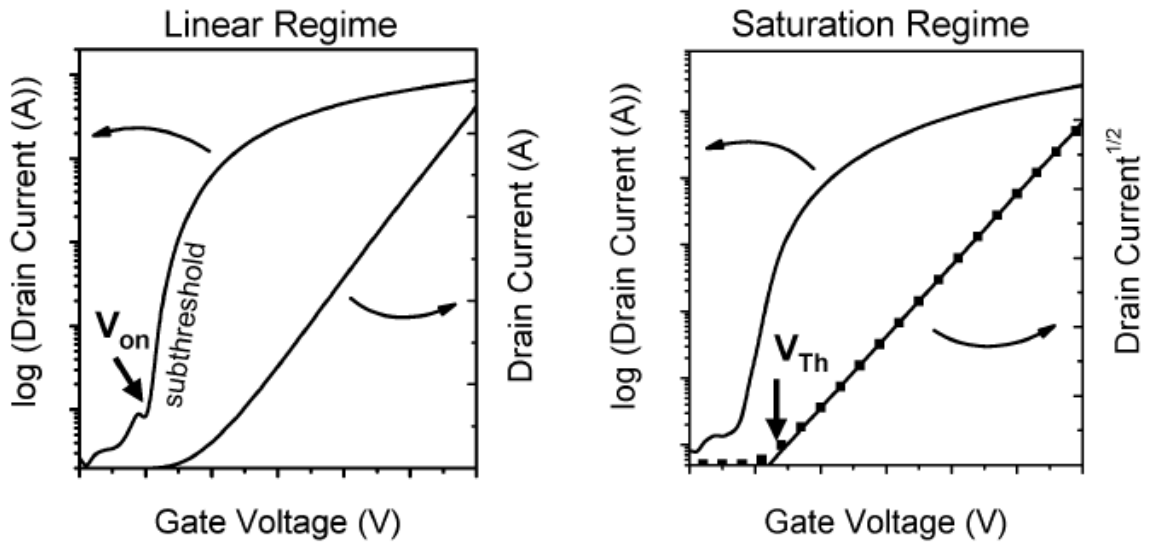

Figure 1.9: Representative transfer characteristics of an n-channel organic field-effect transistor: (left) transfer characteristics for $V_D << V_G$, indicating the onset voltage (V_{ON}) when the drain current increases abruptly; (right) transfer characteristics for $V_{DS} > V_G - V_{th}$, indicating the threshold voltage V_{th}, where the linear fit to the square root of the drain current intersects with the x-axis (taken from [15])

Another method is to extract the threshold voltage from a transfer characteristic

of an OTFT in the linear regime. Figure 1.9 left shows the transfer characteristics of the same transistor for $V_{DS} \ll V_G$(linear regime) in the logarithmic plot and in a linear plot. So from a linear fit to the transfer characteristics the threshold voltage can be extracted. From the logarithmic plot one can easily extract the onset voltage (V_{ON}) (the voltage at which the drain current abruptly increases above a defined low off-current level) and the subthreshold swing S :

$$S = \frac{\delta V_G}{\delta log I_{DS}} \tag{1.4}$$

This parameter is calculated from the transfer characteristic with the data points where $|V_G| < |V_{th}|$. The threshold voltage depends strongly on the semiconductor and the dielectric used, and is very sensitive to several effects: built-in space charge layers, impurities and, in particular charge carrier traps contribute to the threshold voltage. Independent of the cause of V_{th}, it can be reduced by increasing the gate capacitance and thus inducing more charges at lower applied voltages. The threshold voltage is not necessarily constant for a given device. When p-channel organic transistors are operated for an extended time V_{th} tends to shift to more positive values. This bias stress sensitivity has a significant effect on the applicability of organic transistors in electronic circuits.

1.3.3 Contact Resistance

In non-ideal transistors, the channel resistance is only one component of the overall device resistance. In addition to the channel resistance, there are contact resistances at the interfaces between the source and drain electrodes and the organic semiconductor. Typically, these play a major role only if the channel resistance is very small, e.g., in the case of organic semiconductors with very high mobilities or devices with short-channel lengths.

The contact resistance cannot be extracted from simple current-voltage curves. It can be measured as the voltage drop at the electrodes with non-contact scanning probe potentiometry (e.g., Kelvin probe) [20], by four-point probe measurements or with the transfer line method [21].

The transfer line method (TLM) consists of measuring the channel resistance of similar devices with various channel lengths. The measured resistance is actually the sum of the channel and contact resistances. The contact resistance is extracted by plotting the width-normalized resistance as a function of channel length. The extrapolation to zero length gives the contact resistance, when it is independent of I_D (Fig. 1.10).

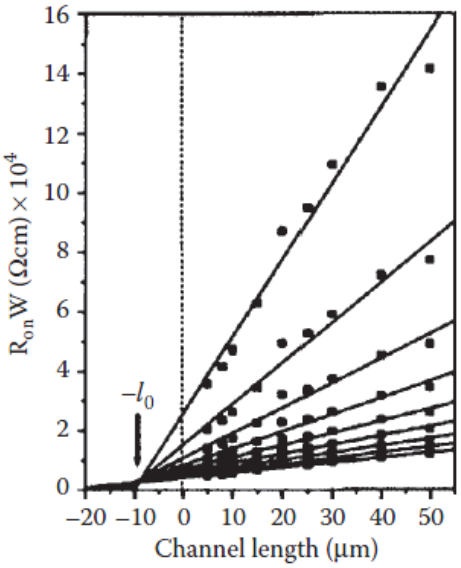

Figure 1.10: Illustration of the transfer line method. A measurement method that makes it possible to extract the contact resistance of several measurements of the channel resistances of similar devices with various channel lengths (taken from [17])

1.3.4 On/Off-ratio

Another important parameter of OTFTs that can be extracted from the transfer characteristics is the on/off ratio, which is the ratio between the drain current in the on-state and the drain current in the off-state for the same drain voltage (I_{on}/I_{off}). This value is strongly dependent of measurement range. For a clear switching behaviour of the transistor, this value should be as large as possible.

1.4 Charge Transport Models

The exact mechanism responsible for charge transport in organic semiconductors is still open to debate. Nevertheless, one can make a clear distinction between disordered semiconductors such as amorphous polymers and highly ordered organic single crystals. This sub chapter is based on [15],[17] and [9].

- Hopping Transport

The charge transport mechanism in disordered semiconductors is generally described by thermally activated hopping of charges through a distribution of localized states or shallow traps. An typical model of this family is the variable range hopping model, where charges can hop a short distance with a high activation energy or a long

distance with a low activation energy. It was introduced by Vissenberg and Matters [22]. It combines variable range hopping transport with an exponential distribution of traps. This model predicts an increase of the field-effect mobility with increasing gate voltage. First the accumulated charge carriers fill the lower-lying states of the organic semiconductor, than additional charges in the accumulation layer will occupy states at relatively high energies. So the additional induced charges will require a lower activation energy to hop between sites. This dependence of the mobility on charge density and thus gate voltage has been observed for many disordered semiconductors. The Vissenberg-Matters model proved to be very useful to model organic field-effect transistors and organic diode structures [23], [24] and [25].

- Bandlike Transport

For highly ordered molecular crystals (e.g., rubrene or tetracene), experimental data seems to exclude hopping transport. Time-resolved tera-hertz pulse spectroscopy [26], [27] and temperature-dependent time-of-flight [28], as well as field-effect transistor measurements [29] on highly ordered molecular crystals showing high mobilities that increase with decreasing temperature(for very low temperatures). This suggests band-like transport in delocalized states instead of hopping transport in localized states. But simultaneously, the mean free path of charge carriers at high temperatures (above 150 K) is found to be comparable with the crystal unit cell lattice parameters. This clearly contradicts delocalized transport [30], [31].

- Multiple Trapping and Thermal Release Model

Additionally to these two extreme cases(hopping transport, bandlike transport) other models that lie in between them have been proposed as well. Models for charge transport in organic semiconductors, such as polycrystalline thin films of small molecules and microcrystalline polymers. A parent model of that by Vissenberg and Matters [22] has been developed for semiconductors made of ordered small molecules. In general the multiple trapping and thermal release (MTR) model was developed for hydrogenated amorphous silicon (a-Si:H) [32]. It assumes charge transport to occur in a delocalized band. But a distribution of traps near the band limits the charge transport [33]. The model does not make any predication on the transport mechanism in the band (delocalized or through polarons). Like for the hopping model the mobility is thermally activated, and follows a power law dependence with gate voltage. The main interest of the model is to explain the charge transport behaviour found in devices made of polycrystalline films of small conjugated molecules [17].

- Charge Transport in Polycrystalline Materials

A frequently occurring problem is the description of the charge transport in polycrystalline materials where the medium is divided into low and high conductivity regions – the grain boundaries and the grains, respectively. Since grains and grain boundaries are connected in series, the overall effective mobility of a polycrystalline medium can be expressed as

$$\frac{1}{\mu} = \frac{1}{\mu_g} + \frac{1}{\mu_b} \tag{1.5}$$

where μ_g and μ_b are the mobilities in a grain and in the grain boundary regions. As long as μ_g is much bigger than μ_b the overall mobility is limited by the mobility within the grain boundaries [34], [35].

Chapter 2

Analytical Methods

In this section the equipment and measurement setup for all the experiments and the analytical characterization of the OTFTs during this diploma thesis are presented. The most powerful tool to analyze and to extract the device parameters of an OTFT is the current-voltage-characteristic. As already mentioned before, there were several possibilities to characterize an OTFT with an I-V-curve, like transfer- and output-characteristics, long time measurements of the drain current and bias stress measurements. Another important measurement tool to investigate the morphology and surface structure of an organic semiconductor is atomic force microscope. To measure the thickness and surface roughness of the layers in OTFTs x-ray reflectivity is used and to investigate the crystal structure, x-ray diffraction measurements were performed. Additionally, contact angle measurements as well as UV/VIS- and IR-spectroscopy measurements were necessary and useful analytical methods during this thesis.

2.1 Electrical Measurements

For the electrical characterization three different measurement setups were used:

- Needle setup in glovebox

Here, the source, drain and gate electrodes are contacted with needles, using MDL positioners from Cascade electronics. Then the devices were electrically characterized with an Agilent E5262A parametric analyzer. With this setup transfer and output characteristics were measured. Subsequently the curves are analyzed with a matlab programm, which extracts the device parameters($\mu_{lin/sat}$,$V_{th,lin/sat}$) of the curves. In the Fig. 2.1 the needle setup in the glovebox is shown.

Additionally it was possible to investigate devices with a Keithley source meter controlled by a software written by Thomas Obermüller, another diploma student,

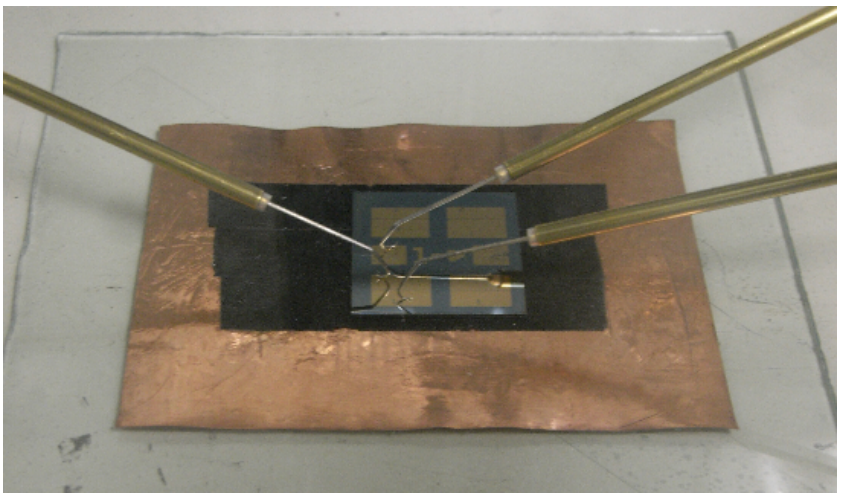

Figure 2.1: Measurement needle setup in glovebox

which is based on LabView and Matlab. It allows a more detailed electrical characterisation of the devices. With this setup it is possible to perform bias stress and long time measurements [36]. These measurements will be explained in detail in the corresponding experimental section. In Fig. 2.2 the front panel of the measurement software for transfer and output characteristics is shown. In the graphs the linear plot of the drain-(left) and the leakage(right) current over the gate voltage is shown. Underneath the graphs the sweep settings can be entered: V_D-, V_G-measurement range and the delay time between measurements. Underneath the right graph it is possible to enter the device name and to add some important comments.

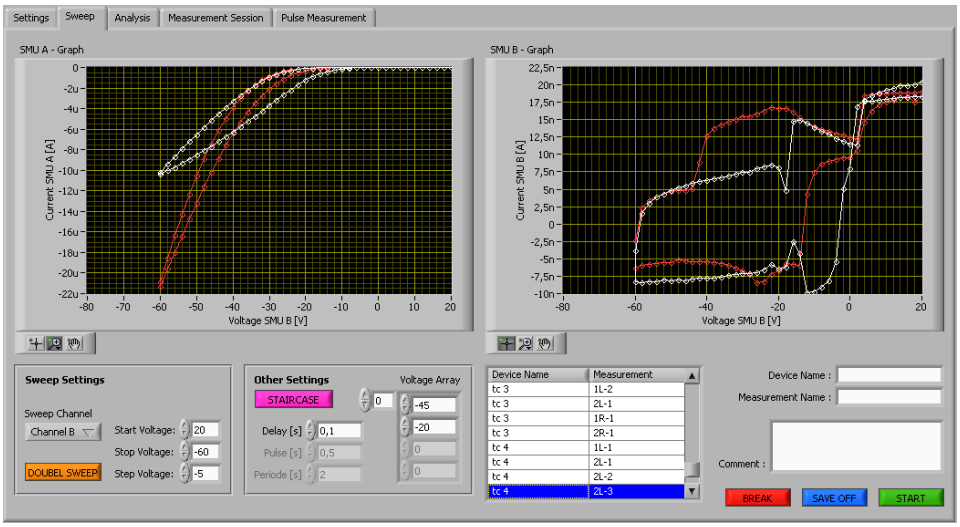

Figure 2.2: Front panel of the Labview program for transfer and output characteristic measurements [36]

- Measuring cell

The measurement cell was designed by Lukas Ladinig and Mag. Simon Ausserlechner. There are some important advantages of the measuring cell(Fig. 2.3) in comparison to the needle setup in the glovebox. First of all the measuring cell is mobile. With a source meter and a laptop it is possible to make measurements everywhere. It is possible to work under ambient conditions, where no inert atmosphere is necessary. This makes it much easier to contact the devices in the measuring cell. Additionally, it is possible to switch between twelve OTFTs during a measurement with an electronic control device from outside.

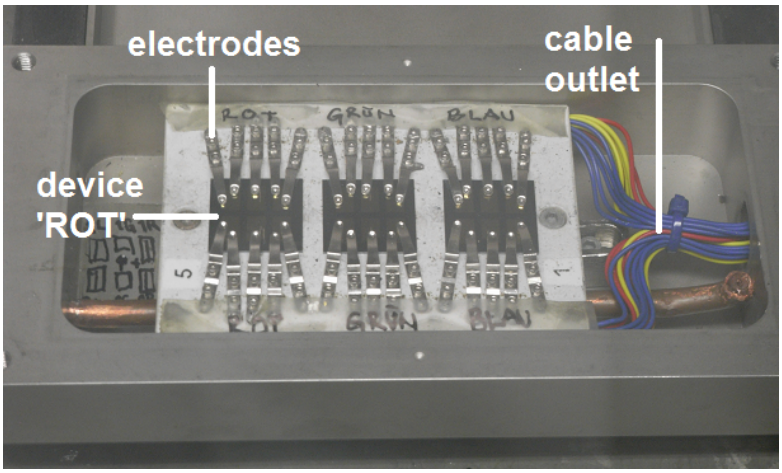

Figure 2.3: Setup of the measuring cell with three devices with four OTFTs on every device. The devices are marked by colours: red, green, blue. The devices are contacted by screwing down the electrodes on the gold pads of the OTFTs

It is also possible to evacuate the measuring cell to about 10^{-6} mbar. After the evacuation, it is also possible to refill the measuring cell with any gas, for example, ammonia when a chemical reaction with that gas is investigated. So the atmosphere in the cell can be clearly defined in comparison to the glove box(solvents). The measuring cell is also suitable for measurements under varying illumination conditions, because a cover with a quartz glass window is available.

- Sample holder for measurements in the cryostat

To enable the investigation of the OTFT behaviour in the low temperature region a sample holder with a special device geometry was designed by DI. Marco Marchl. Namely bottom gate, top contact devices with six OTFTs with six different channel lengths and widths on one device. In this way it is possible to calculate the contact resistance with the transfer line method with just one substrate. In the sample holder the OTFTs were contacted with a SIM-card holder on top, and by a carbon tape with

conductive silver from underneath, the potential was applied by a Keithley source meter. For the analysis of the OTFTs, a bachelor student(Christian Straka) built an electronic control and wrote a suitable LabView program for low temperature measurements [37]. This setup enabled automated low temperature measurements.

For low temperature measurements an Oxford Instruments Continuous Flow Cryostat CF 1204 was used. The principle setup is shown in Fig. 2.4. The cryostat is connected to a nitrogen dewar via a transfer tube. Liquid nitrogen flew from the dewar to the heat exchanger, where it was evaporated. The nitrogen stream was controlled by the VC 30 flow control meter and is pumped out by a membrane pump. The possible temperature range where measurements were performed was between 80 to 400 K [38].

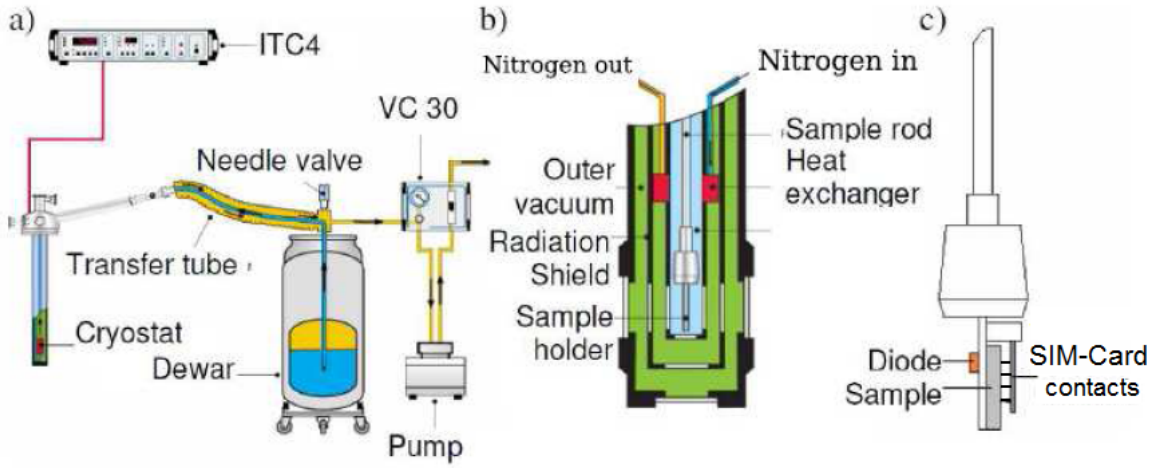

Figure 2.4: (a) Overview of the cryostate setup. (b) Cross section of the sample space in the cryostat. (c) Sample holder with SIM-Card contacts (taken from [38])

2.2 Atomic Force Microscopy

In order to investigate the surface structure and the growth of the active layer on top of the OTFT's, atomic force microscope(AFM) measurements were performed. These were done by DI. Alex Fian and DI. Dr. Anja Haase (Joanneum Research Graz). The AFM was operated in tapping mode [39]. Basically a tip was located on a cantilever, which was excited to its resonance frequency and then scanned laterally along the surface. Very close to the surface the oscillating cantilever is damped due to the presence of short range forces at the surface. The oscillation of the cantilever is measured by a laser beam. A feedback loop keeps the amplitude of the cantilever constant by adjusting the distance between the tip and the sample via a piezo element [40]. The working principle and the components of an AFM-microscope are shown in Fig. 2.5.

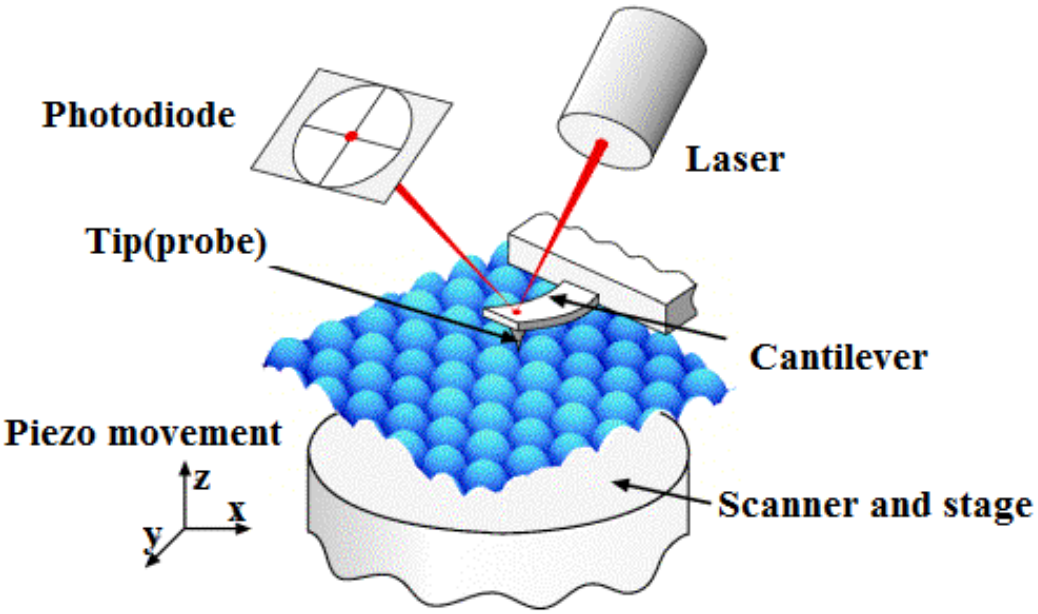

Figure 2.5: Working principle of an atomic force microscope. The most important components are the cantilever with a tip on it, a laser, the piezo elements and the photo detector (taken from [41])

2.3 X-ray reflectivity and diffraction measurements

Alongside AFM measurements, X-ray reflectivity (XRR) and X-ray diffraction (XRD) measurements were important methods of investigation during this thesis. The XRR-measurements were performed by DI. Dr. Heinz Georg Flesch (Graz University of Technology). Here a Bruker diffractometer D8 Discover was set up in Bragg – Brentano configuration(Fig. 2.7) with a copper sealed tube (wavelength = 1.541 $\AA$) as source of

radiation. The layer thickness d was determined by the distance of the minima of the Kiessig fringes in the XRR pattern [42].

$$d = \frac{\lambda}{2(sin\ \alpha_2 - sin\ \alpha_1)} \tag{2.1}$$

α_1 and α_2 defined the positions of the minima of the Kiessig fringes and λ was the wavelength of the X-ray radiation.

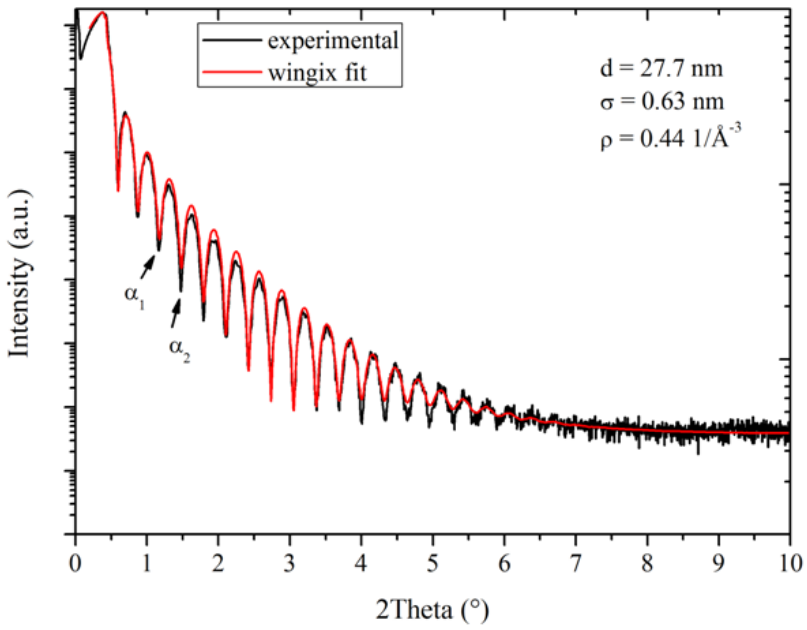

Figure 2.6: Typical X-ray reflectivity pattern of Alp 3 (taken from [43])

The software package WinGIXA [44] was used to simulate the experimental data and to determine the actual layer thickness. Additionally, the electron density ρ and the surface roughness σ can be extracted by this software package as can be seen in Fig. 2.6 for a typical X-ray reflectivity pattern.

X-ray diffraction (XRD) is a measurement technique used to characterize the crystallographic structure and preferred orientation of solid samples. X-ray diffraction is commonly used to identify unknown substances, by comparing diffraction data against a database maintained by the International Centre for Diffraction Data.

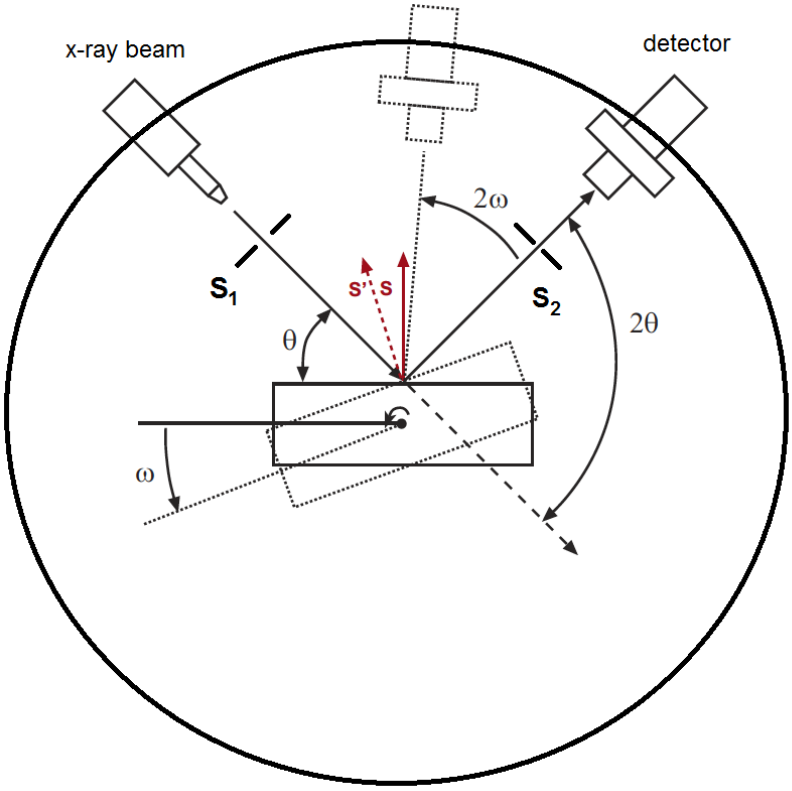

Figure 2.7: Bragg-Brentano geometry for θ / 2 θ scans (taken from [45])

2.4 Contact Angle Measurements

When a small amount of a liquid is deposited on a plane surface a drop occurs, the contact angle between the different materials depends on the surface energies of the materials.(Fig. 2.8)

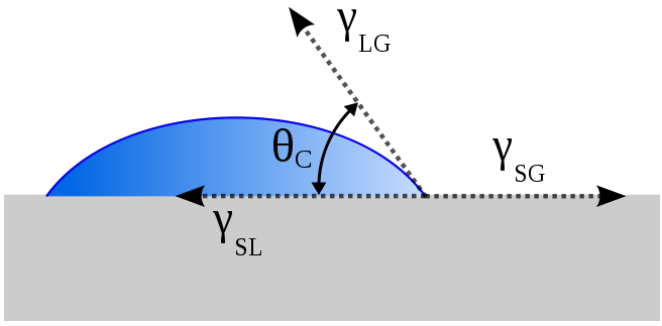

Figure 2.8: Contact angle of a liquid on a solid (taken from [46])

In Fig. 2.8 θ_C is the contact angle, γ_{SG} is the surface tension of the solid, γ_{LG} the

surface tension of the liquid and γ_{SL} the interfacial tension between the solid and the liquid. The equation of Young connects these quantities:

$$\gamma_{SG} = \gamma_{SL} + \gamma_{LG} \cdot cos(\theta_C) \tag{2.2}$$

Following the method of Owens and Wendt [47], the surface energy of a solid can be separated into a polar σ_i^p and into a dispersive part σ_i^d. Thus the interfacial tension can be calculated from:

$$\gamma_{SL} = \gamma_{SG} + \gamma_{LG} - 2(\sqrt{\sigma_{SD}^d \sigma_{LG}^d} + \sqrt{\sigma_{SG}^p \sigma_{LG}^p}) \tag{2.3}$$

By the combining equations (2.2) and (2.3), it is possible to get a linear relationship to extract the surface energy(Fig. 2.9). By using at least two liquids with known σ_{LG}^d and σ_{LG}^p and plotting the result a straight line comes out(Fig. 2.9). By linear regression, the polar component of surface energy (σ_{SG}^p) can be determined from the square of the slope of the line, and the dispersive component of the surface energy of the solid (σ_{SG}^d) can be determined from the square of the intersection of the ordinate and the line.

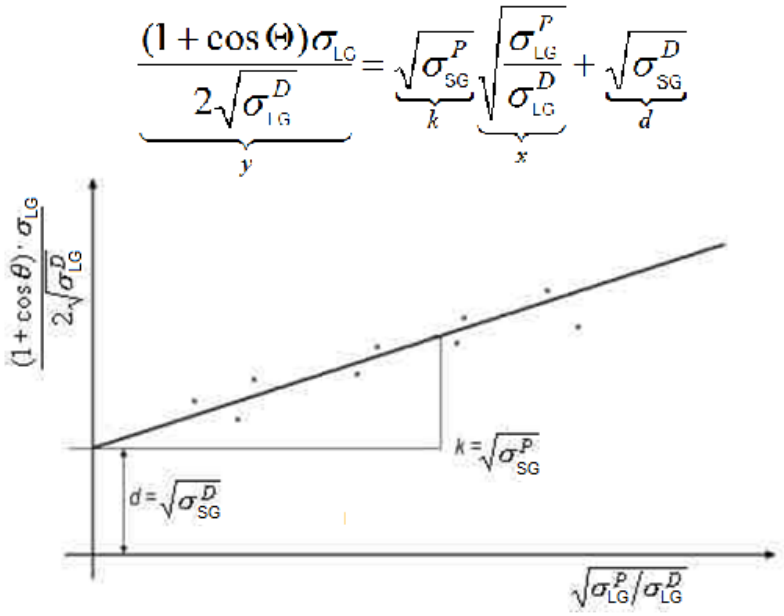

Figure 2.9: Top: Linear equation to extract the surface energy. Bottom: Schematic determination of the dispersive(σ_{SG}^d) and polar(σ_{SG}^p) surface energy components of the solid by linear regression (taken from [47])

In Fig. 2.10 a typical contact angle measurement setup is shown. This technique gave us the possibility to see whether there was a change in the surface energy after

some modifications of our devices.

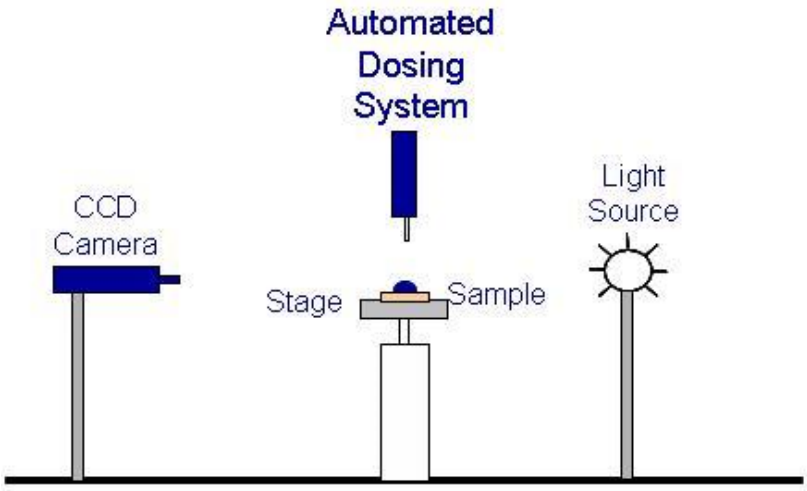

Figure 2.10: Typical contact angle measurement setup, with an automated dosing system, which drops the liquid onto the sample. A light source and a CCD-sensor behind the sample to analyse the shape of the liquid drop are shown (taken from [48])

2.5 UV/VIS/IR - Spectroscopy

During this thesis UV/VIS/IR - Spectroscopy was used to investigate the photo reactive interfacial layers used in the OTFTs. These polymer layers were used to change the OTFT performance by changing their molecular structure after illumination with ultraviolet or visible light. The above mentioned spectroscopic methods made it possible to take a closer look on the photo reaction and on the molecular structures of the photo reaction products. Most of the measurements were performed by DI. Lucas Hauser from the Institute for Chemistry and Technology of Materials, University of Technology Graz and DI. Matthias Edler from the Institute of Chemistry of Polymeric Materials, University of Leoben.

- Ultraviolet and visible light spectroscopy

Ultraviolet and visible light spectroscopy refers to absorption spectroscopy in the ultraviolet and visible spectral region. It is routinely used in the quantitative determination of highly conjugated organic compounds. Organic compounds, especially those with a high degree of conjugation, also absorb light in the UV or visible regions of the electromagnetic spectrum.

The UV/VIS spectrometer measures the intensity of light passing through a sample (I), and compares it to the intensity of light before it passes through the sample (I_0). The ratio I / I_0 is called the transmittance, and is usually expressed as a percentage ($\%$ T). The absorbance(or optical density) A is based on the transmittance:

$$A = -log(\%T/100\%) \tag{2.4}$$

The basic parts of a spectrometer are a light source, a diffraction grating or monochromator to separate the different wavelengths of light, a holder for the sample and a detector.

- Infrared spectroscopy (IR)

Infrared spectroscopy (IR spectroscopy) is the spectroscopy that deals with the infrared region of the electromagnetic spectrum. It covers a range of techniques, mostly based on absorption spectroscopy. As with all spectroscopic techniques, it can be used to identify and study chemicals. Infrared spectroscopy exploits the fact that molecules absorb specific frequencies that are characteristic for their structure. These absorptions are resonant frequencies, i.e. the frequency of the absorbed radiation matches the frequency of the bond or group that vibrates. When infrared light interacts with matter, chemical bonds will stretch, contract and bend. As a result, a chemical functional group tends to absorb infrared radiation in a specific wavenumber range partially regardless of the structure of the rest of the molecule.

Chapter 3

Measurements and Results

The first part of this chapter deals with the pre-treatment and the manufacturing process of organic thin film transistors. The manufacturing processes differed strongly for some organic semiconductors or device structures.

In the second and third part, in an attempt photo-reactive interfacial layers in OTFTs were used to control the morphology and further the mobility of the devices. The theoretical background was a surface energy modification by irradiation to control the growth process of the organic semiconductor(pentacene) on top of the OTFT.

In the fourth part, again a photo-reactive interfacial layer in an OTFT was investigated. In that case, a photo-reactive spiropyran polymer that reversibly changes its molecular structure by irradiation with ultra violet and visible light was investigated. Here, the focus of the investigations was on the reversible shift of the threshold voltage after the illumination with ultra violet or visible light. Additionally, UV- and visible light irradiation experiments were performed.

In the last sub-chapter, investigations of the very promising organic semiconductor TIPS-pentacene are discussed. By using different solvents as well as manufacturing processes it was tried to achieve good OTFT performances with this active layer material.

3.1 Device fabrication and pretreatment

The device structure of the organic thin film transistors produced during this thesis was based on a 2 x 2 cm highly p-doped silicon waver with a thermally grown SiO_2 layer(as the dielectric). The pretreatment of this substrates included several steps [49], and varied with the device setups (bottom / top -contact) and depositioning processes of the active layer material(evaporated, spin-coated, drop-cast). In the following the fabrication of a typical top-contact bottom-gate pentacene thin film transistor with a photo reactive interfacial layer is explained(Fig. 3.1). Here it should be mentioned that the production of some TIPS-pentacene transistors differs fundamentally from that example. These differences are mentioned in the relevant sections.

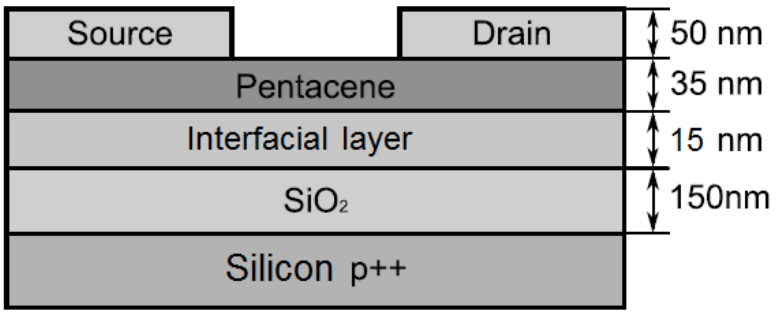

Figure 3.1: Schematic structure of a typical organic thin film transistor used in this thesis

1. **Plasma etching**
   After taking a sample out of the wafer box(the samples were always treated with plastic tweezers to do not harm the insulting layer). The dust from the surface was blown away with CO_2 gas and the sample was given into the plasma etching chamber. Plasma etching was used to remove dirt deposited on the wafers: after evacuating the chamber to 10^{-3} mbar, O_2-gas was constantly flowing through the chamber. Then the plasma was generated by an electromagnetic field and high-energy ions from the plasma interacted with the wafer surface. A regular device was plasma etched for 40 seconds with maximum gas flow in our plasma etching chamber(level 10).

2. **Ultrasonic bath**

   After plasma etching, the sample was put in a small glass half filled with high ohmic water(22 MΩ). Then the glass was put into an ultrasonic bath(half filled with water) for two minutes without heating. After the ultrasonic bath the

samples were washed with high ohmic water(22 MΩ) and dried with CO_2 gas. Apart from cleaning the devices, the ultrasonic bath results a hydrophilic surface.

3. **Deposition of the interfacial layer**

   After the pretreatment, the interfacial layer was deposited. Either by spin-,drop- or dip-coating in the glove box or under ambient conditions. It depended on the interfacial layer material and will be explained in the corresponding sections. For example the photo reactive layers investigated in this thesis were spin coated in the glove box under argon atmosphere with 2000 rounds per minute for 40 seconds in the dark under a red light emitting diode(LED) - lamp. After the spin coating process some devices were dried on a hot plate(70 $^\circ$) in the glove box.

4. **Evaporation of pentacene**

   When the interfacial layer was deposited on the pretreated substrate, the samples were transported in a box under argon atmosphere to the Joanneum Research Institute for Surface Technologies and Photonics in Weiz. Here DI. Dr. Anja Haase or DI. Alexander Fian evaporated an approximately 35 nm thick pentacene layer under a pressure of 10^{-5} mbar on top of the sample. The evaporation procedure was a very well optimized process, where the substrates where heated to 65 degree and the amount of deposited pentacene was controlled over the whole process. The deposition rate of pentacene during the evaporation was 1 angstrom / min and less for the first 0 to 5 nm, 0.05 angstrom / s for the next 5-20 nm and 0.1 Å / s for the last 20-40 nm. The increase of the deposition rates was performed slowly and without overshoot. After the evaporation an AFM picture was usually taken.

5. **Evaporation of gold electrodes**

   The samples were then transported back to Graz in a transport box under ambient conditions(argon atmosphere). First of all the samples were transferred into the glove box, then the evaporation chamber(always the new evaporation chamber) was prepared and the samples were scratched with a diamond cutter at the latter location of contact pads to be able to contact the gate electrode from the top. Furthermore, the samples were positioned in the shadow mask above the place where the gold is evaporated. Hereby, the channel was realized by tungsten wires with a diameter of 25 or 50 μm. Then the chamber was evacuated to a pressure of 3 to 4 $\cdot$ 10^{-6} mbar. When this pressure was reached the

evaporation was performed: in five to ten seconds a 50 nm thick gold layer was evaporated.

6. **Characterization of the OTFTs**

After the evaporation of the gold electrodes, the organic thin film transistor was completed. To reduce the charging current the pentacene layer was scratched away around the electrodes with metal tweezers. This reduced the charging current by one to three orders of magnitude. From that point on it was possible to characterize the OTFT. X-ray reflectivity measurements were performed, to check the thickness and the surface roughness of the deposited layers. Additionally pictures of the deposited active layer material were taken by an optical microscope of the type OLYMPUS BX51.

3.2 Poly formic acid 4-vinyl-phenyl ester as interfacial layer in pentacene based OTFTs

3.2.1 Motivation

Poly(formic acid 4-vinyl-phenyl ester) or P4 is a photo-reactive polymer which was investigated during the bachelor thesis of J.C. Kuhlmann [50] under supervision of DI. Dr. Thomas Griesser at the Institute of Chemistry of Polymeric Materials at the University of Leoben. For the illumination and modification experiments (UV/VIS- and IR-spectroscopy) CaF_2 substrates were used. The substrates were spincoated with 10 mg/ml P4 dissolved in chloroform. The UV/VIS-spectra in Fig. 3.2 showed an increase of the absorption after the illumination. The photo reaction that occurred upon irradiation of the interfacial layer with UV-light at wavelengths shorter than 254 nm is shown in the inset of Fig. 3.2.

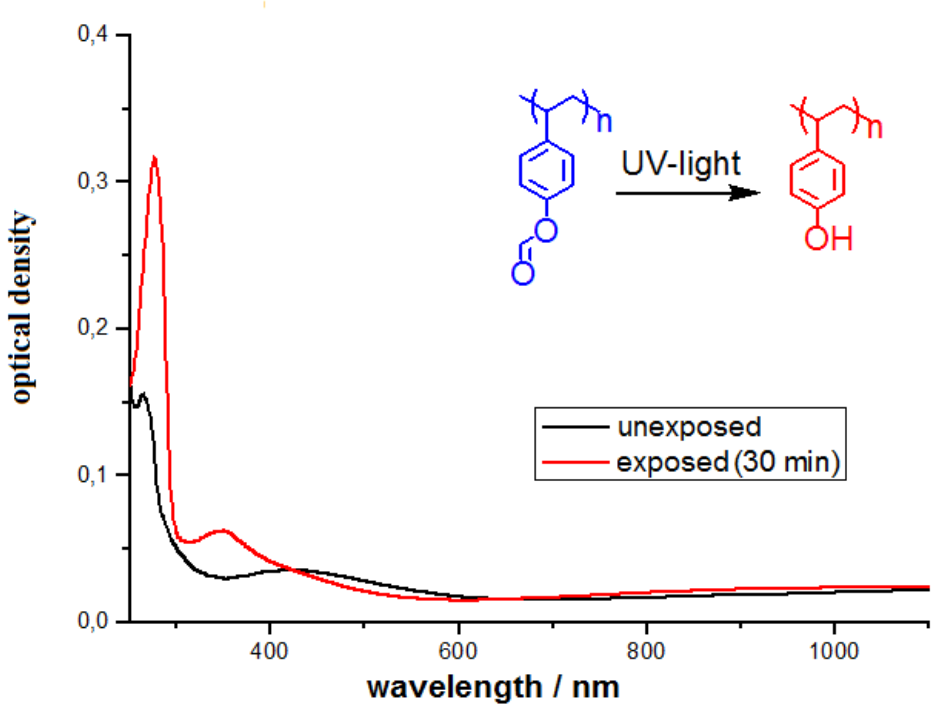

Figure 3.2: UV/VIS-spectra of P4 before and after illumination with UV-light. The inset shows the chemical reaction which occurs by UV-light irradiation (measurement was performed by DI. Matthias Edler) [50]

Based on the IR spectra shown in Figure 3.3, the UV-initiated decarbonylation (dissociation of the C=O group) was recognized by the appearance of characteristic bands. In the spectrum of the unexposed polymer (black), the typical bands of an

ester were seen at 1750 cm^{-1} (C=O stretching oscillations) and at 1191 cm^{-1} (C-O-C stretching oscillations). These bands disappeared after the illumination (blue) and at 3380 cm^{-1} stretching oscillations of the hydroxyl group appeared [50].

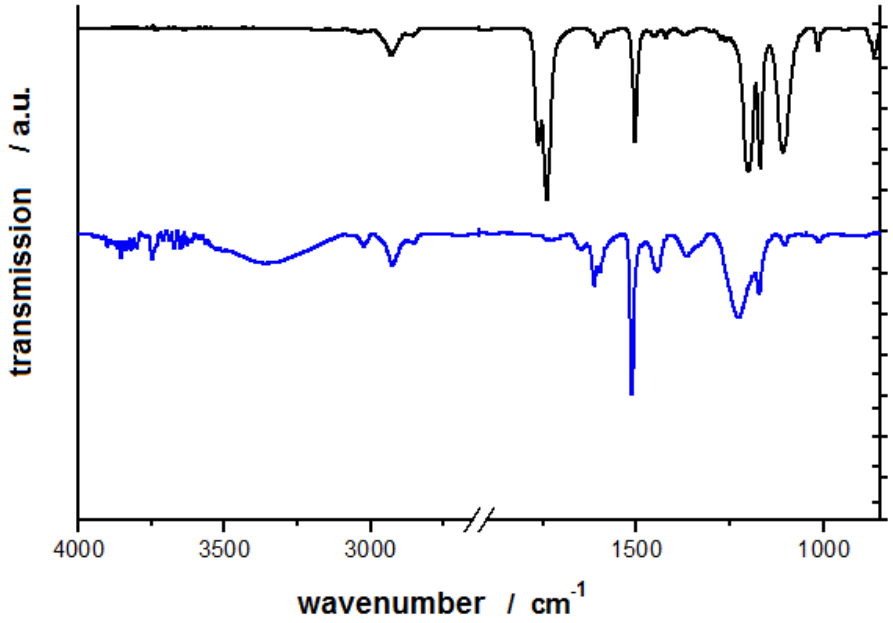

Figure 3.3: IR-spectra of P4 before and after illumination with UV-light (measurement was performed by DI. Matthias Edler) [50]

The conversion of the ester group into a phenol was expected to change the surface energy with the net effect depending on the irradiation time. The latter was varied between 10 seconds and 7 minutes. To measure changes in the surface potential, the contact angles of H_2O and CH_2I_2(diiodomethane) on spincoated P4 layers on Si/SiO_2 substrates were investigated. Data for the former were adversely affected by the fact that the polymer became water soluble upon irradiation. Therefore, the contact angle was measured five seconds after deposition of the droplet.

Like can be seen in Tab. 3.1 the contact angle slightly increased for CH_2I_2 and clearly increased for H_2O as a function of the irradiation time. This confirmed that the surface energy is controllable by the illumination time. The idea behind the variation of the surface energy of the P4 layer by irradiation with a UV - lamp was to tune the surface energy to values similar to the surface energy of pentacene, to optimize the growth process and to enhance the grain size of the pentacene layer on top of the P4 layer [51].

Table 3.1: Contact angle measurements of H_2O and CH_2I_2 on Si/SiO_2 wafers with a spincoated photo reactive P4 layer on top. Before the CA-measurement the devices were illuminated with an UV-lamp for different time periods.

Sample number	illumination time / s	$CA - H_2O$ / deg	$CA - CH_2I_2$ / deg
REF	<5	<5	36
P4-1	<5	41	28
P4-2	<5	47	29
P4-3	10	48	28
P4-4	30	55	31
P4-5	60	77	33
P4-6	120	81	32
P4-7	300	85	34

3.2.2 Results

Based on the promising results of the above described experiments, pentacene-based organic thin film transistors with a P4-interfacial layer were built. All the results presented in this thesis are OTFTs which were built in the glove box under argon atmosphere. The interfacial layer consisted of 4 mg/ml P4 solved in tetrahydrofuran(THF). The solution was spincoated with 2000 rpm for 40 seconds. As a next step, pentacene was evaporated onto the polymer layer and an AFM picture was taken. Finally top source and drain contacts were evaporated and the impact of the interfacial layer on the carrier mobility and threshold voltage was investigated. Additionally one device was investigated by XRR-measurements to check the thickness of the spincoated and the evaporated layer.

In Fig. 3.4 on the left transfer characteristics of a regular pentacene OTFT are presented. To the right side a set of transfer curves of an OTFT with a P4 interfacial layer exposed to UV-light for 30s is shown. As can be seen in this figure, there was no big difference in the behaviour of the OTFTs. The analysis of the I-V-characteristics showed small differences in the mobility and the threshold voltage of the devices.

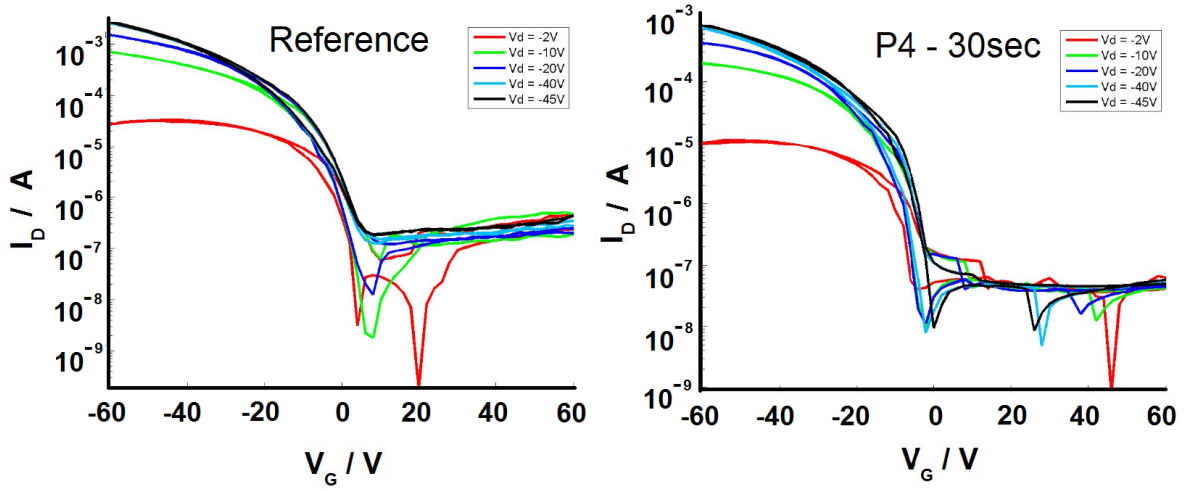

Figure 3.4: Transfer characteristics of a reference pentacene OTFT(left) and an OTFT with a P4 interfacial layer illuminated with UV light for 30 seconds

In addition to that, the output characteristics of an OTFT with and without P4 interfacial layer exposed to UV-light for 30s was measured, as can be seen in Fig. 3.5. In (Fig. 3.5 right) the good saturation behaviour of the transistor for the forward sweep of the P4-OTFT and a big hysteresis was observed.

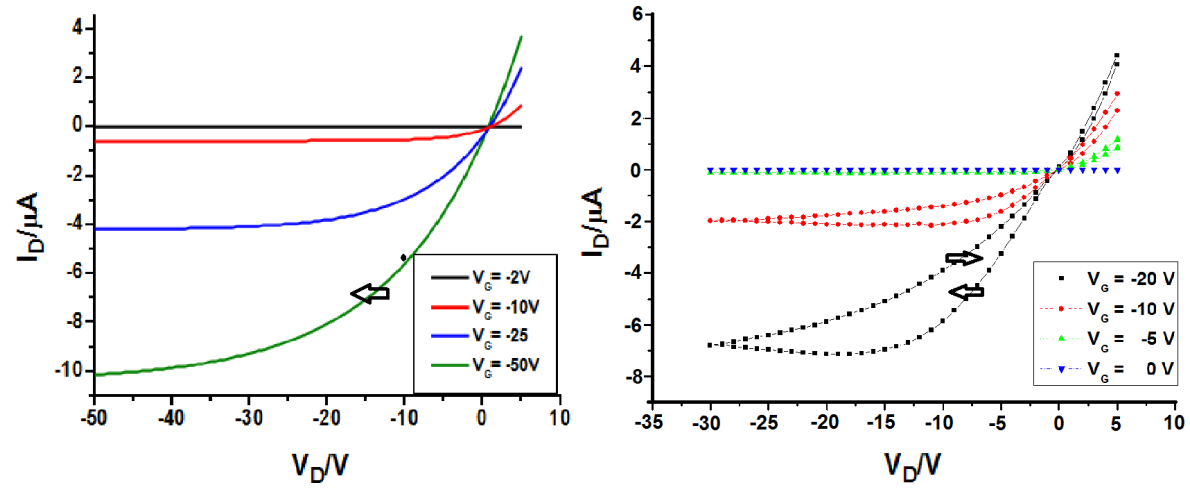

Figure 3.5: Left: Single sweep output characteristic of a regular pentacene based OTFT. Right: Double sweep output characteristic of a pentacene based OTFT with a P4 interfacial layer illuminated for 30 seconds

The analysis of the threshold voltage and the mobility of the devices was done in the saturation regime. These investigations did not show any clear impact of the interfacial layer, after different periods of illumination, on the carrier mobility or threshold

voltage. This can be seen in Fig. 3.6 where the mobility and the threshold voltage are plotted as a function of the UV-exposure time of the P4-OTFTs. The regular pentacene based OTFTs had a constant mobility and threshold voltage of μ= 0.3 $\frac{cm^2}{Vs}$ and V_{th}= -2V.

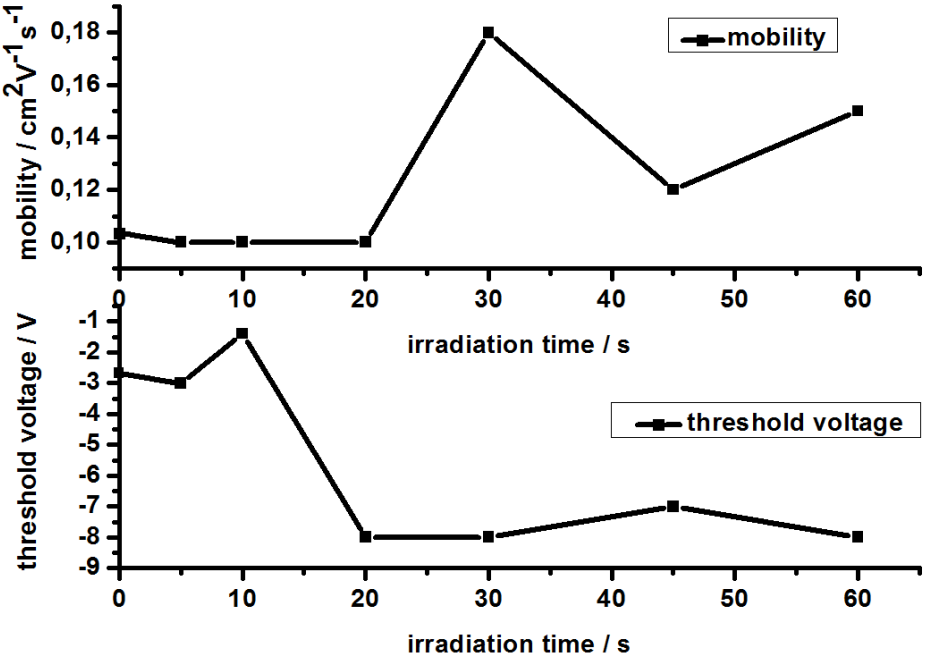

Figure 3.6: Mobility and threshold voltage of a pentacene based OTFT with an P4 interfacial layer plotted over the UV-exposure time

For this set of P4-OTFTs the mobility increased from 0.10 to 0.18 $\frac{cm^2}{Vs}$ after illumination periods longer than 20 seconds and decreased for illumination periods longer than 30 seconds to about 0.14 $\frac{cm^2}{Vs}$. The threshold voltage shifted to more negative values for illumination times longer than 10 seconds(from -1 to -7 volts). This trend for the mobility and threshold voltage, however, was not reproducible. In this set of pentacene based OTFTs with a P4 interfacial layer the maximum mobility and grain size was measured for an UV exposure time of thirty seconds (Fig. 3.6), but the next set showed a maximum grain size and thus a maximum mobility [51] for OTFTs illuminated for ten seconds, as can be seen in the AFM images in Fig. 3.7.

Analyzing the mobilities of the devices and comparing the device parameters with the AFM pictures(Fig: 3.7) showed a clear already known trend: the bigger the grain size the higher the mobility. A correlation between UV exposure time and grain size as described in [51] could, however not be observed.

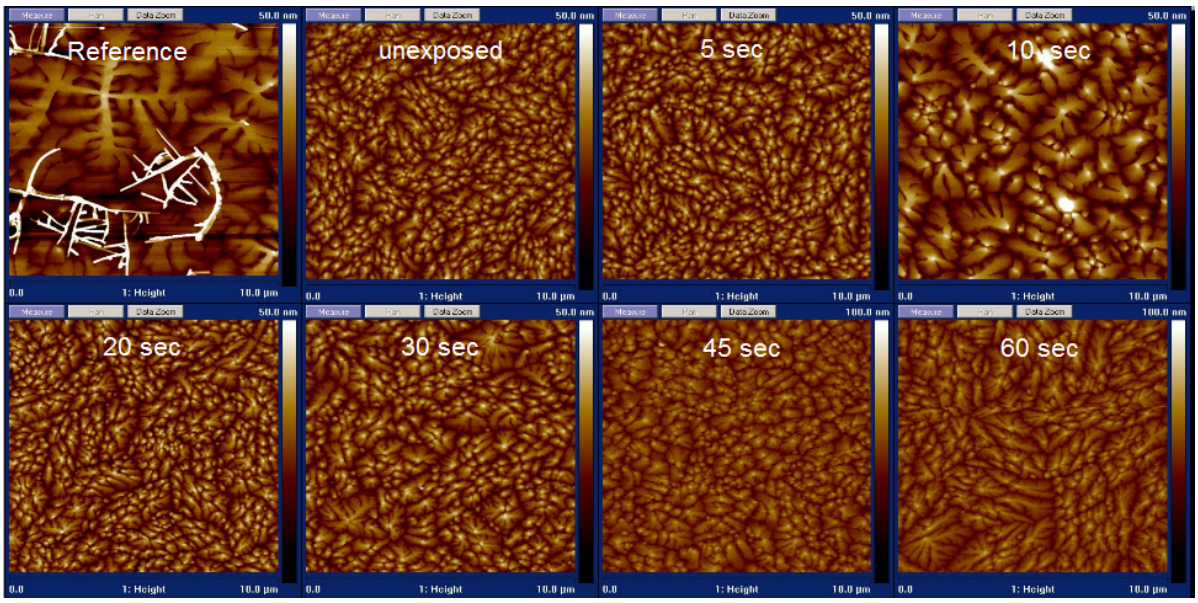

Figure 3.7: 10 x 10 μm atomic force microscope images of a pentacene based OTFT with an P4 interfacial layer exposed to UV-light for different time periods (measurement was performed by DI. Dr. Anja Haase)

Additionally x-ray reflectivity measurements showed the thickness of the dielectric and of the interfacial layer(Fig. 3.8). The thickness of the oxide layer was d_{oxide}= 145,5 nm and the thickness of the P4 interfacial layer was d_1= 11,5 nm.

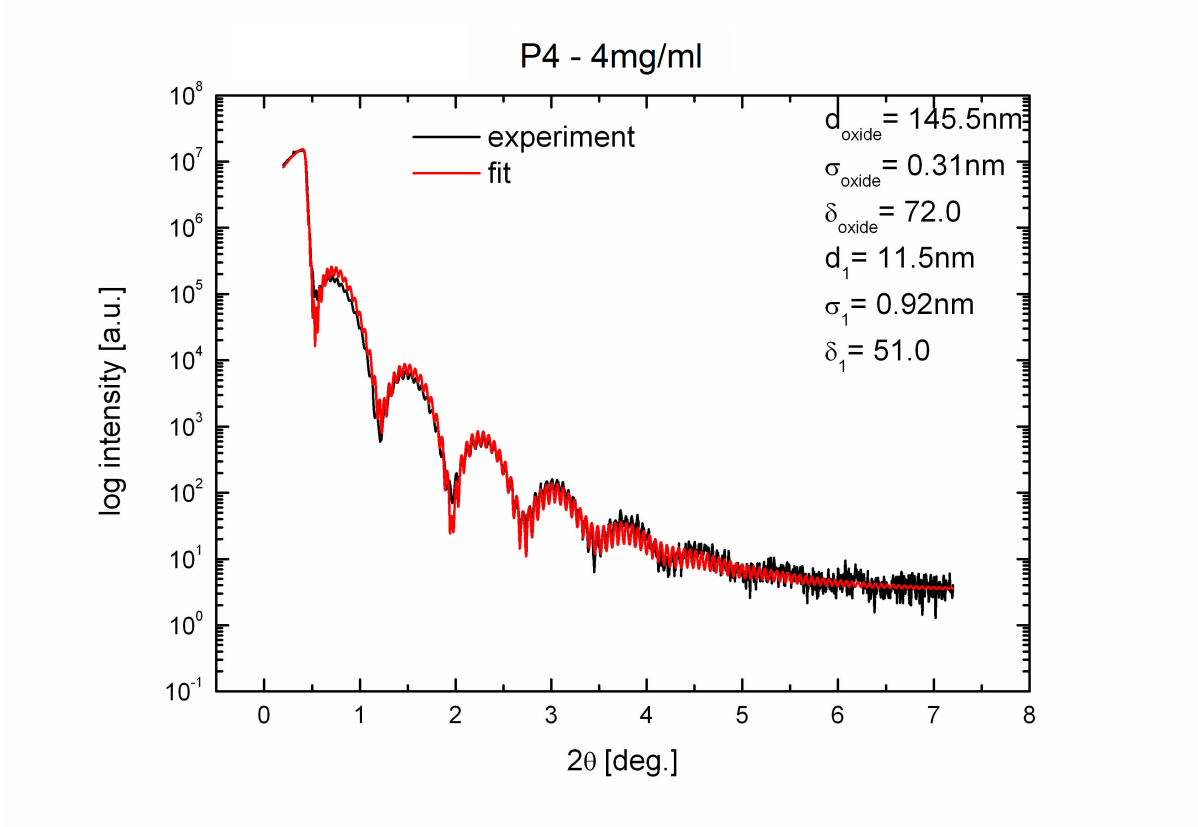

Figure 3.8: X-ray reflectivity measurement of a Si/SiO_2 substrate with a spin coated layer of 4 mg/ml poly formic acid 4-vinyl-phenyl ester solved in THF on top (measurement was performed by DI. Dr. Heinz Flesh)

3.2.3 Conclusion

Finally it can be noticed that no fundamental connection between the change of the surface energy of the photo-reactive polymer Poly formic acid 4-vinyl-phenyl ester and the device parameters (mobility μ, threshold voltage V_{th}), was recognized.

3.3 Poly(VBT-CO-stryrene) as interfacial layer in pentacene based OTFTs

3.3.1 Motivation

In this sub-chapter Poly(4-vinylbenzl thiocyanate-co-stryrene) or short PVBT a photo reactive polymer is investigated and used as interfacial layer in OTFTs. PVBT (Fig. 3.9) was investigated by Matthias Edler during his Ph.D. thesis at the Institute of Chemistry of Polymeric Materials at the University of Leoben. It is a co-polymer consisting of a mass fraction of 50 % styrene and 50% VBT. The illumination experiments were analysed by contact angle measurements and FT-IR spectroscopy. CaF_2 was used as substrate for these investigations. The substrates were cleaned with acetone and distilled water. PVBT was dissolved in CH_2Cl_2 (or THF) in a concentration of 10 mg/ml). After that the dissolved polymer was spincoated on the CaF_2 substrates with 2000 rpm for 30 seconds. All these steps were performed under ambient conditions, meanwhile the solution was always protected from light.

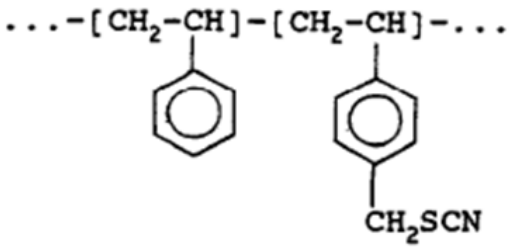

Figure 3.9: Chemical structure of a PVBT monomer (taken from [52])

Under the influence of UV-light (254 nm) the photosensitive thiocyanate (-SCN) group reacted to an isothiocyanate (-NCS) group(Fig. 3.10). UV-irradiation experiments were carried out with an ozone free low pressure Hg lamp (Hereaus Noblelight; 254 nm). In these experiments, the light intensity (power density; in mW cm^{-2}) at the sample surface was measured with a spectroradiometer (Solatell, Sola Scope 2000TM, spectral range from 230 to 470 nm). The light intensity was 2.1 mW cm^2 for 254 nm, respectively. All UV illuminations were carried out under inert gas atmosphere (N_2).

- **Photo reaction of PVBT**

The conversion of the photoreactive thiocyanate (-SCN) group into an isothiocyanate (-NCS) group was investigated with a FT-IR-spectrometer as can be seen in Fig. 3.10.

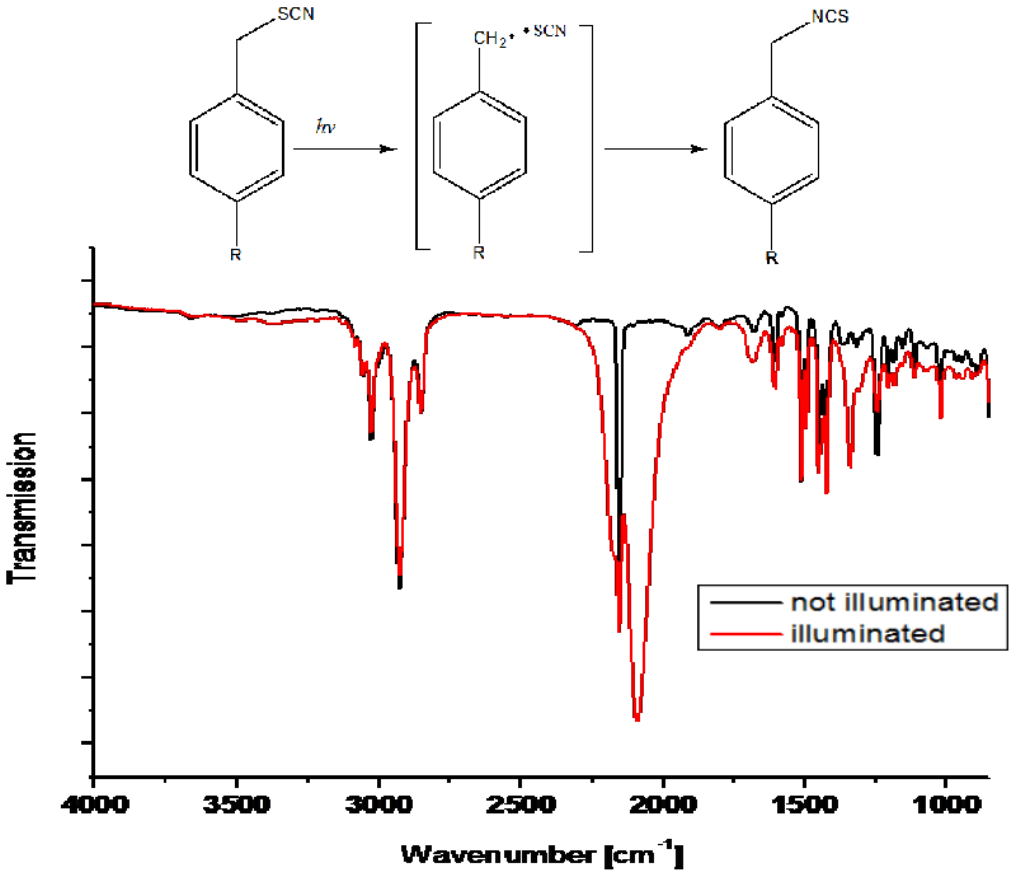

Figure 3.10: Top: molecular imaging of the conversion of the photoreactive thiocyanate (-SCN) group into an isothiocyanate (-NCS) group. Bottom: detection of the conversion with a FT-IR-spectrometer (measurement was performed by DI. Matthias Edler) [52]

In figure 3.10 the spectra of the exposed and unexposed PVBT film are shown. The unexposed PVBT spectrum (black) shows a sharp SCN-peak at 2151 cm^{-1}. After the illumination (red), a new peak at 2086 cm^{-1}, and another peak at 1338 cm^{-1} were detected. These two peaks are attributed to the formation of isothiocyanate. After 10 minutes exposure approximately half of the thiocyanate reacted. After about 35 minutes, almost all groups became isothiocyanate.

Additionally, the contact angles of the unexposed and the exposed sample were compared. The contact angle changed from 83 ° (water) and 30 ° (diiodomethane) for the unexposed sample to 87 ° (water) and 36 ° (diiodomethane) for the exposed sample. The contact angle measurements in this sub-chapter were performed by DI. Matthias Edler.

3.3.2 Post modifications

Based on the formation of this photo product(isothiocyanate) several interesting post-modifications were performed that will be introduced subsequently. Most of this modification reaction were performed under ambient conditions. If not, then it is mentioned in the respective point. the post-modification of the exposed samples in the vapour phase were performed with 200 mg derivatization reagent per ml solvent (about 3-5molar).

- **Derivatization with propylamine**

After the photo reaction of PVBT the polymer was exposed to a vapor phase of toluene or THF with a few drops of propylamine for 60 minutes (Fig. 3.11). Here, the contact angle changed from 87.0 ° (water) and 36.1 ° (diiodomethane) to 82 ° (water) and 35 ° (diiodomethane).

- **Derivatization with trifluoroethylamine**

After the photo conversion of PVBT the polymer was exposed to a vapor phase of toluene or THF with a few drops of trifluoroethylamine for 60 minutes (Fig. 3.12). The contact angle of water changed from 87 ° to 100 °. For the rest of the post modifications no contact angle measurements with diiodomethane were performed. The significant increase of the contact angle of water was explained by the fluorinated end group.

- **Ethylenediamine**

After the photo reaction of PVBT the polymer was exposed to a vapor phase of toluene or THF with a few drops of ethylenediamine for 30 minutes(Fig. 3.13). Apparently the ethylenediamine reacted with the water in the air and made the PVBT film cloudy. Therefore, this experiment was repeated in the glove box. There no turbidity was detected. The contact angle of water changed from 87 ° to 82 °.

- **Ethylenediamine + HCl-vapour**

Because of the small changes in the contact angle the post-modified polymer film was held under HCl vapour for 30s(Fig. 3.14). For the HCl vapour treated samples the contact angle of water changed from 87 ° to 61 °. The significant decrease of the contact angle is explained by the fluorinated end groups.

On the following pages the molecular structure of the reaction products and the FT-IR-spectroscopy investigations of the post modification reactions are shown. On top of this figures the molecular structures before and after the modification are shown. Underneath that the FT-IR-spectroscopy investigations are presented. They always show the spectra of the not illuminated, the illuminated and the post modified device. So the first two look always the same in the figures because the illuminated PVBT layer was always the starting point for the different post modifications.

The post-modified films showed a distinct peak at about 3450-3150 cm^{-1}. It is attributed to the secondary amine. Also a thiourea-peak at 1550 cm^{-1} appeared. In addition the peak of the NCS group and the SCN group disappeared almost completely after the post modification. So the post modification reaction was almost complete and just a few NCS-groups were still present.

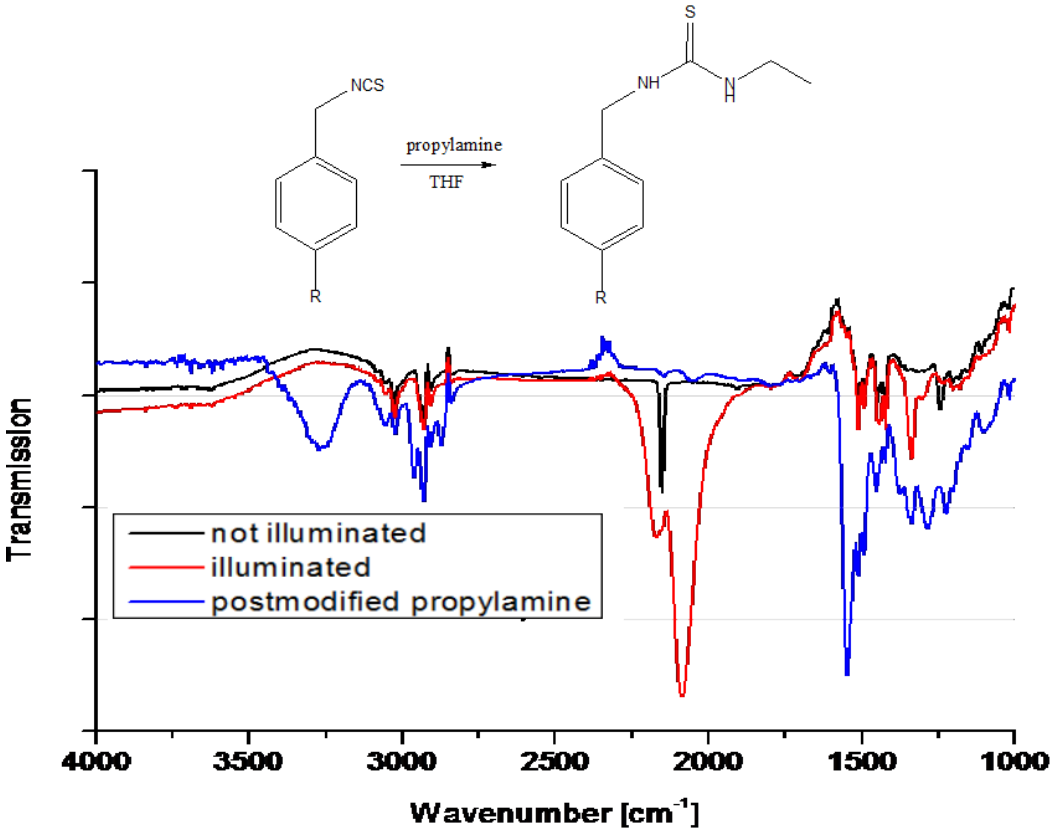

Figure 3.11: Top: molecular imaging of the post modification reaction of the illuminated PVBT with propylamine. Bottom: FT-IR spectrum of the unexposed, exposed and a with propylamine-modified PVBT film (measurement was performed by DI. Matthias Edler) [52]

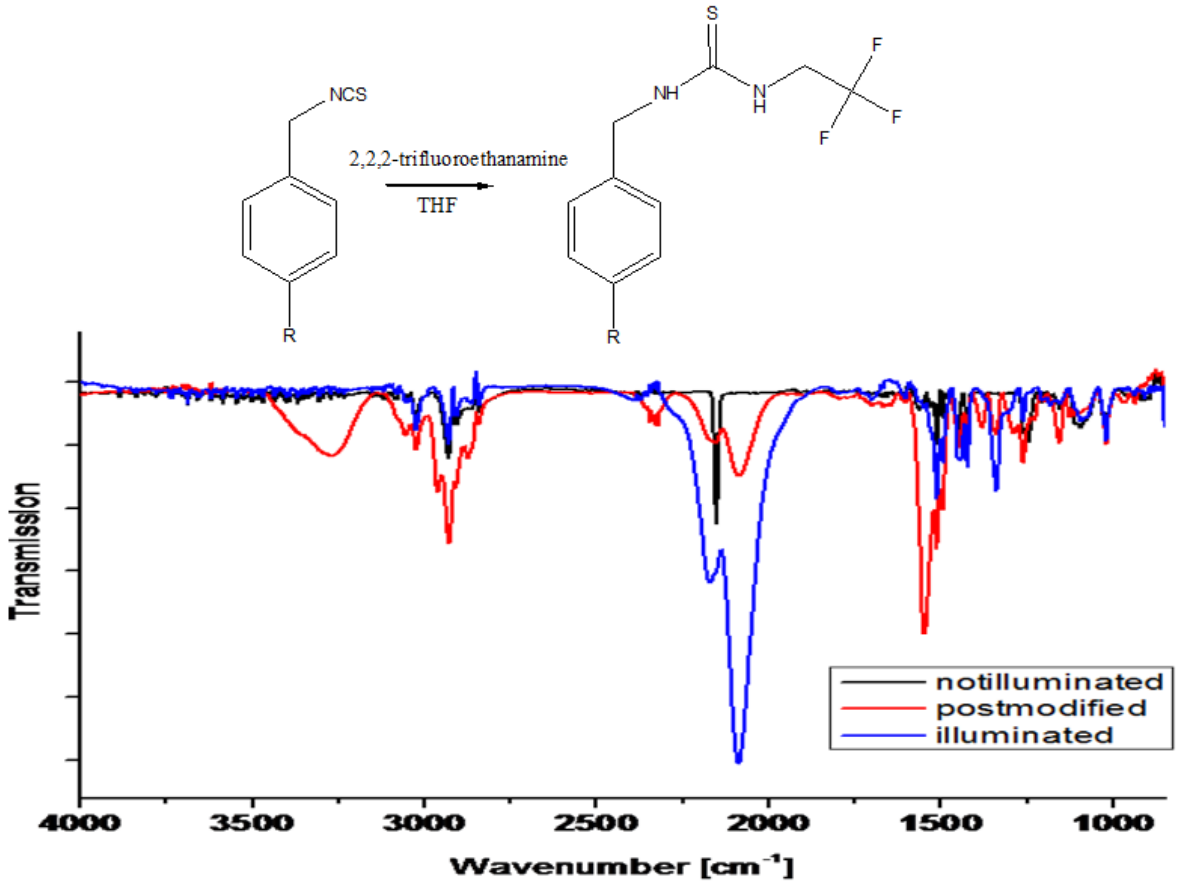

Figure 3.12: Top: molecular imaging of the post modification reaction of illuminated PVBT with trifluoroethylamine. Bottom: FT-IR spectrum of the unexposed, exposed and a with trifluoroethylamine modified PVBT film (measurement was performed by DI. Matthias Edler) [52]

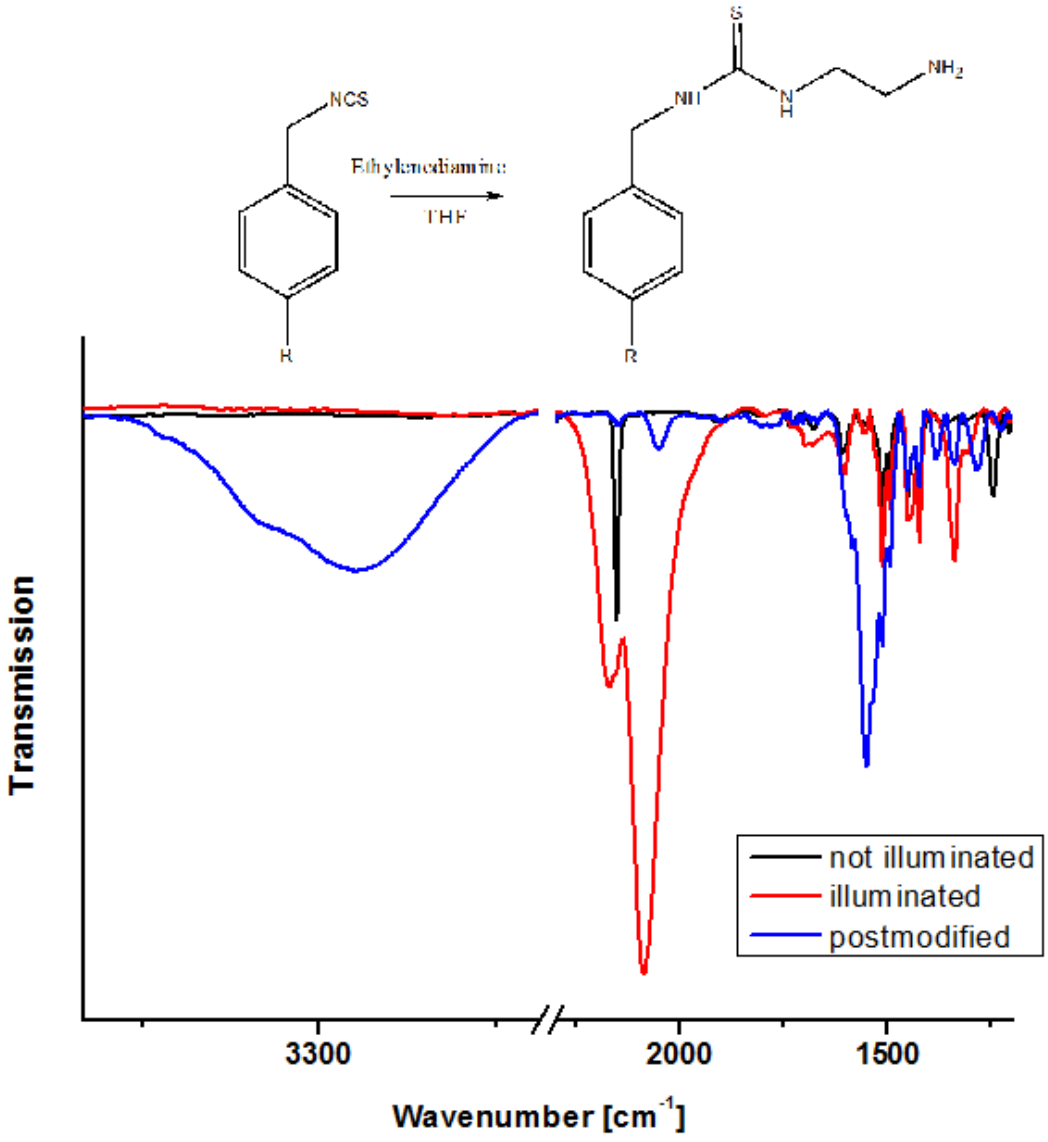

Figure 3.13: Top: molecular imaging of the post modification reaction of illuminated PVBT with ethylenediamine. Bottom: FT-IR spectrum of the unexposed, exposed and a with ethylenediamine modified PVBT film (measurement was performed by DI. Matthias Edler) [52]

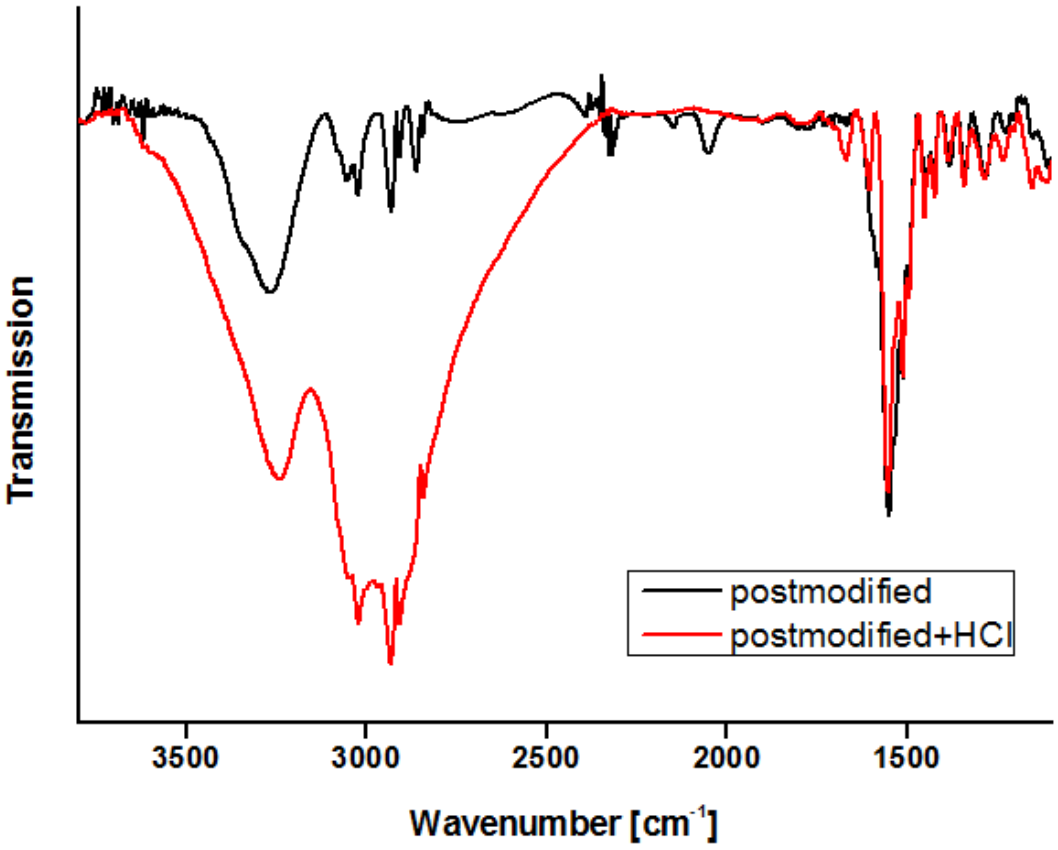

Figure 3.14: Top: FT-IR spectrum of the with ethylenediamine post-modified and the additionally with HCl vapour treated PVBT film (measurement was performed by DI. Matthias Edler) [52]

With this variety of surface energy changing polymer layers promising tools for the optimization of the electronic and structural properties of the active layer were available. Therefore, as a next step we applied them in OTFT device structures.

3.3.3 Devices

Here the Si/SiO_2 substrates were cleaned with CO_2 gas. Then the device substrates were transported under ambient conditions to the Institute of Chemistry of Polymeric Materials at the University of Leoben. Then they were plasma etched(O_2,100 W) for one min under a pressure of 40 mtorr. After that the PVBT solution(15mg/ml in anisole) was spincoated for 100 seconds with 2000 rpm with a Electronic Micro Systems LTD, Spin Coater Model 4000.

To find a possibility to optimize the electronic and structural properties of the active layer, devices with the already mentioned post-modifications of PVBT were built:

- Sample1 Si/SiO_2/PVBT/not illuminated
- Sample2 Si/SiO_2/PVBT/illuminated with UV-light with 254 nm for ten minutes
- Sample3 Si/SiO_2/PVBT/illuminated/reaction with vapour phase of THF and trifluoroethylamine for 60 minutes
- Sample4 Si/SiO_2/PVBT/(half illuminated)/post-modified with propylamine/ reaction with vapour phase of THF and trifluoroethylamine for 60 minutes
- Sample5 Si/SiO_2/PVBT/illuminated/reaction with THF and ethylenediamine in glovebox for 60 minutes
- Sample6 Si/SiO_2/PVBT/illuminated/reaction with THF and ethylenediamine in glovebox for 60 minutes + kept under HCl gas for 20 seconds

After the post-modification the devices were again transported under ambient conditions to the Institute of Solid State Physics at the University of Technology, Graz. Then the devices were transported under inert conditions to the Institute of Nanostructured Materials and Photonics, Joanneum Research, Weiz where the pentacene layer was evaporated by DI. Alexander Fian. After that the gold electrodes were evaporated on top of the device. In the following investigations of the differently modified samples, the transfer characteristics and the from the linear region extracted device parameters of the samples are presented. The mobility of the reference OTFT(a regular pentacene OTFT) was 0.3 $\frac{cm^2}{Vs}$, and the threshold voltage was 0V.

- Sample1: Si/SiO_2/PVBT/not illuminated

The first sample was a pentacene based OTFT with a PVBT interfacial layer.

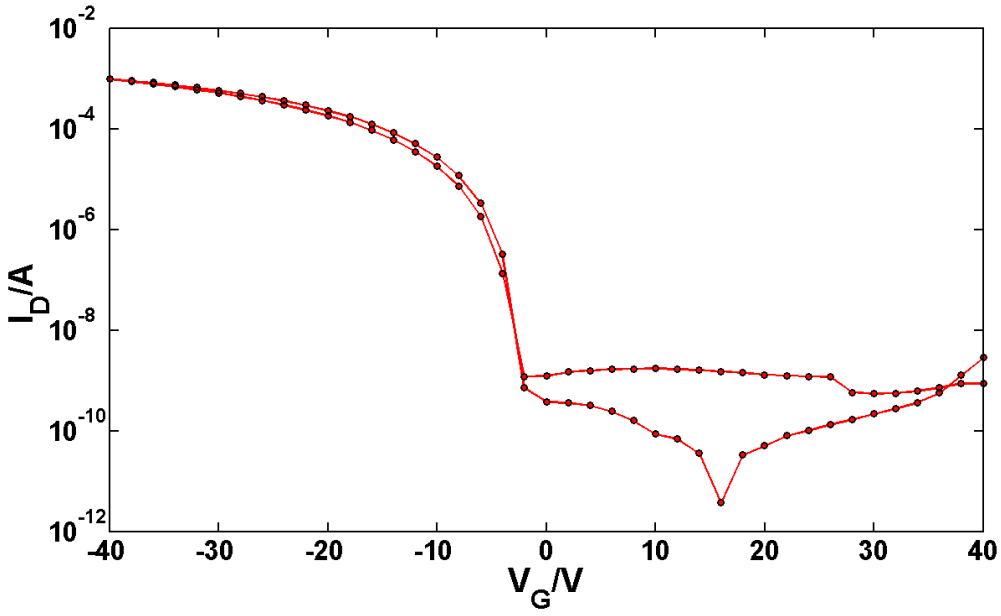

Figure 3.15: Transfer characteristic of a pentacene based OTFT with a PVBT interfacial layer. V_D = -20V

On this sample all transistors worked very well. There was almost no hysteresis in the transfer curves, the mobility was 0.25 $\frac{cm^2}{Vs}$ and the threshold voltage was -5 V. The onset voltage was -2 V. The leakage current was very low, approximately 10^{-8} A, and therefore the on/off ratio was very good.

- Sample2: Si/SiO_2/PVBT/illuminated with UV-light with 254 nm for ten minutes

The second sample was again a pentacene based OTFT with an interfacial layer(PVBT) illuminated with UV-light with 254 nm for ten minutes(Fig. 3.10).

Three of four transistors worked very well on this sample. There was almost no hysteresis in the transfer curve, the mobility was 0.27 $\frac{cm^2}{Vs}$ and the threshold voltage was -6 V. The onset voltage was 0 V. The leakage current was again very low, approximately 10^{-8} A, and therefore the on/off ratio was very good.

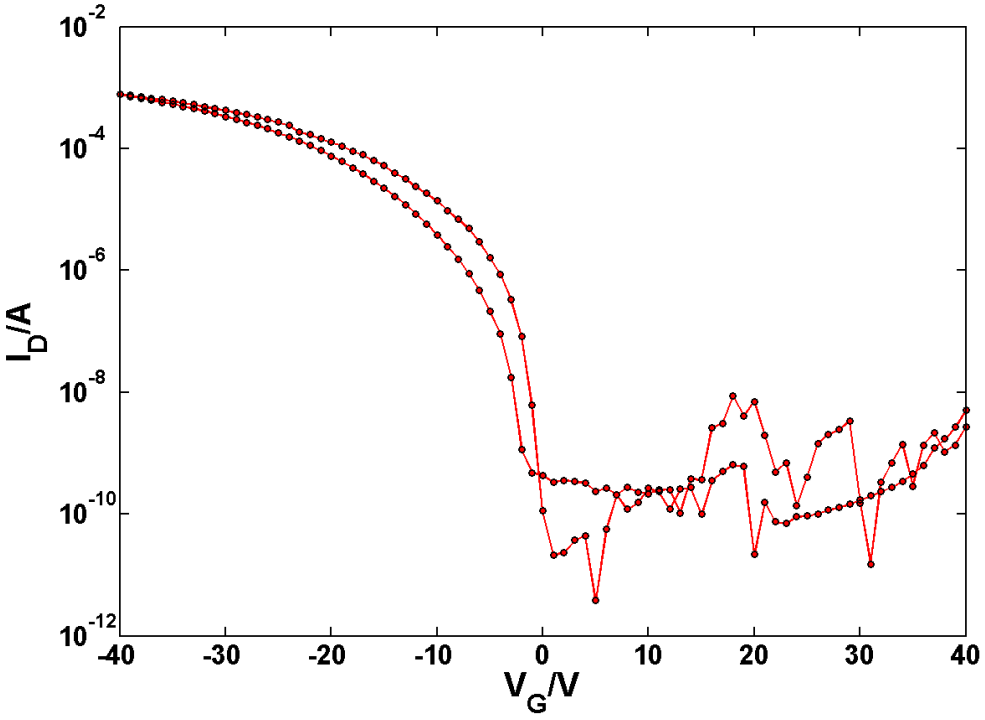

Figure 3.16: Transfer characteristic of a pentacene based OTFT with a PVBT interfacial layer after illumination with UV-light for 10 minutes. V_D = -20V

- Sample3: Si/SiO_2/PVBT/illuminated/reaction with vapour phase of THF and trifluoroethylamine for 60 minutes

The interfacial layer of the third sample was illuminated with UV-light with 254 nm for ten minutes, and post-modified by a reaction with the vapour phase of THF and trifluoroethylamine for 60 minutes (Fig. 3.12).

Here three of four transistors worked very well, there was a little bigger hysteresis in the transfer curve than before, the mobility was 0.2 $\frac{cm^2}{Vs}$ and the threshold voltage was -5 V. The onset voltage was 0 V. The leakage current was low, approximately 10^{-7} A.

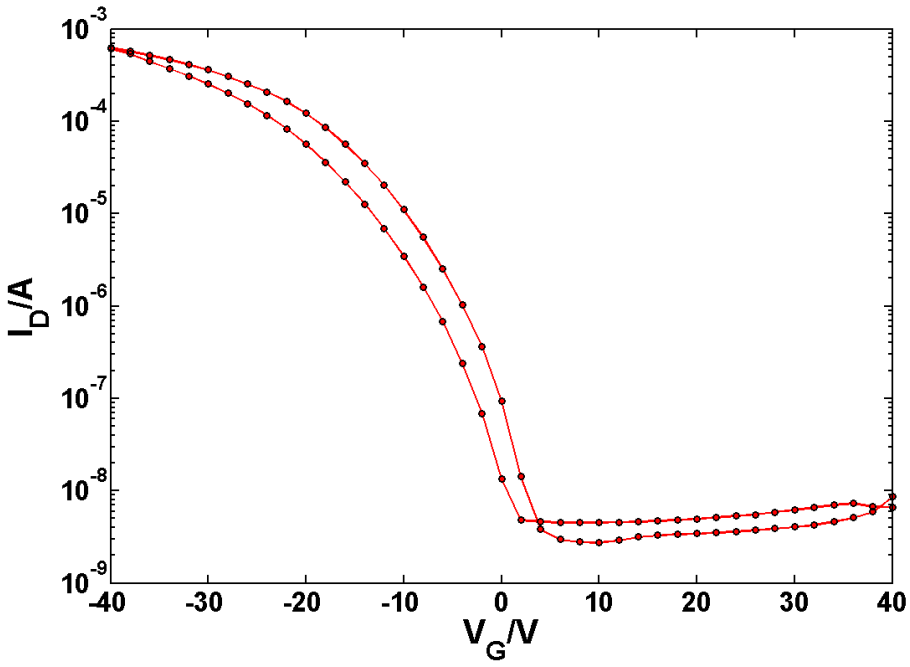

Figure 3.17: Transfer characteristic of a pentacene based OTFT with a PVBT interfacial layer after an illumination with UV-light(254 nm) for 10 minutes, and a post modification in the vapour phase of THF and trifluoroethylamine for 60 minutes. V_D = -20V

- Sample4: Si/SiO_2/PVBT/(half illuminated)/post-modified with propylamine/ reaction with vapour phase of THF and trifluoroethylamine for 60 minutes

One half of the interfacial layer of the fourth sample was illuminated with UV-light with 254 nm for ten minutes, then the whole sample was modified with propylamine, and after that modified by a reaction with the vapour phase of THF and trifluoroethylamine for 60 minutes. Here two of four transistors showed transistor behaviour (Fig. 3.11).

The two transistors on the non illuminated half of the sample showed a very high off-current(bulk doping or a related mechanism). These transistors never really turned off(on/off-ratio: 10^1). The other transistors on this sample showed a clear transistor behaviour with a small hysteresis, a little lower mobility than before of 0,15 $\frac{cm^2}{Vs}$, a threshold voltage of -3 V. The leakage current was not low, approximately $5 \cdot 10^{-7}$ A.

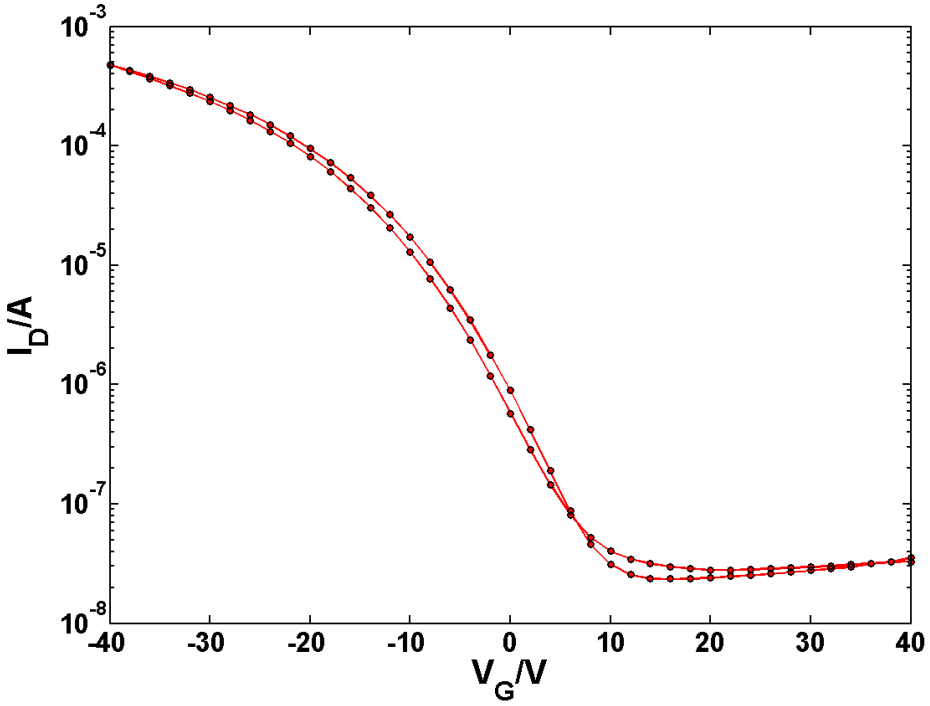

Figure 3.18: Transfer characteristic of a pentacene based OTFT with a PVBT interfacial layer after an illumination with UV-light(254 nm) for 10 minutes and after a modification reaction with the vapour phase of THF and trifluoroethylamine for 60 minutes. V_D = -20V

- Sample5: Si/SiO_2/PVBT/illuminated/reaction with THF and ethylenediamine in the glovebox for 60 minutes

The interfacial layer of the fifth sample was illuminated with UV-light with 254 nm for ten minutes, and post-modified by a reaction with the vapour phase of THF and ethylenediamine in the glovebox for 60 minutes (Fig. 3.13).

Here three of four transistors worked and showed transistor behaviour, but the hysteresis of the devices in the transfer characteristic was big. The mobility was 0.02 $\frac{cm^2}{Vs}$ and the threshold voltage was -8 V. The leakage current was $5 \cdot 10^{-8}$ A.

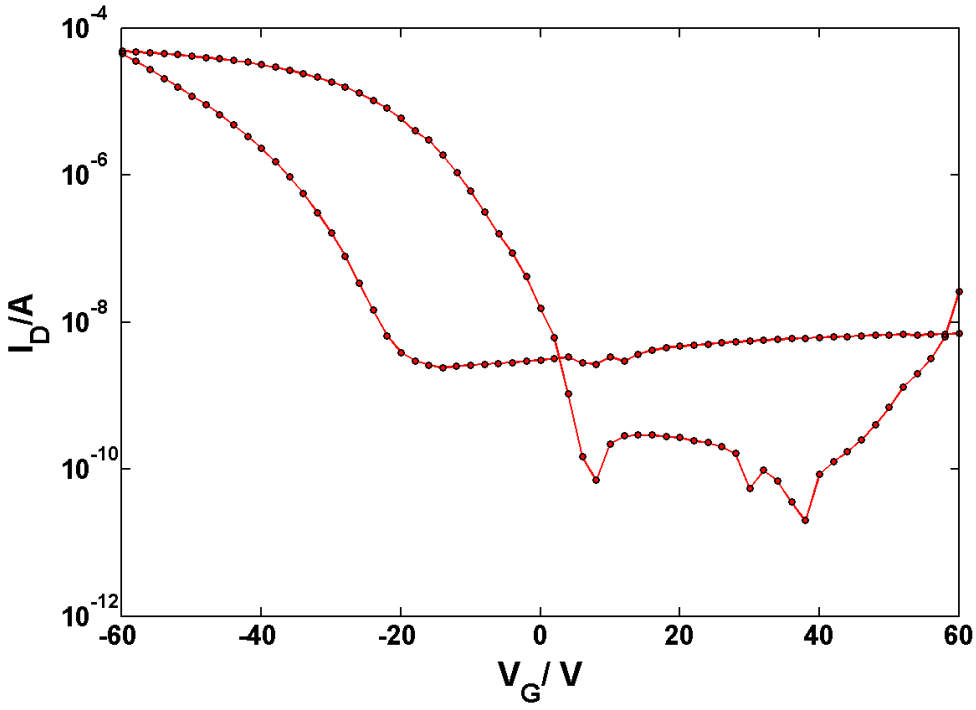

Figure 3.19: Transfer characteristic of a pentacene based OTFT with a PVBT interfacial layer after an illumination with UV-light(254 nm) for 10 minutes and a post-modification with the vapour phase of THF and ethylenediamine in the glovebox for 60 minutes. V_D = -20V

- Sample6: Si/SiO_2/PVBT/illuminated/reaction with THF and ethylenediamine in glovebox for 60 minutes + kept under HCl gas for 20 seconds

The interfacial layer of the sixth sample was illuminated with UV-light with 254 nm for ten minutes, post-modified by a reaction with the vapour phase of THF and ethylenediamine in the glovebox for 60 minutes and in the end the sample was kept under HCl gas for 60 seconds (Fig. 3.14).

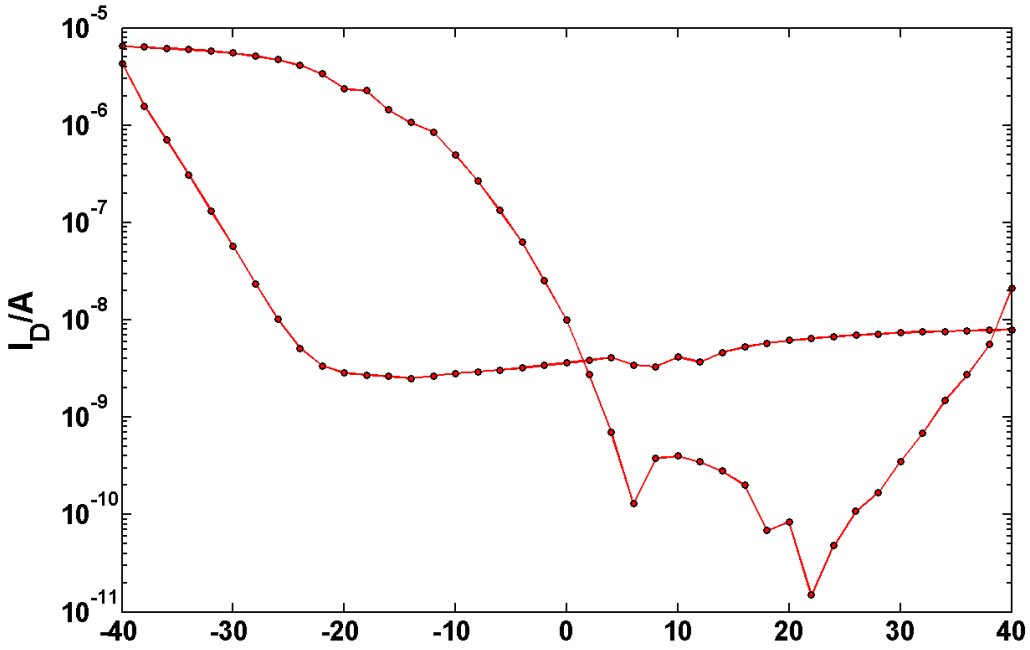

Figure 3.20: Transfer characteristic of a pentacene based OTFT with a PVBT interfacial layer after an illumination with UV-light(254 nm) for 10 minutes and a post-modification with the vapour phase of THF and ethylenediamine in the glovebox for 60 minutes. Additionally this device was kept under HCl gas for 60 seconds. V_D = -20V

Here all of the four transistors showed transistor behaviour, but the hysteresis of the devices in the transfer characteristic was enormous. The mobility was 0.001 $\frac{cm^2}{Vs}$ and the threshold voltage shifted to more positive values to +7 V. The leakage current was $5 \cdot 10^{-8}$ A.

After the analysis of the transfer characteristics of the differently post-modified devices AFM images of the three devices with the best OTFT behaviour were taken. These are the OTFTs with a not illuminated PVBT layer, an illuminated PVBT layer and the OTFT with an illuminated PVBT layer that was post-modified by a reaction with the vapour phase of THF and triflouroethylamine for 60 minutes(Fig. 3.21).

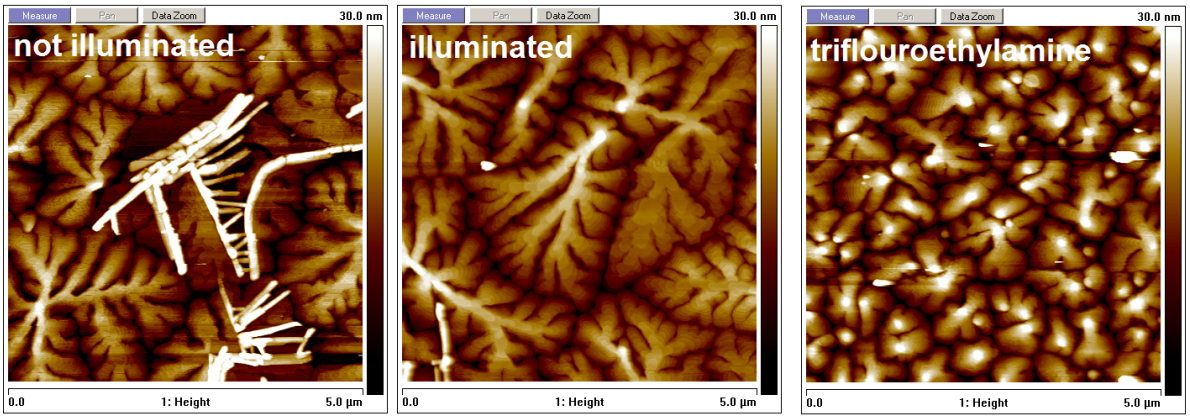

Figure 3.21: AFM images(5x5 μm) of a pentacene layer on: a not illuminated PVBT layer(left), an illuminated(UV-light with 254 nm for ten minutes) PVBT layer(middle) and on an illuminated(UV-light with 254 nm for ten minutes) PVBT layer that was post-modified by a reaction with the vapour phase of THF and triflouroethylamine for 60 minutes(right) (measurements were performed by DI. Alexander Fian)

The AFM-images showed the already known trend: the bigger the grain size the bigger the mobility. But beside that, the illumination or the post modification did not improve the device performance or the morphology of the pentacene layer.

3.3.4 Conclusion

In Tab. 3.2 the results of the device sub-chapter are compared with each other. In detail the contact angles of H_2O and CH_2I_2, the mobility μ, the threshold voltage V_{th} and the hysteresis of the differently post modified devices are listed up in this table.

Table 3.2: Results of the investigations of the OTFTs with a PVBT interfacial layer. Here, the the contact angles of H_2O and CH_2I_2, the mobility μ, the threshold voltage V_{th} and the hysteresis(measured at the drain current I_D = 10^{-6}) of the differently post modified devices are listed up. The X in the table symbolise that that CA-measurement was not performed for that liquid

Sample	$CA - H_2O$ / °	$CA - CH_2I_2$ / °	μ / $\frac{cm^2}{Vs}$	V_{th} / V	hysteresis / V
Sample 1	83 ± 2	30 ± 3	0.25 ± 0.02	-5	1
Sample 2	87 ± 2	36 ± 3	0.27 ± 0.02	-6	3
Sample 3	100 ± 2	X	0.2 ± 0.03	-5	4
Sample 4	82 ± 2	35 ± 3	0.15 ± 0.05	-3	2
Sample 5	82 ± 2	X	0.02 ± 0.008	-8	25
Sample 6	62 ± 2	X	0.001 ± 0.0005	+7	24

Unfortunately, despite the promising results of the preliminary experiments (contact angle measurements, infra red spectroscopy) no improvement of the device parameters of the OTFTs was observed. As can be seen in Fig. 3.21 and Tab. 3.2 neither large nor small changes of the contact angle or the surface energy improved the grain growth of the evaporated active layer material(pentacene) or the device performance. In the case of the post modification with ethylenediamine, the reaction even led to a strong deterioration of the device performance. Additionally, the post-modification of sample 6 resulted to a shift of the threshold voltage to more positive values. But this is just a fit value and because of the enormous hysteresis of more than 20 volts this value should not be taken to serious.

3.4 Photo reactive Spiropyran interfacial layer in pentacene based organic thin-film transistors

In OTFTs photo-reactive interfacial layers are a interesting possibility to imrove the electronic properties of the active layer. The goal of this study was to elucidate, whether a photochromic layer consisting of the spiropyran containing polymer poly(bis(7-(3‘,3‘-dimethyl-6-nitrospiro [chromene-2,2‘-indolin]-1‘-yl)heptyl)bicyclo[2.2.1]hept-5-ene-2,3-dicarboxylate) on top of the gate oxide, allows to photochemically and reversibly modify the electronic properties of the active layer and thus control the device characteristics.

3.4.1 Motivation

For the monomer-synthesis spiropyran-alcohol was treated with trans-5-Norbornene-2,3-dicarbonyl chloride. The polymer was synthesized by ring-opening metathesis-polymerization(ROMP) (synthesis was performed by DI. Lucas Hauser) [53].

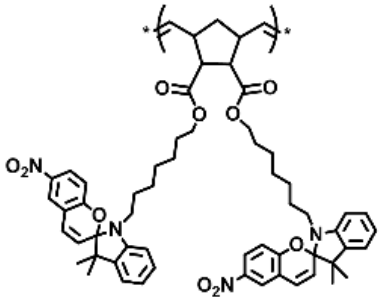

Figure 3.22: Molecular structure of a spiropyran containing polymer (taken from [53])

The photochromic behaviour of this polymer can be associated by the switching between two isomeric forms of the spiropyran ring system. Upon irradiation of the polymer with UV-light at wavelengths shorter than 365 nm(Lamp: EXFO Novacure, 10000 mW, distance: 10 cm, illumination under Argon as well as under air, irradiation time: 1 minute), the stable closed ring isomeric form (SP-1, colourless or pale yellow) of the spiropyran changed to a metastable open ring merocyanine (MC, violet) form [54], [55], as shown in the inset of Fig. 3.23. The originally colourless form (SP-1) was restored either via visible light irradiation(simple tungsten 50 W lamp, distance: 10 cm, irradiation time: 10 minutes) with wavelengths higher than 500 nm or thermally. The photochromic process was verified by UV/VIS spectroscopy, as can be seen in Fig. 3.23. Before starting a UV-vis measurement, the absorption of the CaF_2 plate was measured to get the sample-background.

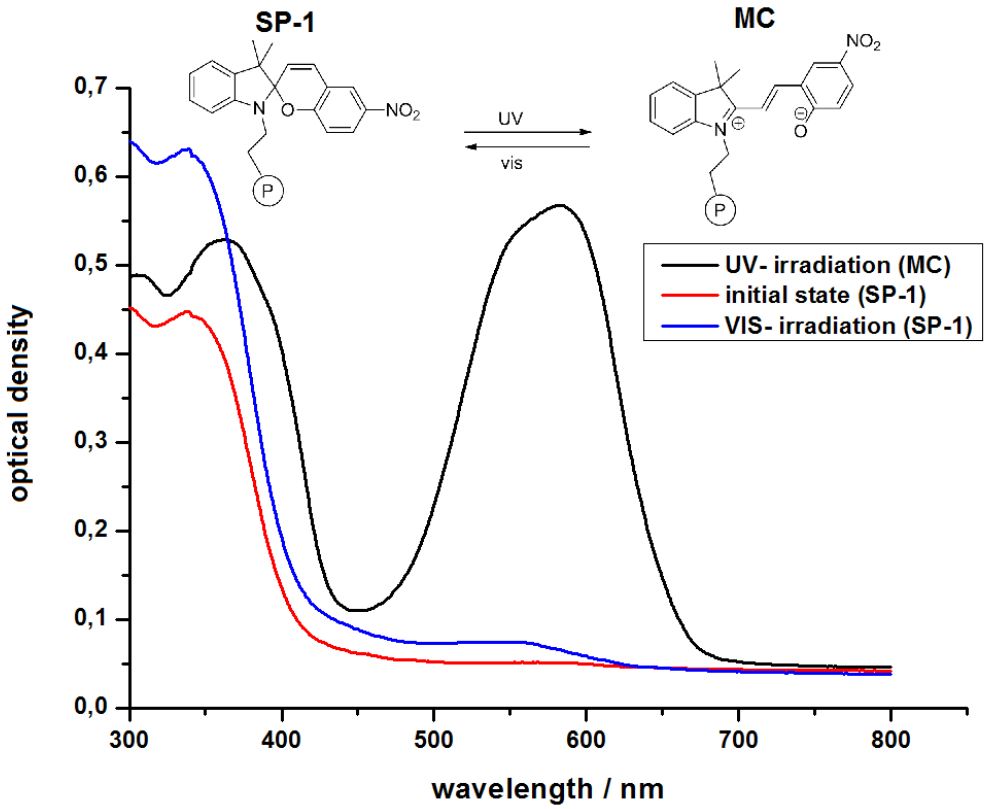

Figure 3.23: UV/VIS-spectra of spiropyran after UV- and VIS-light irradiation. Inset: chemical structure of the spiropyran before and after irradiation (measurement was performed by DI. Lucas Hauser)

The black curve is the absorption spectrum of the closed spiropyran, which has its maximum at around 360 nm. After the illumination with UV-light the zwitterionic merocyanine state of the spiropyran appeared with a new absorption-maximum at 570 nm. After illumination with visible light at wavelengths longer than 500 nm, the ring closed again and the former maximum at 360 nm appeared again. The reversible process was also investigated by IR-spectroscopy, as can be seen in Fig. 3.24.

In the IR-spectra, three main differences were observed, at 1276 cm^{-1}, the sharp peak got broader after illumination. This is attributed to the formation of the new C=N+ bond in the merocyanine form. The second difference was a new peak at 1422 cm^{-1}. It is associated with the formation of the C-O bond in the merocyanine. Finally, a peak at 1595 cm^{-1} due to the C=C double bond in the middle of the molecule appears. All changes are reversed upon illumination with visible light.

Additionally, contact angle measurements were performed to investigate the impact of the photo-isomerisation on the surface energy. The results that are presented in Fig. 3.25 were obtained for very thick spincoated polymer layers on a glass sub-

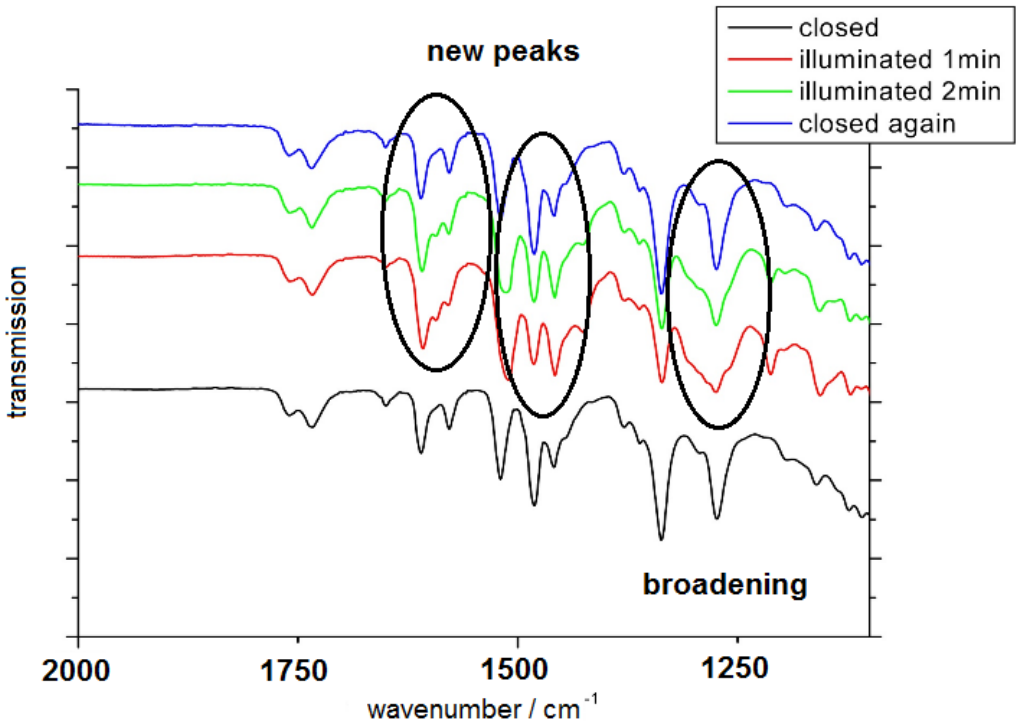

Figure 3.24: IR-spectra of spiropyran after UV- and VIS-light irradiation (measurement was performed by DI. Lucas Hauser)

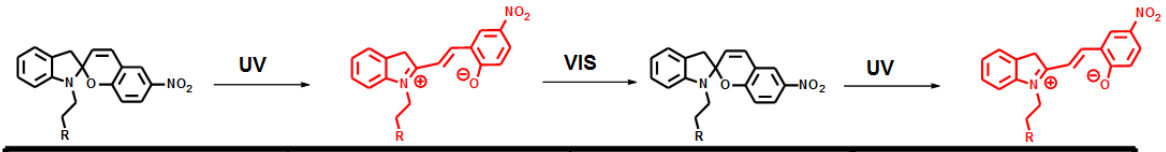

untreated	365 nm	572 nm	365 nm
106 ± 1	91 ± 1	105 ± 1	93 ± 1

Figure 3.25: Contact angle measurement of the spiropyran polymer in the untreated state and after UV- and VIS-light illumination(measurement was performed by DI. Lucas Hauser)

strate. Contact angle measurements with water on a Si/SiO_2 substrate and a normally thick polymer layer (4mg/ml in Chloroform spincoated with 2000 rpm for 20 seconds) showed the same trend. The contact angle of water on this substrate in the not illuminated state was (90 $\pm$ 2) $^\circ$ and (73 $\pm$ 4) $^\circ$ in the UV-light illuminated state. Due to the higher polarity of the zwitterionic merocyanine, the contact angle of water decreased.

Spiropyranes have already been used for several applications, for example, to

work as a photo switchable DNA- binder in chemical biology [56], and as photo sensitive switches for information recording using the electrical signal as a non-destructive detection method of the mode of the device [57]. Due to the photochromic behaviour of the spiropyran polymer, it is a very promising material for organic thin film transistor applications. Therefore we tested whether a reversible change of device parameters could be achieved by illumination of a spiropyran-based interfacial layer with ultraviolet and visible light.

3.4.2 Results

To fabricate OTFTs, after the typical pretreatment(plasma etching, ultrasonic bath), the photo-reactive polymer was spincoated(2000 rpm for 20 seconds) onto a SiO_2 gate dielectric under inert conditions. After that, pentacene was evaporated and gold top source and drain contacts were deposited through a shadow mask. The structure of a pentacene based organic thin-film transistor with an interfacial spiropyran layer and the chemical structures of the organic layers are shown in Fig. 3.26.

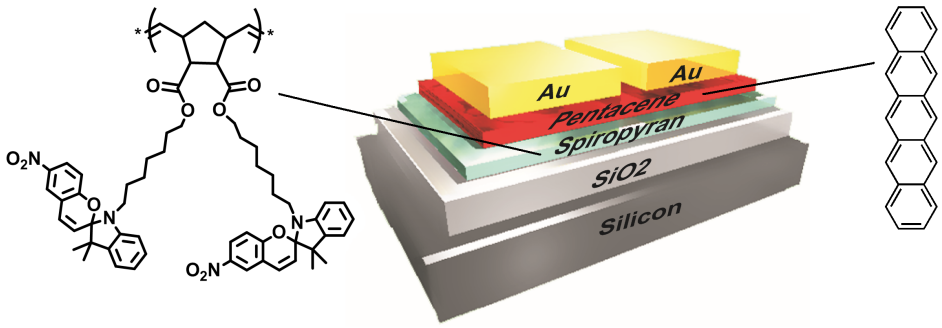

Figure 3.26: Structure of a pentacene based organic thin film transistor with a spiropyran interfacial layer. The chemical structures of the organic layers are also shown (taken from [49])

A typical transfer characteristic of a pentacene based thin film transistor with a spiropyran interfacial layer is shown in Fig. 3.27. Here, the linear(left) and logarithmic(right) plot of the transfer characteristic for V_D= -45 V and a gate voltage measurement range from +60 to -60 volts are shown.

In comparison to an OTFT without the interfacial spiropyran layer, the device has a much larger hysteresis and a two orders of magnitude lower mobility. Therefore AFM-measurements on the OTFTs with and without that spiropyran interfacial layer were performed (Fig. 3.28). Compared to the reference pentacene OTFT, the samples with the interfacial layer showed a much smaller grain size and a smaller degree of order. Interestingly, images b, c and d in Fig. 3.28 should look exactly the same.

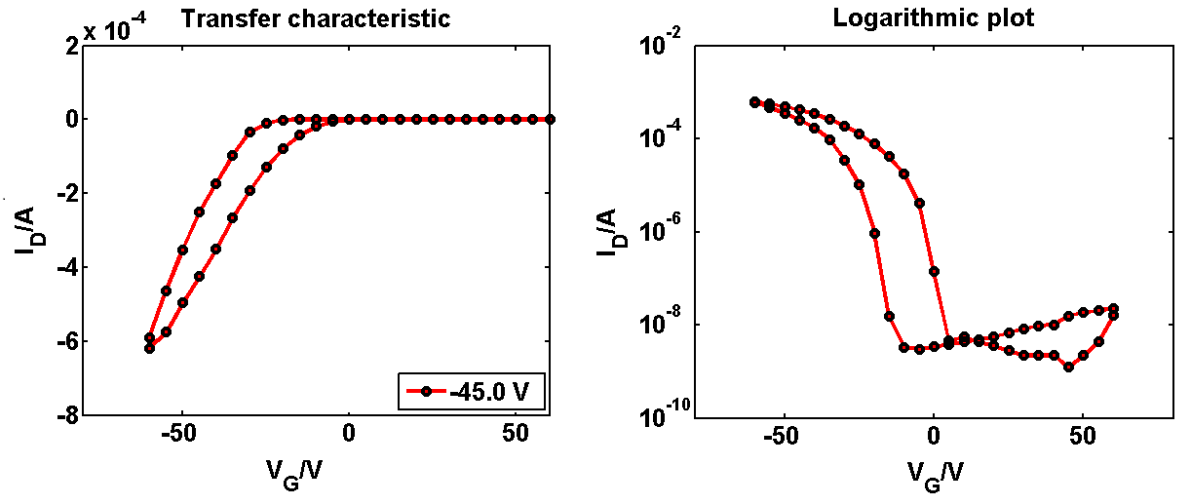

Figure 3.27: Linear and logarithmic transfer characteristic of a pentacene based thin film transistor with a photo reactive spiropyran interfacial layer

But obviously the structure of the pentacene layer on top of the spiropyran layer is strongly differing between the three samples.

Then the impact of the interfacial layer on the carrier mobility and the threshold voltage was investigated for the open-ring merocyanine and the closed ring isomeric form by alternating illumination with UV and visible light for several minutes which can be seen in Fig. 3.29.

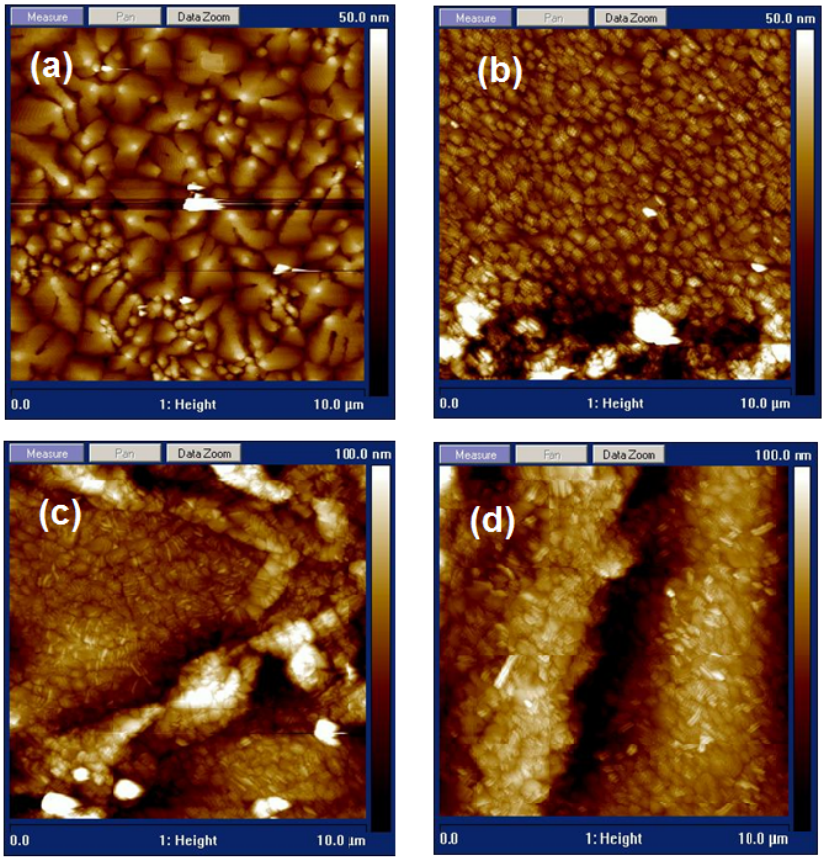

Figure 3.28: Atomic force microscope pictures of pentacene based thin film transistor with(b,c,d) and without a photo reactive spiropyran interfacial layer (measurements were performed by DI. Alexander Fian)

These experiments indicated a shift of the threshold voltage to more negative values upon UV illumination, but additionally larger hysteresis occurred and so it was difficult to get an accurate value for the threshold or onset voltage. After several measurements it was noticed that the shift of the threshold voltage to more negative values, was dominated the bias stress effects.

Increasing the measurement range in the transfer characteristic to more negative gate voltages, shifted the threshold voltage significantly into the negative region(Fig. 3.30). Interestingly, no shift to more positive values was recognized when the measurement range was increased into the positive region.

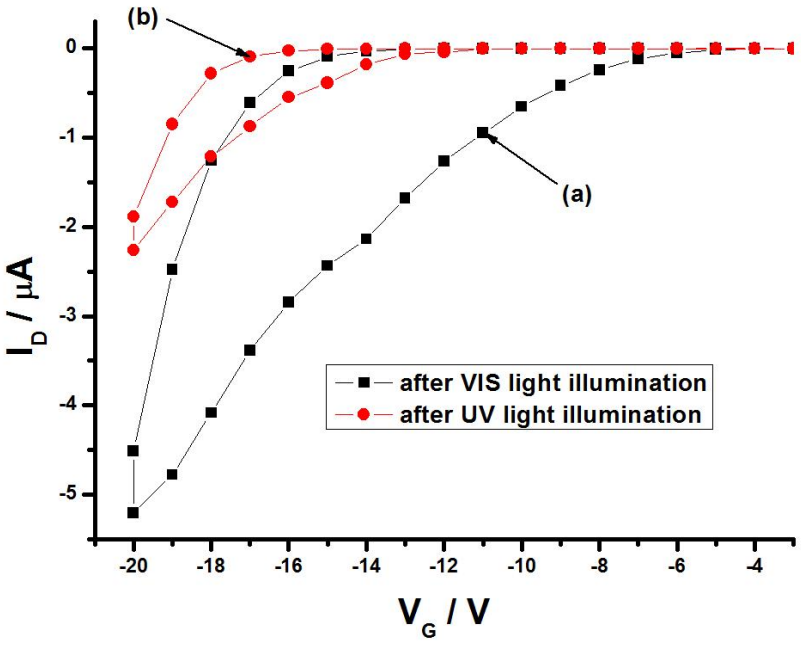

Figure 3.29: Transfer characteristics of a pentacene based thin film transistor with a photo reactive spiropyran interfacial layer after UV-(left)and visible light(right) illumination with V_{DS} = -20V

As can be seen in Fig. 3.30 a very large hysteresis occurred for the curve in the bigger measurement range. This hysteresis decreased significantly after some measurements. But the turn-on and threshold voltage remained in the negative region for several minutes. So the system was strongly time dependent and in half an hour the OTFT shifted back to the initial state.

Similarly, in measurements with a larger number of measuring points, a much bigger hysteresis was found. These results showed clearly that the spiropyran interfacial layer induced large bias stress effects. Therefore, bias stress and long term measurements were performed and analyzed in detail in the following.

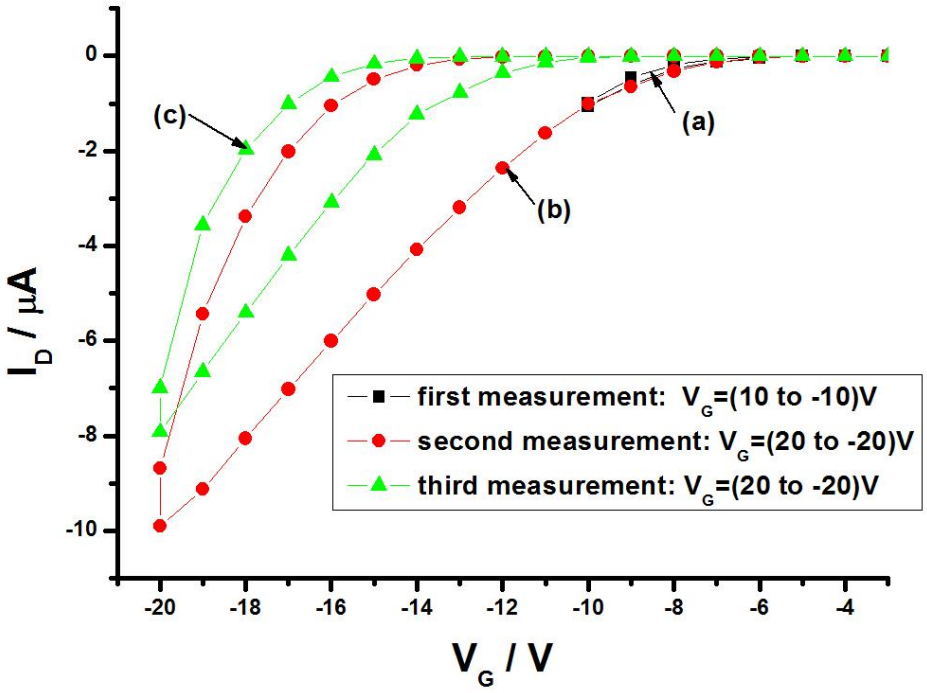

Figure 3.30: Transfer curves of a pentacene based OTFT with a spiropyran interfacial layer in the SP-1 state for V_{DS} = -20V. The first curve (a) was measured in the range of V_G = (10 to -10)V. For the second measurement (b) the range was increased to V_G=(20 to -20)V. Here a big hysteresis occurs. The last measurement (c) was done in the same gate voltage range like (b), but here the hysteresis was smaller and the threshold voltage shifted to more negative values.

What can be seen in Fig. 3.31 and 3.32 are long time measurements of the drain current I_D over time, for a fixed set of parameters(V_D=-20V, V_G=-20V) for a pentacene TFT with and without a spiropyran interfacial layer. The OTFTs with spiropyran interfacial layer were always measured in the initial SP-1 state.

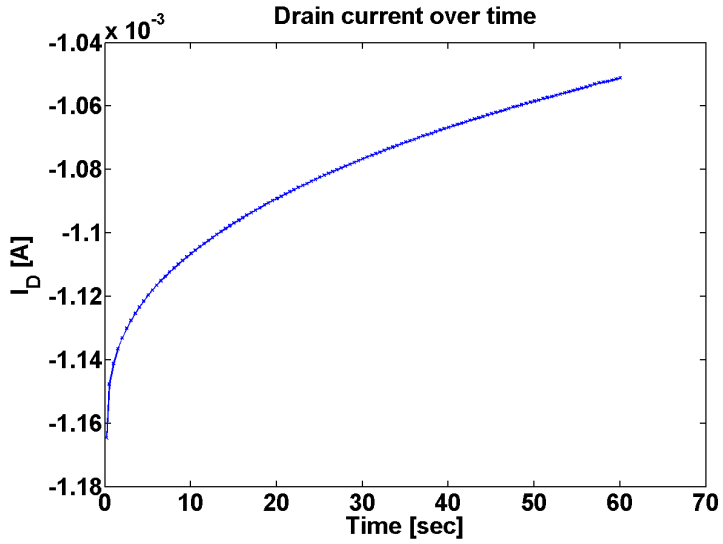

Figure 3.31: Long time measurements of the drain current I_D over time, for a fixed set of parameters(V_D=-20V, V_G=-20V), for a pentacene TFT without a spiropyran interfacial layer

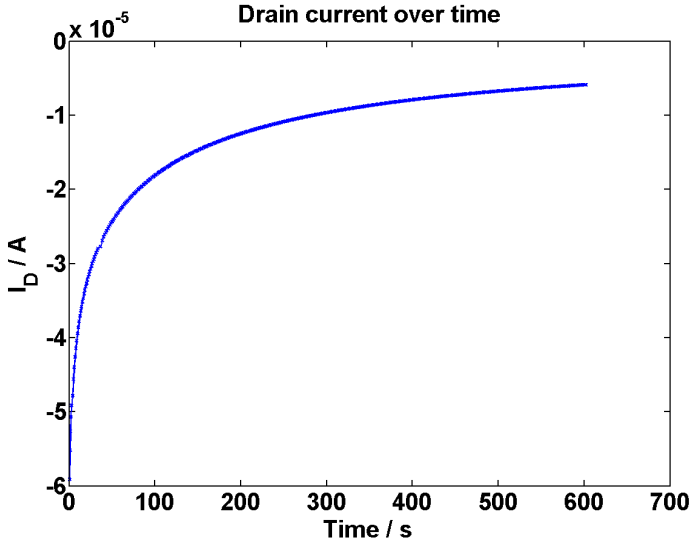

Figure 3.32: Long time measurements of the drain current I_D over time, for a fixed set of parameters(V_D=-20V, V_G=-20V), for a pentacene TFT with a spiropyran interfacial layer

It was found that the drain current I_D in a pentacene based TFT with a spiropyran interfacial layer decreases much faster than in a regular pentacene TFT. This is because of the strong bias stress sensitivity due to the spiropyran layer. At the interface a lot of charge carriers get trapped and the current decreases because of the loss of mobile charge carriers.

To further investigate the transistor behaviour of pentacene based OTFTs with a spiropyran interfacial layer long time measurements of the transfer characteristics are used in the following. In these measurements several transfer characteristics are measured successively.

Fig. 3.33 and 3.34 show long time measurements of transfer characteristics for a fixed drain voltage V_D=-20V, for pentacene TFTs with and without spiropyran interfacial layer. The measurements were carried out directly one after another for 600 seconds.

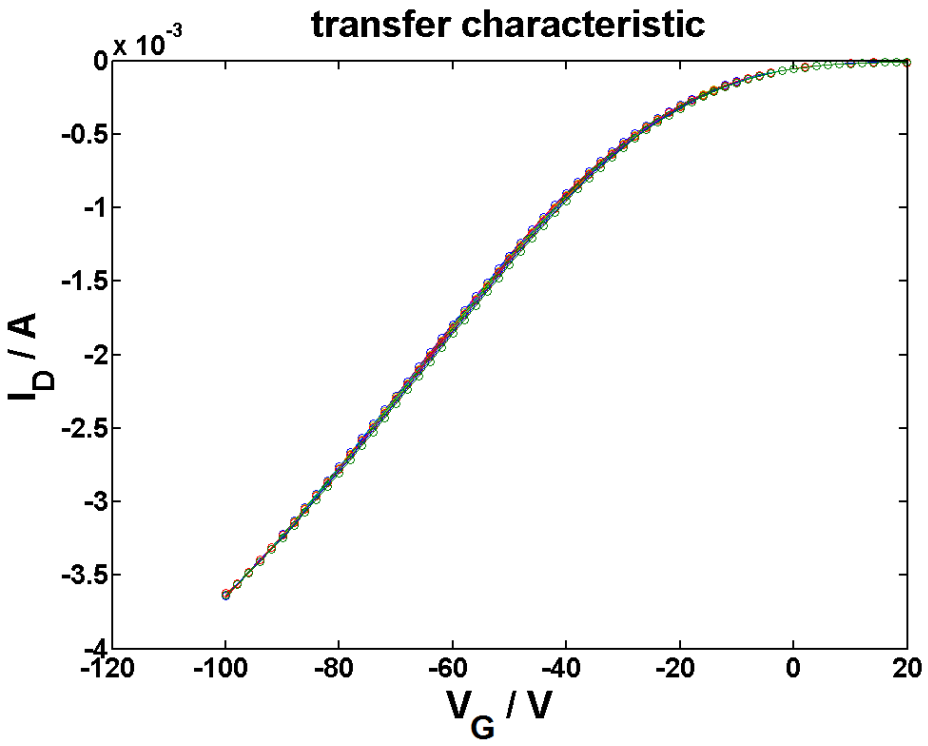

Figure 3.33: Long time measurements of transfer characteristics over time, for a fixed drain voltage(V_D=-20V), for a pentacene TFT in the measurement range from +20 to -100 volts

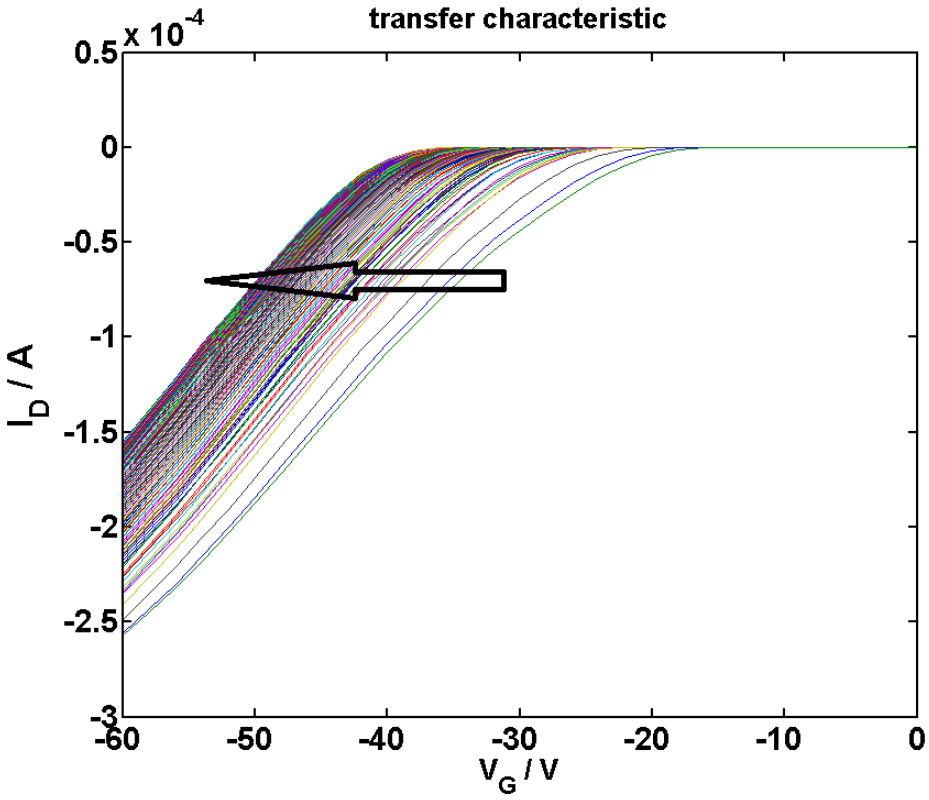

Figure 3.34: Long time measurements of the tranfer characteristics over time, for a fixed set of parameters(V_D=-20V, V_G=-20V), for a pentacene TFT with a spiropyran interfacial layer

Obviously, the threshold voltage, respectively, the onset voltage in pentacene based OTFTs with a spiropyran interfacial layer was shifted to more negative values through several successive measurements (Fig. 3.35,3.36). In contrast to that, the shift of the threshold voltage in regular pentacene based TFTs was very small. There was a small increase of the mobility and a small shift to more negative values of the threshold voltage. OTFTs with spiropyran interfacial layer showed a clear shift of the threshold voltage into the more negative region of about 15 volts. The mobility approximately remained the same after a small increase in the beginning of the measurement.

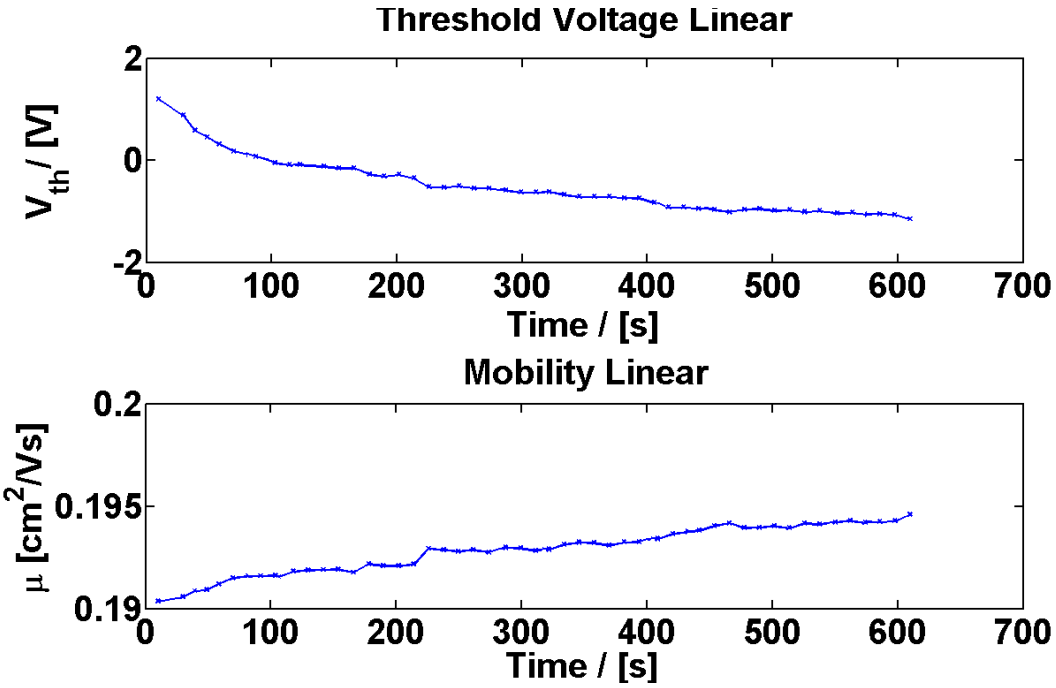

Figure 3.35: Evolution of the mobility and the threshold voltage of regular pentacene based OTFTs without a spiropyran interfacial layer

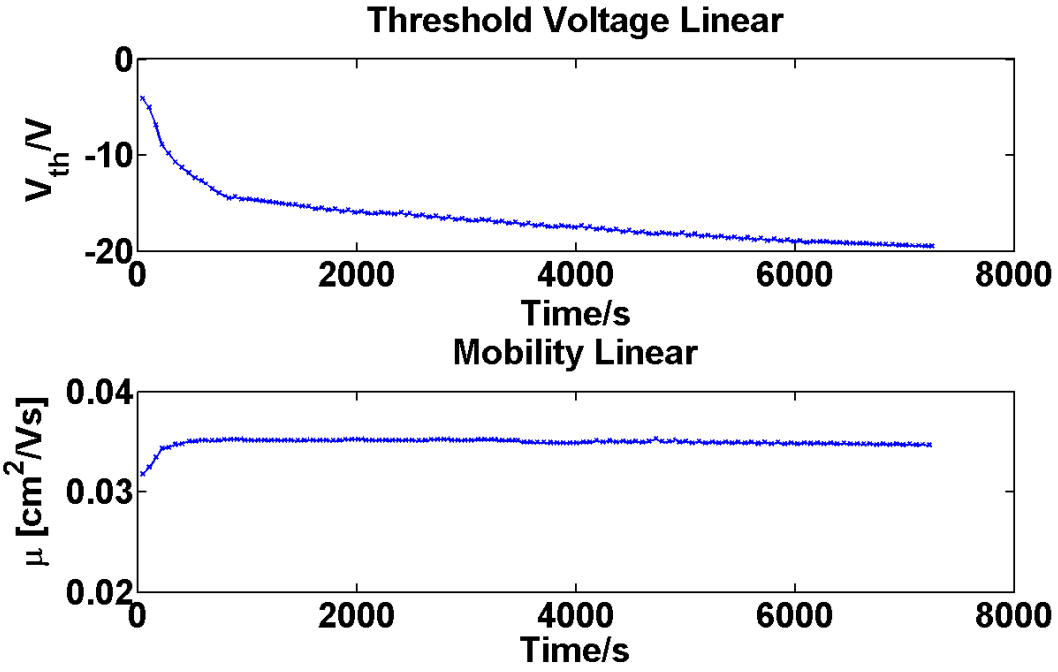

Figure 3.36: Evolution of the mobility and the threshold voltage of pentacene based OTFTs with a spiropyran interfacial layer

To investigate the behaviour of pentacene based OTFTs with a spiropyran interfacial layer on the irradiation with visible or ultra violet light long time measurements in the measurement cell were performed. Here it was possible to illuminate the samples with ultraviolet and visible light during a measurement.

So it was possible to investigate the behaviour of the drain current during the illumination of the OTFT. The following figures show long time measurements of the drain current over the time. During the measurements the sample was illuminated with ultraviolet(low pressure Hg lamp, Hereaus Noblelight) or visible light(simple light bulb 60 W in 10 cm distance). The curve was taken for a fixed set of parameters(V_D = -20V, V_G = -20V), for a pentacene based OTFT with and without a spiropyran interfacial layer(Fig. 3.37 and 3.38). The ranges marked with UV or VIS in the figures mark the periods in which the OTFT was irradiated with ultra violet or visible light.

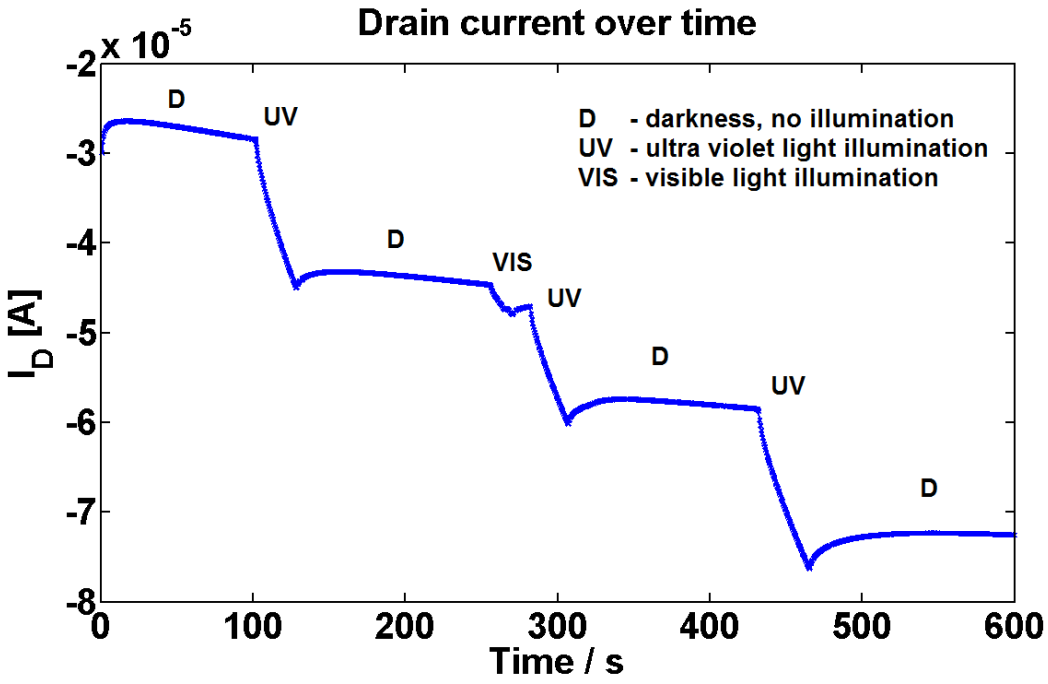

Figure 3.37: Long time measurements of the drain current over the time during the illumination with UV / VIS light, for a fixed set of parameters(V_D=-20V, V_G=-20V), for a regular pentacene TFT

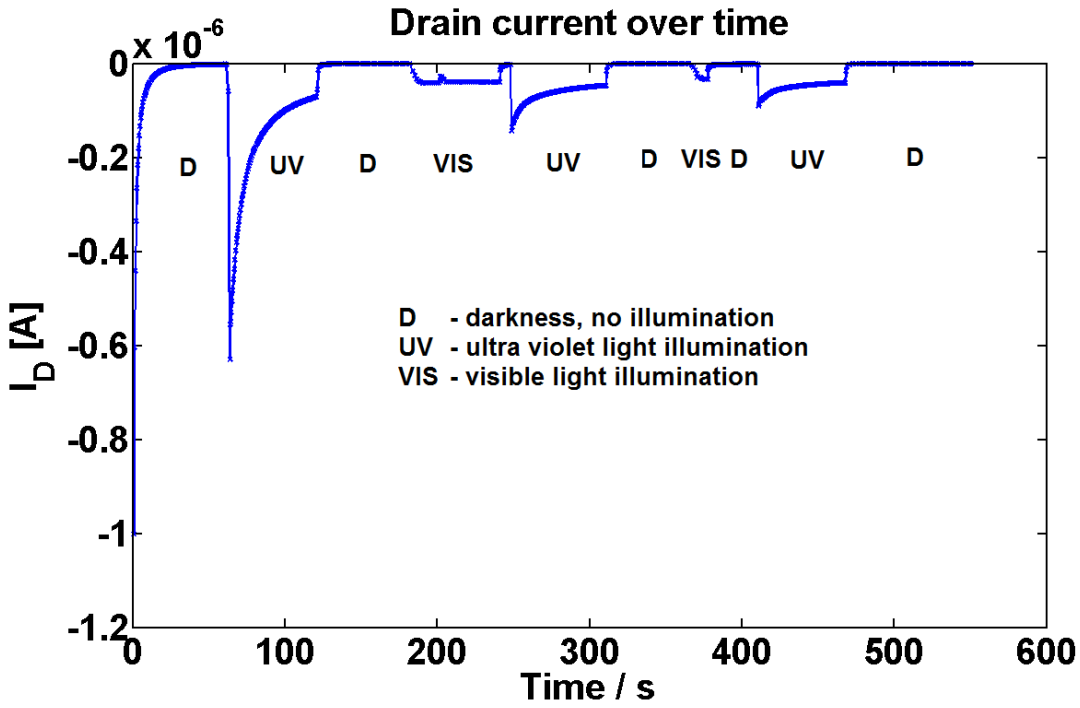

Figure 3.38: Long time measurements of the drain current over time during the illumination with UV / VIS light, for a fixed set of parameters(V_D=-20V, V_G=-20V), for a pentacene TFT with a spiropyran interfacial layer

Obviously the illumination of the OTFTs with ultraviolet or visible light has a strong effect on the transistor behaviour. The increase of the drain current through illumination can be explained by a shift of the threshold voltage. According to V. Podzorov and M. E. Gershenson [58], the magnitude of the shift of the onset voltage depends mainly on the applied gate voltage V_G. But also other parameters, such as the intensity and wavelength of light and the transverse electric field at the semiconductor-dielectric interface are important for that effect.

For regular pentacene based OTFTs without an interfacial layer, a strong increase of the drain current was detected during the illumination with visible and ultraviolet light. The stronger increase of the drain current was noticed when the devices were illuminated with ultraviolet light. During the dark periods where the sample was not illuminated, the drain current slightly decreased. Again this can be explained with a shift of the threshold voltage.

During the illumination of OTFTs with a spiropyran interfacial layer with visible and ultraviolet light a small increase of the drain current was detected. The drain current increased significantly when the devices were illuminated with ultraviolet light. But exactly after the illumination period where the sample was not illuminated the drain current decreased rapidly. This was expected anyway, because of the big bias

stress sensitivity of the interfacial layer. Another interesting form of this bias stress sensitivity is the form of the drain current curve during a illumination period with ultraviolet light. In the beginning of the illumination period the drain current increased rapidly but after the first seconds the drain current started decreasing again. But because of the very small drain current it is not sure whether this device showed transistor behaviour any more.

To find an explanation for the enormous bias-stress effect the redox process [54] of the spiropyran polymer was investigated. Therefore cyclovoltammogramms were measured to get some information about the electrochemical behaviour of the molecule. It was measured from -1.8 V to +0.8 V, with a scan rate of 800 mV/s and the supporting electrolyte $TBAPF_6$. As shown in Fig. 3.39, two main differences were seen between the closed spiropyran and the open merocyanine. In the range of 0.2 V the peak increased after illumination, which can be assigned to a single electron transfer in the nitrogen from the C-N-C bond to the C=N+ bond in the centre of the molecule. The second one was the increasing of the peak at -0.8 V. This one shows the easier reducibility of the nitro-group at the end of the molecule by the creation of the new OH-group.

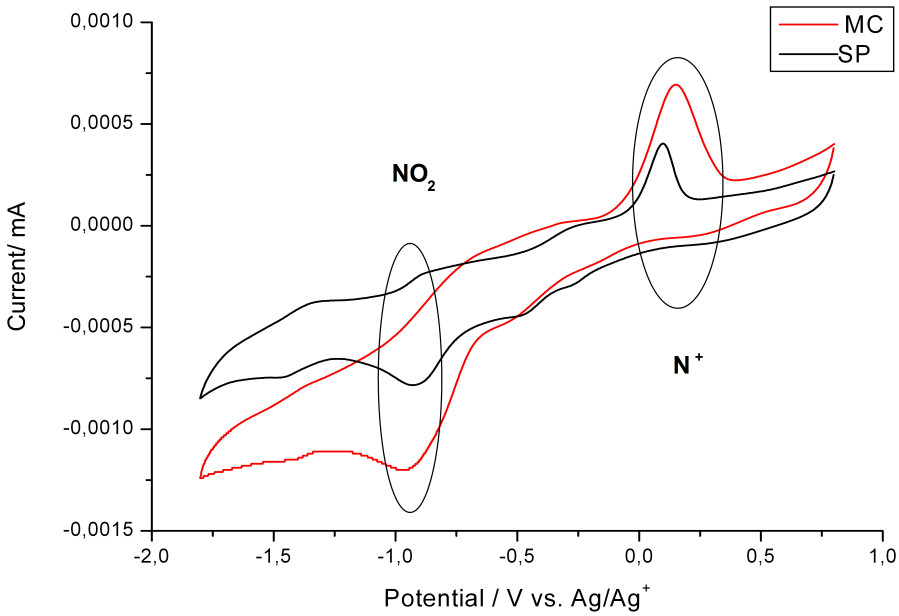

Figure 3.39: IV-curve of an electrochemically measurement to investigate the redox process between the two states of spiropyran polymer (measurement was performed by Laura Kaltenböck and Lucas Hauser from the Institute for Chemistry and Technology of Materials, University of Technology Graz)

The main information is that after the illumination the open MC-form is much more reactive, which means the polymer is easier to oxidize or to reduce(the NO_2 is easier to oxidize and N^+ is easier to reduce), depending on the voltage-range. This should have an effect on the transistor characteristics, but whether this effect occurs through hole-trapping is still under investigation.

3.4.3 Conclusion

The reversible tuning of electronic properties holds high promise for various applications. Unfortunately, the enormous bias stress effect we found in devices containing a spiropyran polymer shifts the threshold voltage to more negative values during every measurement. This makes this polymer interfacial layer impractical for regular OTFT application.

3.5 6,13-bis (triisopropylsilylethynyl) pentacene as semiconducting material in organic field effect transistors

3.5.1 Motivation

Pentacene has been identified as a promising material in organic thin film transistors and is therefore often used as reference material. It is normally deposited by vacuum evaporation onto the substrate. It arranges in a herringbone structure resulting in an overlap of the individual π-electron systems and thus an overall highly delocalized π-electron system. This gives rise to a very good charge transport parallel to the pentacene layers. Unfortunately, pentacene is not soluble and therefore it can not be deposited by spin coating, drop casting or dip coating.

To avoid the time consuming evaporation step, there is serious interest in a modification that makes pentacene available for solvent-based production methods. Unfortunately, functional groups usually disrupt the electrical properties of pentacene [59]. A basic approach is the so-called precursor concept. Here, soluble derivatives serve as precursors of pentacene. After the coating step the functional groups can be eliminated by a thermal treatment, resulting in pentacene and volatile reaction products. The second approach is to make the functional groups in a way that they do not affect the electrical properties of pentacene and, therefore, do not have to be removed. 6,13-bis (triisopropylsilylethynyl) pentacene (TIPS-PEN) is such a functionalized pentacene. Because of these functional groups it shows very good packing properties. In Fig. 3.40 the molecular structure of TIPS-PEN can be seen [59].

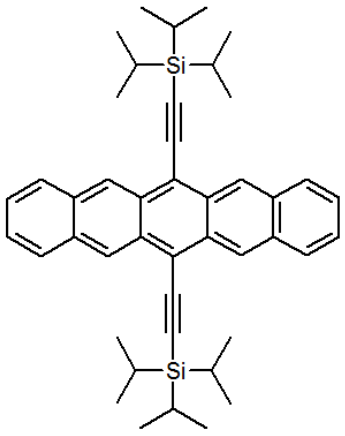

Figure 3.40: Molecular structure of 6,13-bis (triisopropylsilylethynyl) pentacene (TIPS-PEN)

It should be mentioned that since the first time TIPS-PEN was mentioned by John

E. Anthony in 2001 [60], and the first OTFT was produced in 2004 by C.D. Sheraw, several working groups have already dealt with that subject [61] [5]. With TIPS-PEN, it is now possible to produce transistors, with comparable device performances(mobility, turn on voltage, on/off ratio) as pentacene transistors [5]. This was a big step for the production of cheap organic devices and a promising method for the production of solution processed OTFTs in our group.

In literature papers about TIPS-PEN usually differ in the choice of the solvent and in the device structure of the OTFTs. In this work the solvents toluene and 3,4-dimethylanisol were used. In the cause of my investigations top and bottom contact transistors were produced. The active layer was deposited by spin-coating or drop-casting. Furthermore, TIPS-PEN was blended with poly (α-methylstyrene) and deposited on the substrate [62], [63]. To investigate the crystal structure of the deposited active layer XRD-measurements were performed.

The goal was to establish TIPS-PEN in our group as reliable alternative OSC material that can be used for interface modifications in the future.

3.5.2 Device pretreatment and manufacturing steps

In this subsection the steps of the pretreatment and device manufacturing process are explained in detail. It needs to be mentioned that only because of the great cooperation with DI. Sebastian Dunst and the working group from the Institute of Nanostructured Materials and Photonics, Joanneum Research, Weiz it was possible to achieve the following results.

- **Solvents**

During our investigations the solvents toluene and 3,4-dimethylanisole were used. TIPS-PEN is easily soluble in both. These two solvents have significantly different boiling points (toluene: 110 degree and 3,4-dimethylanisole: 200 degree). So 3,4-dimethylanisole takes much longer until it evaporates under ambient conditions. The idea was that due to the slower evaporation of solvents with higher boiling points, larger granularity and a higher degree of crystallinity in the semiconductor layers are achieved, what could probably lead to better electrical properties(mobility). In this work concentrations in the range of 10-30 mg/ml TIPS-PEN dissolved in toluene and 3,4-dimethylanisole were tried. But as can be seen in the sub chapter Best results, the best OTFT performances were achieved when TIPS-PEN was solved in 3,4-dimethylanisole with a concentration of 15 mg/ml.

- **Cleaning and Pretreatment**

The production of the first thin layers of TIPS-PEN as active layer material on the substrate showed that TIPS-PEN dissolved in toluene or 3,4-dimethylanisol has different film forming properties on differently pretreated Si/SiO_2 surfaces(Fig. 3.42). So beside the traditional pretreatment (plasma etching, ultrasonic bath) another pretreatment option was implemented during the experiments with TIPS-PEN. The silicon wafer was coated with First Contact ® before the active layer was deposited on it. First Contact ® is an acrylic polymer solution that can be coated onto various surfaces. It dries under ambient conditions and after about 15 minutes the dried film can be removed with some tweezers(Fig. 3.41).

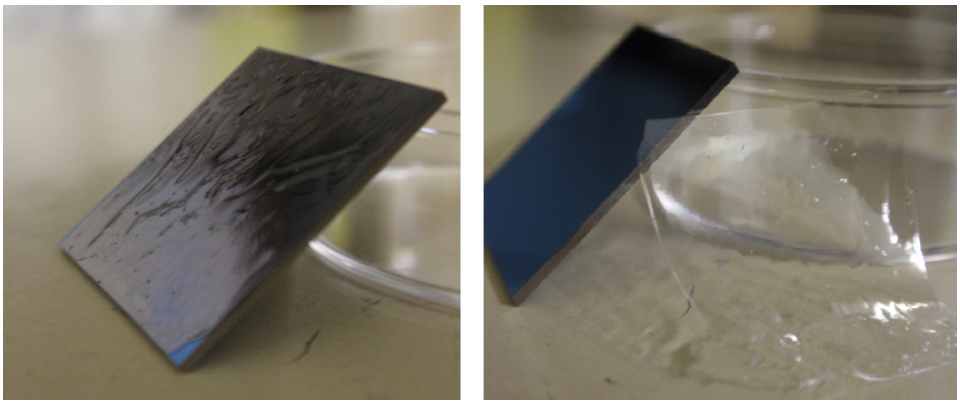

Figure 3.41: Left: First Contact ® coated on a Si/SiO_2 substrate. It dries under ambient conditions for at least 15 minutes. Right: the cleaned Si/SiO_2 substrate and the with some metal tweezers removed dried First Contact ® film (taken from Reinhold Hetzel)

Surface adhering particles and dirt can be efficiently removed by this pretreatment. After some time we found out that the pretreatment works even better when First Contact ® was removed after two or more days. Because then then it was easier to remove the dried solution from the surface and the surface seemed optically cleaner.

- **Deposition of the active layer material**

The active layer of the TIPS-pentacene OTFTs produced during this thesis was deposited by spin coating or drop casting. The best transistor characteristics of the TIPS-PEN OTFTs produced in this work are presented in the sub chapter Best Results. In the following the parameters of the spin coating and drop casting process are presented in detail.

Spin coating is one of the most common methods to form a thin film on a substrate. During this work all the spin coating processes were performed under ambient conditions and lab light in a flow box. Like already mentioned in the Cleaning and Pretreatment subsection before, it is really important to use the right pretreatment to achieve a good thin film by spin coating. According to [64] the parameters of the spin coating process were changed from 30 seconds with 2000 rpm to 9 seconds with 500 rpm plus 20 seconds with 2000 rpm. With that set of parameters a more homogeneous layers was formed on the Si/SiO_2 substrate. Another important aspect is the concentration of the TIPS-PEN solution. As already mentioned for this process the best devices were produced with concentrations of 15 mg/ml TIPS-PEN dissolved in 3,4-dimethylanisol.

As can be seen in Fig. 3.42 the pre-treatment with First Contact ® improves the film forming behaviour of the active layer.

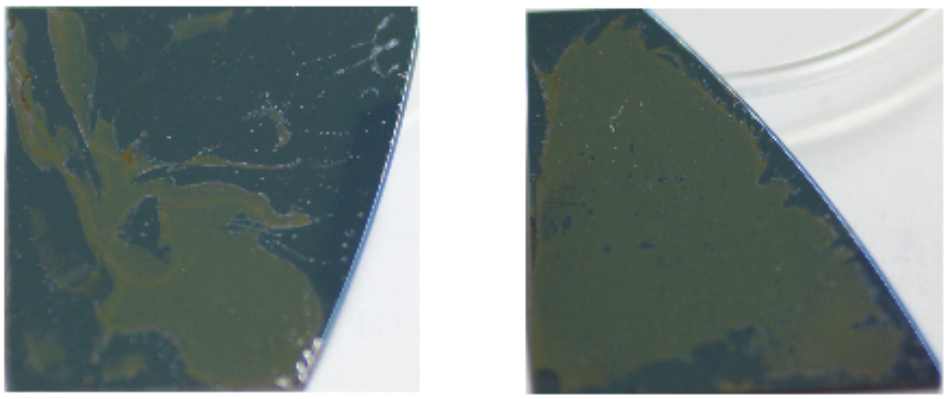

Figure 3.42: 10 mg/ml TIPS-PEN solved in 3,4-dimethylanisol spincoated on a (20x20)mm Si/SiO_2 substrate pretreated by plasma etching and ultrasonic bath(left) and pretreated with First Contact ® (right)

Additionally, it was noticed that TIPS-PEN dissolved in toluene shows a very good film forming behaviour, but after a closer investigation of the device it was seen that no homogeneous layer but a lot of small colloids formed on the substrate(Fig. 3.43). Thus for spincoated TIPS-PEN dissolved in toluene no transistor behaviour

was realized.

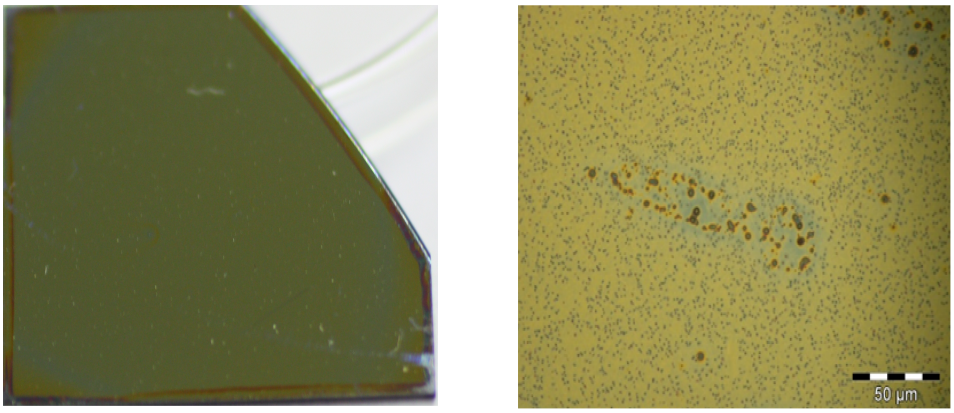

Figure 3.43: (20x20)mm Si/SiO_2 sample pretreated with First Contact ®, spincoated with 10 mg/ml TIPS-PEN solved in toluene. In the left image the whole sample is shown, the right figure is a microscope picture from inside the channel

Another possibility for depositing the active layer onto the dielectric is drop casting. In this process, the dissolved TIPS-PEN was dropped onto the sample. In Fig. 3.44 three images of drop cast samples with TIPS-PEN dissolved in 3,4-dimethylanisol are shown. It can be seen that very large crystals formed. The size of the crystals depended on the solvent and the drying time. For long drying times(24 hours) very big crystals were formed like can be seen in Fig. 3.44 to the left, but the layer was very inhomogeneous . For the drop cast devices in principle it can be said that the shorter the drying times the better results were achieved. Because of that the devices were tempered on a hot plate directly after the deposition of the active layer as can be seen in the sub chapter Tempering steps.

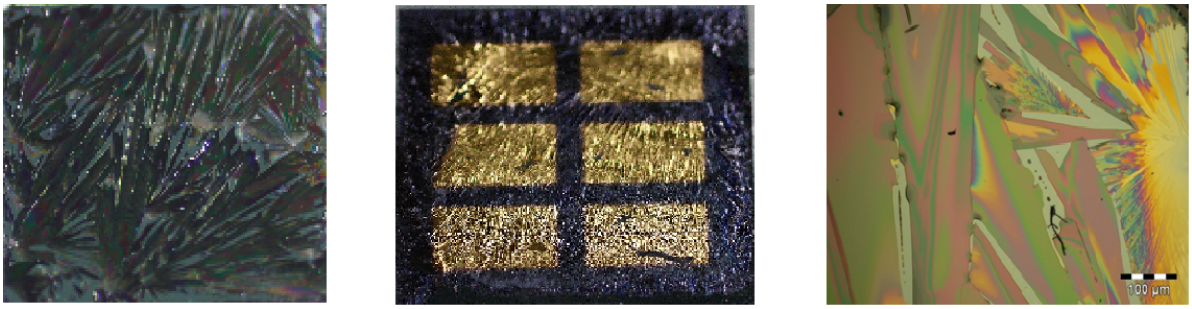

Figure 3.44: Left: Picture of a (20 x 20)mm Si/SiO_2 substrate drop cast from 15 mg/ml TIPS-PEN solution in 3,4-dimethylanisol(left). Middle: Picture of that drop cast device(left) with gold electrodes evaporated on top of the active layer. Right: Microscopic picture of the active layer in high resolution

As can be seen in Fig. 3.44 (left) the active layer shows a high roughness. Because of that, it was not was not possible to evaporate a homogeneous layers of gold onto the drop cast active layer surface. So it was not possible to produce top contact OTFTs with drop cast active layers.

After the deposition of the active layer material by spin coating or drop casting the sample was put in a petri dish under ambient conditions and it was waited for 24 hours until the solvent was evaporated. Another possibility was to temper the device directly after the depositioning process(this tempering process is presented in the subsection Tempering steps).

- **Tempering steps**

During this work the effect of three different tempering steps were investigated:

The first tempering step was after the pretreatment and before the deposition of the active layer. The devices were tempered on a hot plate (150 $^{\circ}C$) under ambient conditions for five minutes to reduce water on the sample surface. This tempering step showed no effect or difference in the device performance. Probably because the spin coating process was again under ambient conditions.

The second tempering step was directly after the deposition of the active layer. The samples were given on a hot plate(100 $^{\circ}C$) for two minutes to evaporate the solvent and to form a homogeneous active layer. This tempering step showed a big effect: a much higher percentage of the devices showed transistor behaviour(now three of four instead of one of four on a substrate), the mobility of the devices increased(from $5 \cdot 10^{-5}$ to $2 \cdot 10^{-4}$) and the hysteresis was reduced(from seven to two volts) as can be seen in Fig. 3.45.

The third tempering step was performed after the finished manufacturing of the TIPS-PEN OTFTs. Here the devices were given on a hot plate(80 $^{\circ}C$) for two hours under inert conditions, or on a (120 $^{\circ}C$) hot plate for one hour under ambient conditions. This tempering step showed no effective improvement of the device performance.

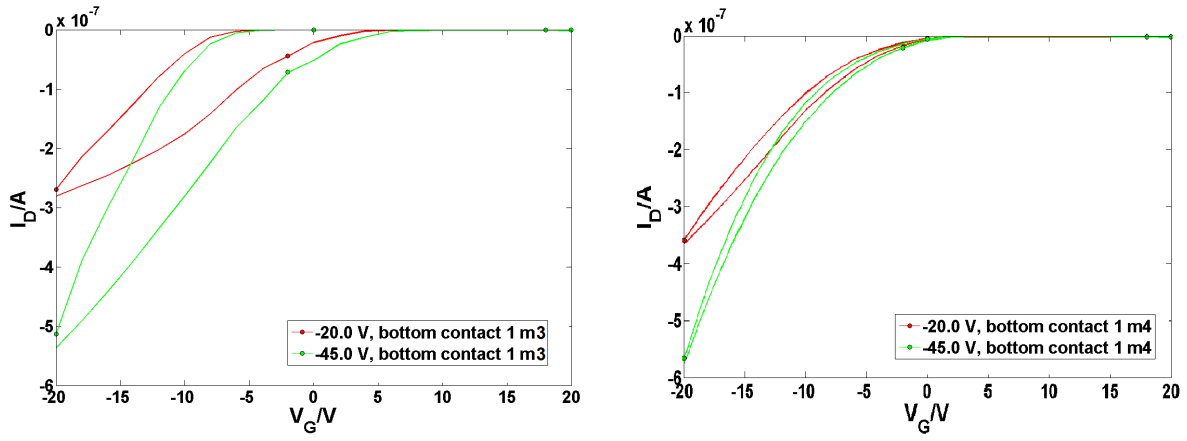

Figure 3.45: Transfer characteristics of a spin coated bottom contact OTFT with TIPS-PEN dissolved 3,4-dimethylanisol as active layer material, produced without(left) or with(right) a tempering step on a hot plate(100 $°C$) for two minutes after the deposition of the active layer

- **HMDS-layer**

As already mentioned before, the surface energy of the dielectric affects the crystallization of the organic semiconductor on top. So optionally, the substrates were treated with hexamethyldisilazane (HMDS) prior to the semiconductor deposition (Fig. 3.46).

Silicon dioxide has OH groups on the surface, which provide a hydrophilic character. This negatively affects on the wettability when using organic solvents. To make the surface hydrophobic, there is the possibility to functionalize the OH bonds. Here, silanes react with the OH groups and form self-assembled monolayers (SAMs) on the surface. In this way, a reduction of the surface energy is achieved. In this work hexamethyldisilazane (HMDS) was used. HMDS reacts with the hydroxyl groups on the silicon dioxide surface through elimination of ammonia. Here HMDS was spin coated with 4000 rpm for 20 seconds and then the sample was tempered at 150$°C$ for 15 minutes [65].

During this thesis no improvement of the wettability or the device parameters by treatment with HMDS was observed. Possibly this is because optimally HMDS is coated by a stream of nitrogen that leads the HMDS to a heated substrate(such a device is called a "Bubbler") [66].

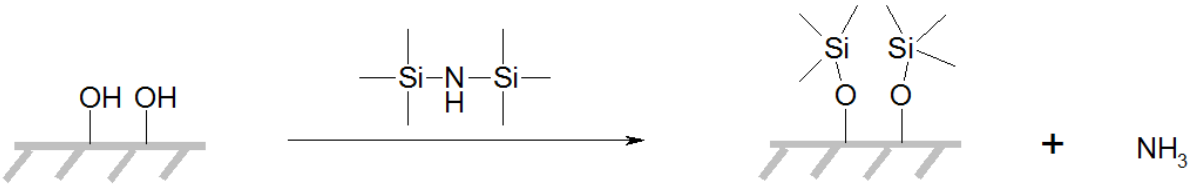

Figure 3.46: Chemical modification of silicon-dioxide surfaces by treatment with hexamethyldisilazane(HMDS) (taken from [59])

- **Poly(α-methylstyrene)(PαMS)**

According to the research results of another working group(Sebastian Dunst, Dr. Barbara Stadlober, Joanneum Research, Weiz), the mixture of TIPS-PEN dissolved in 3,4-dimethylanisole and poly(α-methylstyrene)(PαMS) improves the mobility and the coating properties of the OTFTs significantly [59]. The mixture consisted of 15 mg/ml TIPS-PEN dissolved in 3,4-dimethylanisole and the same amount of PαMS dissolved in 3,4-dimethylanisole. During the production of OTFTs with an active layer of TIPS-PEN mixed with PαMS very homogeneous layers were produced, as can be seen in Fig. 3.47. But unfortunately no improvement of the mobility nor transistor function was measured.

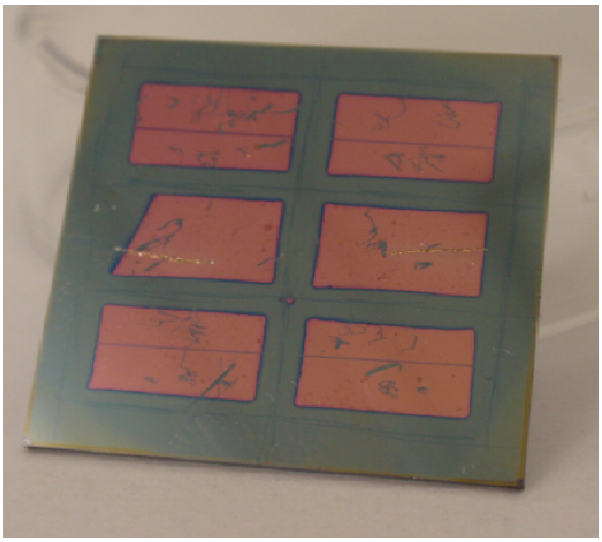

Figure 3.47: Image of a top contact spin coated OTFT with a mixture of TIPS-PEN dissolved in 3,4-dimethylanisole and poly(α-methylstyrene)(PαMS) as active layer material. Here the gold electrodes were already evaporated onto the substrate, and the pentacene layer was scratched away around the electrodes with metal tweezers.

- **evaporation of the gold electrodes**

Like already explained in the sub chapter Device fabrication and pretreatment: in the new evaporation chamber in five to ten seconds a 50 nm thick gold layer was evaporated onto the device surface.

3.5.3 Best results

In this subsection the best results of the TIPS-PEN OTFTs, produced by spin coating or drop casting, in a top or bottom contact device geometry, of this work are shown. These devices were pretreated, spin coated,drop cast and stored under ambient conditions and laboratory light. The electrical measurements were performed with a Keithley source meter and measurement needles in the argon glove box. The Si/SiO_2 substrates were pretreated with First Contact ®. The spin coating processes were performed with 9 seconds with 500 rpm plus 20 seconds with 2000 rpm in a flow box. After the deposition of the active layer the samples were tempered on a hot plate(100 $^{\circ}C$) for two minutes. If anything differs from this or further manufacturing steps were used, they are mentioned in the respective case.

- **Spin coated top contact OTFTs with TIPS-PEN as active layer material**

The first spin coating experiments were performed with TIPS-PEN dissolved in toluene and 3,4-dimethylanisol with a concentration of 10 mg/ml. These attempts were not successful, hence no transistor function was measured. After the optimization of the process(different spin coating parameters, tempering steps, higher concentrations) good results were achieved. In Fig. 3.48 the transfer characteristic of a spin coated top contact OTFT with 15 to 20 mg/ml TIPS-PEN dissolved in 3,4-dimethylanisol is shown .

There was almost no hysteresis in the transfer curve, the mobility was in the range of 10^{-4} $\frac{cm^2}{Vs}$ and the threshold voltage was -2 V. The leakage current was very low, approximately 10^{-9} A.

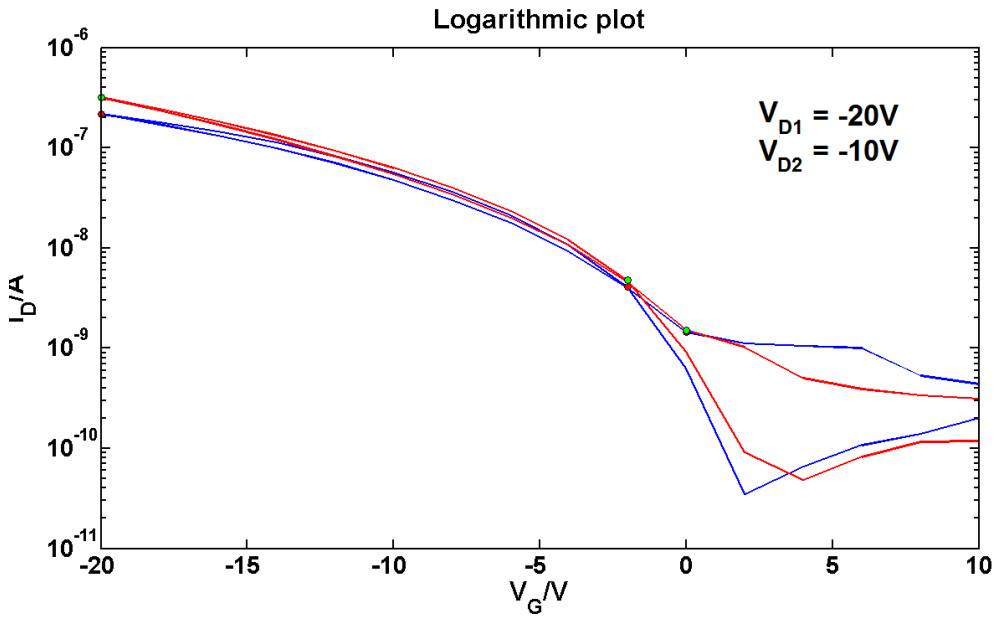

Figure 3.48: Transfer characteristic of a spin coated top contact OTFT with TIPS-PEN solved in 3,4-dimethylanisol as active layer material

- **Spin coated bottom contact OTFTs with TIPS-PEN as active layer material**

During this work, a lot of bottom contact OTFTs were produced, first the electrodes were evaporated, then the active layer was spin coated onto the substrate. The first devices that showed transistor behaviour were built with that type of setup. This is mainly because of the much better wettability of the dissolved TIPS-PEN on the gold pads than on the bare Si/SiO_2 surface (Fig. 3.49). Quite contrary to previous devices, the channel between the drain and source electrode was completely coated with the active layer material.

Even for the improved manufacturing process we see a big difference in the wettability of the dissolved TIPS-PEN on the gold pads and on the blank Si/SiO_2 surface as can be seen in Fig. 3.49. Here just for high concentrations the channel was completely filled with the organic semiconductor. For lower concentrations there was no OSC film on Si/SiO_2 respectively in the channel.

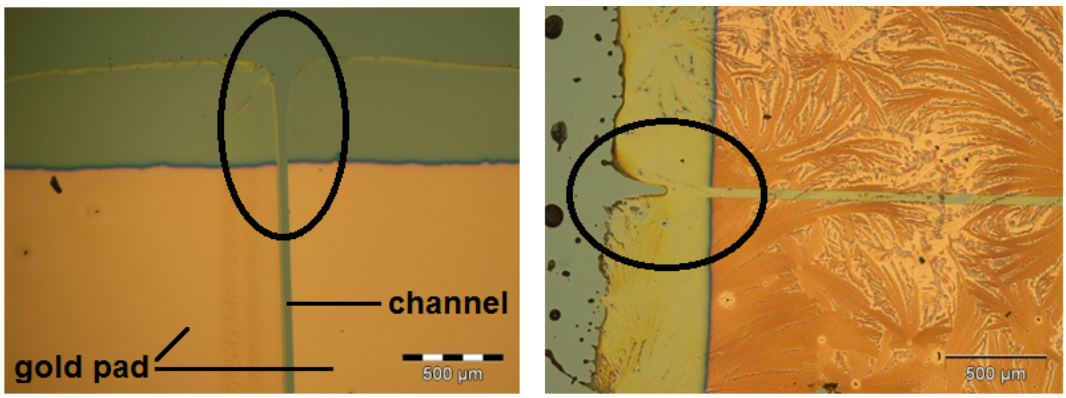

Figure 3.49: Microscope pictures of a spin coated bottom contact OTFT with 10(left) and 20(right) mg/ml TIPS-PEN solved in 3,4-dimethylanisol as active layer

In Fig. 3.48 the transfer characteristic of a spin coated bottom contact OTFT with TIPS-PEN solved in 3,4-dimethylanisol is shown.

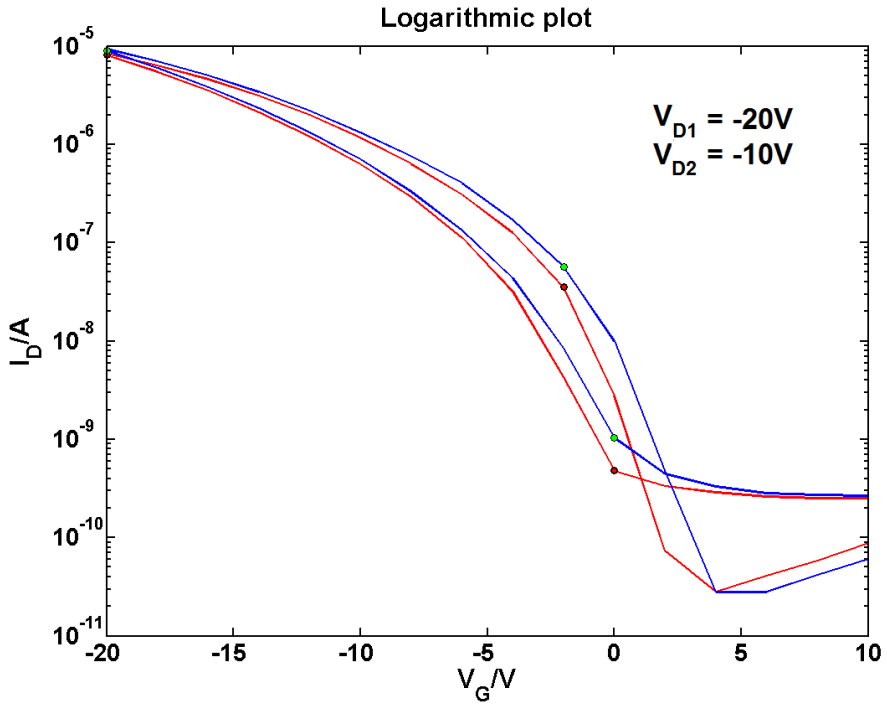

Figure 3.50: Transfer characteristic of a spin coated bottom contact OTFT with 15 mg/ml TIPS-PEN solved in 3,4-dimethylanisol as active layer material

These were the best transfer characteristics of TIPS-PEN as active layer material during this thesis. There was a small hysteresis(about 2 volts for a drain current of

10^{-7}) in the transfer curve, the mobility was 5 $\cdot 10^{-3}$ $\frac{cm^2}{Vs}$ and the threshold voltage was +1 V. The leakage current was very low, approximately 10^{-8} A, and therefore the on/off ratio was about 10^5.

- **Drop cast OTFTs with TIPS-PEN as active layer material**

During this work several different setups of drop cast OTFTs were built, but as already mentioned just bottom contact OTFTs showed transistor behaviour. So bottom contact OTFTs with active layers with concentrations from 10 to maximum 30 mg/ml TIPS-PEN solved in toluene or 3,4-dimethylanisol were built. High concentrations reduced the device performance significantly, and for concentrations of 30 mg/ml no transistor behaviour was measured. The best results for drop cast OTFTs were achieved with bottom contact OTFTs with 10 mg/ml TIPS-PEN solved in toluene.

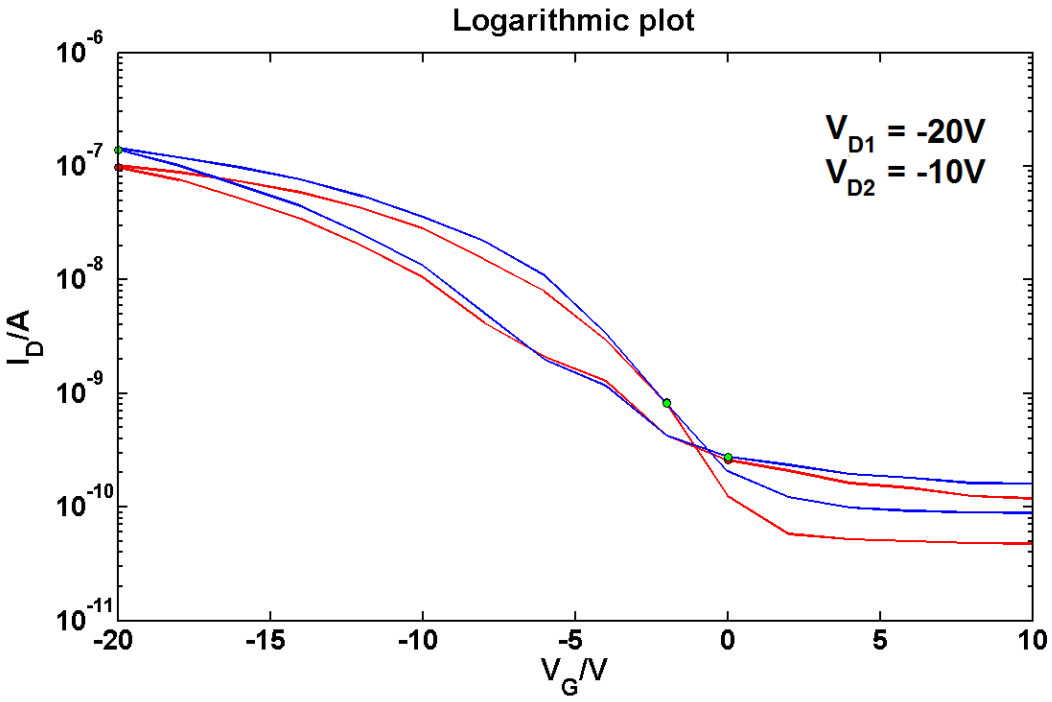

Figure 3.51: Transfer characteristic of a drop cast bottom contact OTFT with 10 mg/ml TIPS-PEN solved in toluene as active layer material

The best results of drop cast bottom contact OTFTs showed small hysteresis in the transfer curve, the mobility was 10^{-5} $\frac{cm^2}{Vs}$, and the threshold voltage was 0V. The leakage current was 10^{-8} A.

But generally speaking the device parameters of the drop cast devices produced during this thesis were not good enough to suggest further investigations. In comparison to the results from literature the device performance was far beyond the results from Park et al [5].

In Tab. 3.3 the results of the investigations of TIPS-PEN OTFTs are presented. Here the the different solvents, pretreatments, depositioning processes, mobilities and threshold voltages are listed up. The TIPS-PEN OTFTs presented in this table were all tempered(Tempering steps) subsequently after the depositioning process(drop casting, spin coating) of the active layer material.

Table 3.3: Results of the investigations of TIPS-PEN OTFTs. Here the different solvents, pretreatments, depositioning processes, mobilities and threshold voltages are listed up. The word 'standard' in the pretreatment column means that the devices were plasma etched and were than given into a ultrasonic bath(Device fabrication and pretreatment). The X in the mobility and threshold voltage column symbolises that for that sort of sample no transistor function was measured. The word 'both' in the table means that the results were the same for example for both OTFT structures(bottom- and top-contact). Toluene and 3,4-dimethylanisol(here just called anisol) were used as solvents

top/bottom	solvent	pretreatment	spin/drop	μ / $\frac{cm^2}{Vs}$	V_{th} / V
both	both	standard	spin	X	X
both	toluene	both	spin	X	X
bottom	toluene	First Contact ®	drop	10^{-5}	0
top	anisol	First Contact ®	spin	10^{-4}	-2
bottom	anisol	First Contact ®	spin	5*10^{-3}	1

3.5.4 Change of the mobility over time: X-ray diffraction measurements to investigate the crystallization and the drying process

During the investigations of thin film transistors with TIPS-PEN as active layer material an interesting effect, precisely a special time dependent development of the mobility was noticed. The OTFTs achieved their maximum mobility after a week to ten days, and then the device performance uniformly decreased with time. During this time the devices were stored under ambient conditions. This effect was already recognized by other research groups as can be seen in Fig. 3.52.

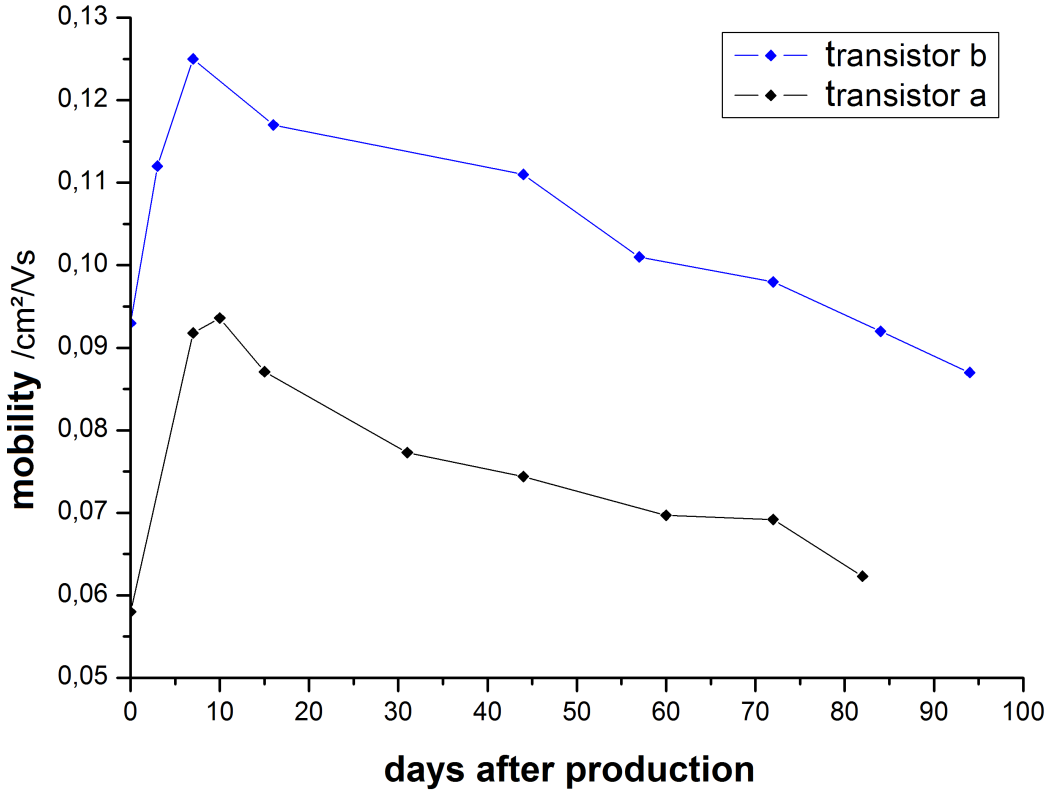

Figure 3.52: Development of the mobility of two TIPS-PEN based OTFTs over time (taken from [59])

The decrease of the drain current and thus the mobility over two weeks can be seen in Fig. 3.53.

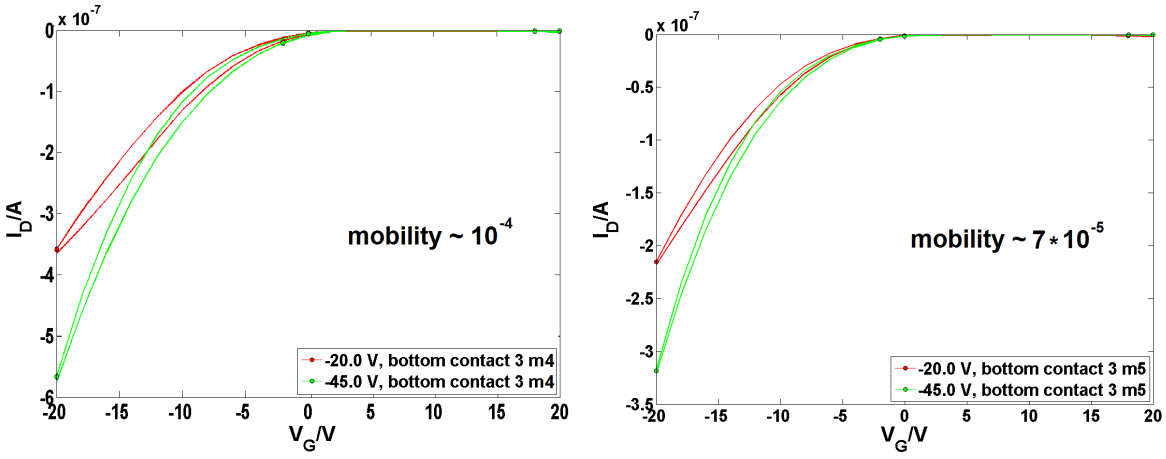

Figure 3.53: Transfer characteristics of a spin coated bottom contact TIPS-PEN OTFT one week(left) and three weeks(right) after the OTFT was built. One can see the decrease of the drain current and the mobility over time.

So there were two points of interest: the increase of the mobility after the preparation to the maximum mobility and the decrease of the mobility over time after the maximum was exceeded. Thus the drying process, as well as the development of the crystal structure over a long period of time was investigated by x-ray diffraction measurements.

Before the samples were investigated by XRD-measurement the substrates were pretreated and than the active layer material was drop cast on top of the Si/SiO_2 substrate. The samples in this sub chapter were all plasma etched for 40 seconds and were put into the ultrasonic bath for two minutes, like it is explained in the chapter Device fabrication and pretreatment. Over the whole process the samples were handled under ambient conditions.

Fig. 3.54 shows the result of a short time XRD measurement of a Si/SiO_2 sample drop cast with TIPS-PEN dissolved in toluene with a concentration of 10 mg/ml under ambient conditions. This measurement was performed immediately after the active layer was drop cast on the substrate and built into the measurement setup.

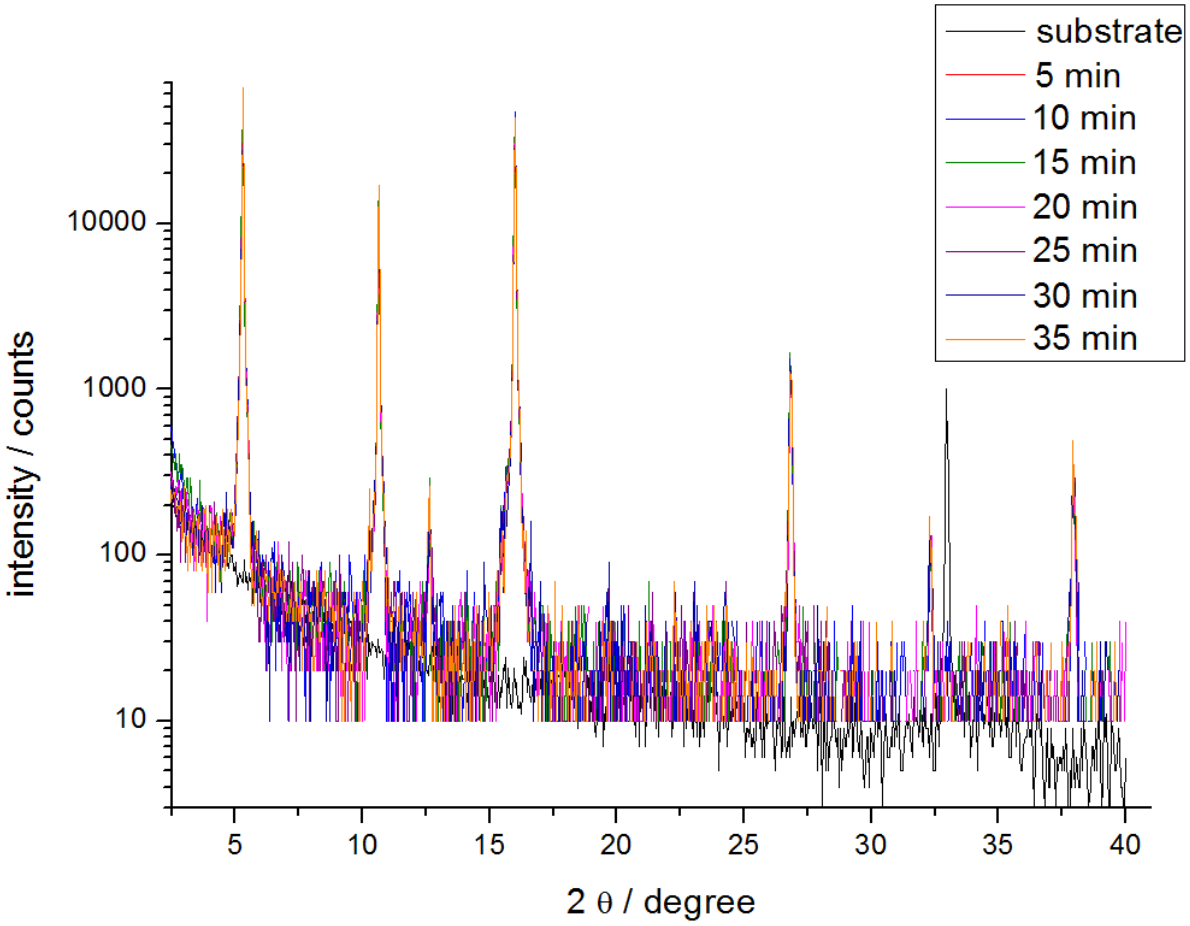

Figure 3.54: Short time x-ray diffraction measurements of a Si/SiO_2 sample drop cast with 10 mg/ml TIPS-PEN solved in toluene. The short time measurement was performed seven times. The black curve comes from the substrate.

This measurement was done in the shortest possible measurement period(3 minutes) for our measurement rang for seven times. But unfortunately the signal to noise ratio is to small to get concrete results from this measurement. So this was not the right way to investigate the drying process directly after the deposition of the active layer: the measurement period should be at least 10 minutes to get an accurate result.

Additionally long time measurements(6 hours for one measurement period) were performed, to analyse the decrease of the mobility. During this measurements one measurement was performed every day for two weeks. Here the pretreated Si/SiO_2 substrates were drop cast with 10 mg/ml TIPS-PEN solved in 3,4-dimethylanisole and in toluene. After the deposition of the active layer material the sample was put in a petri dish under ambient conditions and it was waited for 24 hours until the solvent was evaporated. Then the samples were built into the measurement setup. The results of this measurements for TIPS-PEN solved in 3,4-dimethylanisole and in toluene are presented in Fig. 3.55 and 3.56.

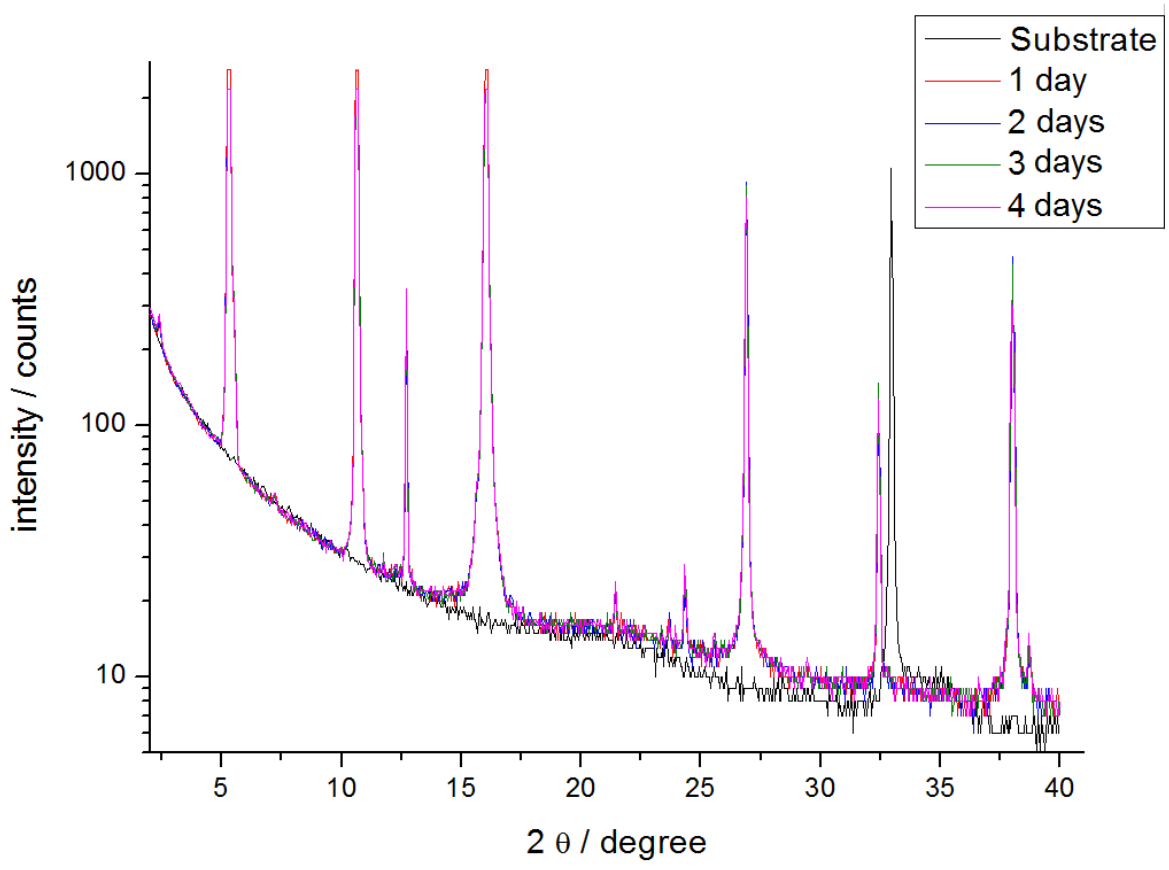

Figure 3.55: Long time x-ray diffraction measurement of a Si/SiO_2 sample drop cast with TIPS-PEN solved in 3,4-dimethylanisole. The black curve comes from the substrate.

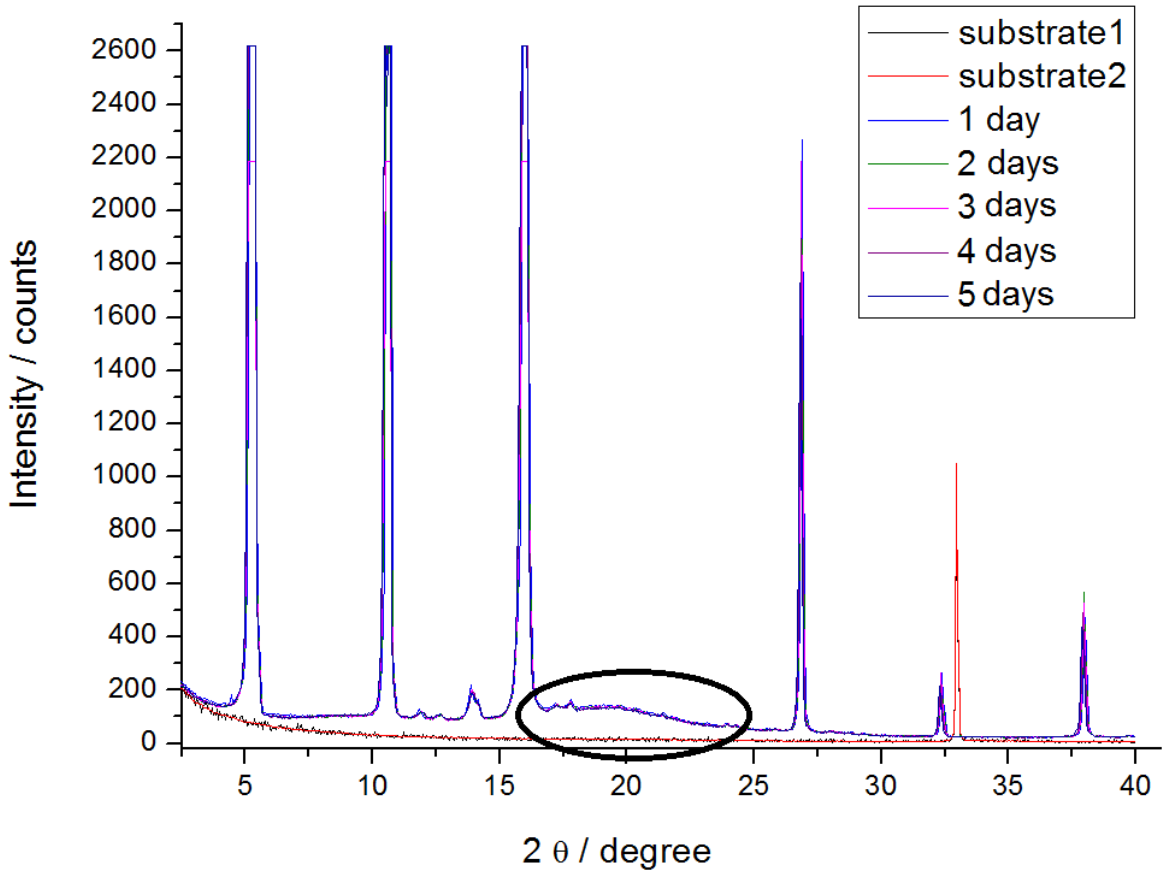

Figure 3.56: Long time x-ray diffraction measurement of a Si/SiO_2 sample drop cast with TIPS-PEN solved in toluene. The black and the red curve are from the substrate.

These measurements were performed with one sample for four(Fig. 3.55) respectively five (Fig. 3.56) times, always one measurement per day. In the two XRD-patterns of the samples some small differences were observed. In the long time x-ray diffraction measurement of a sample of TIPS-PEN dissolved in toluene, drop cast onto a Si/SiO_2 substrate(Fig. 3.55) we saw a broad peak in the marked region between 17 and 22 °. In the other long time measurement of a sample of TIPS-PEN dissolved in 3,4-dimethylanisole, drop cast onto a Si/SiO_2 substrate 3.56 this peak does not occur. According to Ao. Univ. Prof. DI. Dr. Roland Resel this peaks gives us information about the amorphous fraction of the active layer. So the amorphous fraction of the active layer in the second sample is much higher. This is not surprising, because the boiling point of toluene(110 °) is much lower than that of 3,4-dimethylanisole(200 °) and so the drying process of the the drop casted TIPS-PEN solved in toluene is much shorter than the drying process of the drop cast TIPS-PEN dissolved in 3,4-dimethylanisole.

Another point that was recognized in Fig. 3.56 was a small shift of the whole XRD-pattern to smaller scattering angles, as can be seen in Fig. 3.57. Here the peak

between 26.7 and 27.0 degree is shown, but this shift was seen for all peaks of the XRD-pattern. What this small shift of the XRD-pattern means about the structure of the active layer material is currently under investigation.

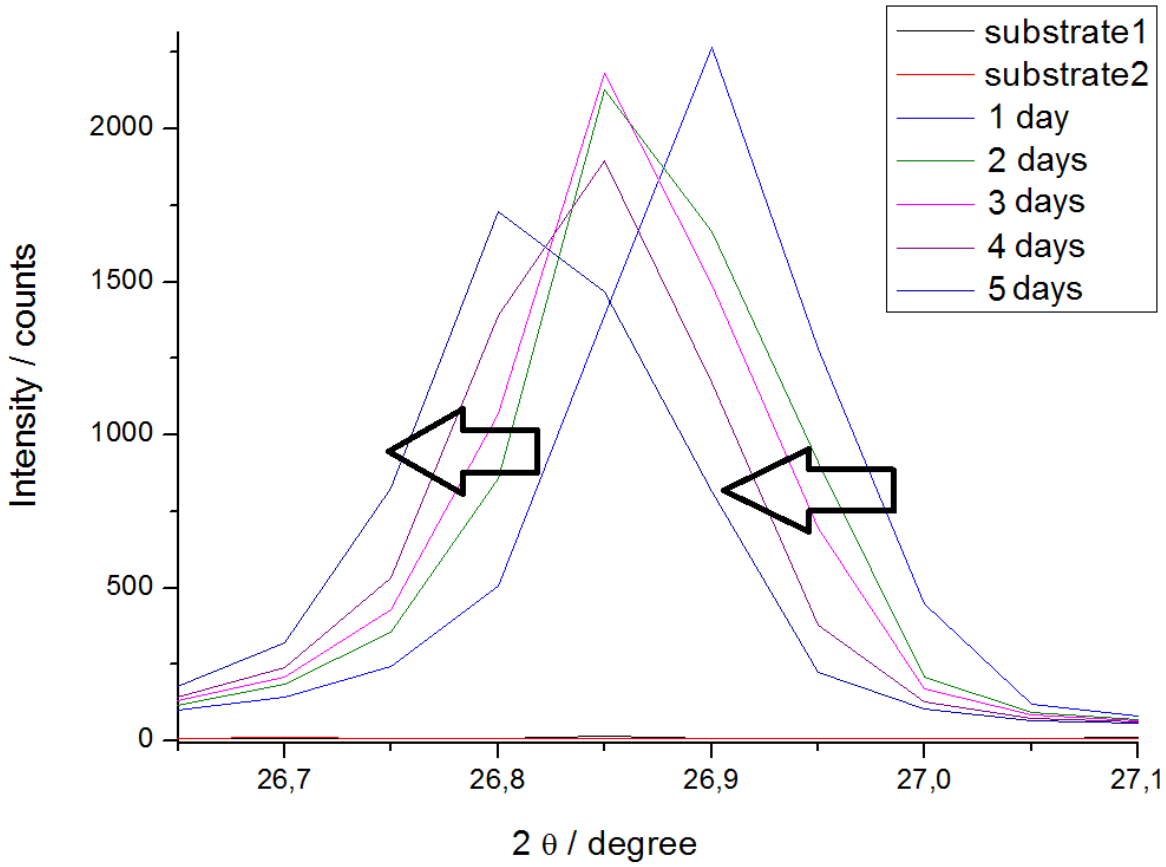

Figure 3.57: Small section of the long time x-ray diffraction measurement of a Si/SiO_2 sample drop cast with TIPS-PEN solved in toluene. The black and the red curve are from the substrate

But this measurement results might have nothing to do with the change of the mobility, probably this change has nothing to do with a change of the crystal structure over the time. Probably the increase of the mobility in the first ten days was because of the slow evaporation of the solvent out of the crystal structure, and the long term decrease of the mobility was a typical material degradation process like in regular pentacene based OTFTs.

3.5.5 Conclusion

Within the tested range of parameters the optimized pretreatment and manufacturing process of TIPS-PEN OTFTs turned out to be the following (for a bottom contact device):

1. pretreatment with First Contact ® with a long drying process (for at least two hours)
2. evaporation of the gold electrodes
3. spin coating/drop casting of dissolved TIPS-PEN with optimized spin coating parameters(9s with 500rpm and 20s with 2000rpm for a 15 mg/ml TIPS-PEN solution in 3,4-dimethylanisol)
4. tempering on hot plate ($100°C$ for two minutes) to dry the deposited active layer

The OTFTs with TIPS-PEN as active layer material produced during this thesis showed relatively good device parameters. But they were not yet comparable with regular evaporated pentacene based OTFTs. This would require an optimization of the entire production process.

Chapter 4

Conclusion and Outlook

In this chapter a conclusion and an outlook on the subjects investigated during this thesis are presented. Here every section will be started with a summarizing sentence and than a discussion and outlook about the specific theme is given.

- Interfacial layers to control the surface energy and thus the growth process of the active layer are a interesting method to improve the OTFT device performance

Obviously the change of the contact angle and thus of the surface energy of the polymer interfacial layer are not the only important parameters in this scenario. The performance of the pentacene layer also depends on the interfacial layer itself, and the evaporation process of pentacene. During the AFM investigations of the P4-OTFTs we saw different surface structures of the pentacene layer for every device series but no clear change of the device performance upon irradiation. For poly(4-vinylbenzl thiocyanate-co-stryrene) and the poly(formic acid 4-vinyl-phenyl ester) OTFTs no improvement of the transistor performance was realized so these polymers are not suitable for OTFT applications.

- Photo reactive spiropyran interfacial layers are a promising material to reversibly change device parameters but we observed an enormous bias stress and strongly time dependent characteristics

Upon irradiation, the spiropyran polymer was just going into a metastable zwitterionic state. So no doping process occurred nor a space charge layer formed and so no clear change of the device performance or parameters was realized. The use of spiropyran polymers in regular transistor applications is very impractical: it decreases the device performance by orders of magnitudes, it results in an enormous bias stress effect and strongly time dependent characteristics.

- TIPS pentacene dissolved in toluene and 3,4-dimethylanisol as active layer material showed medium performance for spin coated and drop cast devices

During the production of solution processed TIPS pentacene OTFTs the best results were achieved for spin coated bottom contact devices. This was the case because the wettability of the surface during the spin coating process was the most crucial point. This problem was partly solved with the new pretreatment procedure, but to further improve the device performance the process of manufacturing still needs to be improved. For that reason a tempering step directly after the deposition of the active layer was included. This and the increased concentration showed small improvements in the device performance. If this process will be further improved, the device performance of OTFTs produced with TIPS-pentacene will probably keep up with the performance of regular pentacene OTFTs. Possible improvements of the manufacturing process could be a heating setup, that heats the devices during the spin coating process(like the setup built by Reinhold Hetzel). Another possibility to improve the wettability of the spin coated active layer material on the substrate could be a blend with a polymer that improves the film forming properties like [62] and [63].

Bibliography

[1] J.E. Lilienfeld. Method and apparatus for controlling electric currents, 1930. 1

[2] D. Kahng. Electric field controlled semiconductor device, 1963. 1

[3] H. Koezuka, A. Tsumura, and T. Ando. Field-effect transistor with polythiophene thin-film. *Synthetic Metals*, 18(1-3):699–704, February 1987. 1

[4] Samsung. www.samsung.com. 1

[5] S. K. Park, T. N. Jackson, J. E. Anthony, and D. A. Mourey. High mobility solution processed 6,13-bis(triisopropyl-silylethynyl)pentacene organic thin film transistors. *Appl. Phys. Lett.*, 91:063514–063514–3, 2007. 2, 72, 83

[6] A. Neuhold. Polymer heterostructure based light emitting devices and light emitting organic sensors. *Master thesis, Graz University of Technology*, 2009. 3, 4, 5, 6

[7] Institut fuer Angewandte Photophysik Technische Universität Dresden. *http://www.iapp.de/orgworld*. 3, 4, 5, 6

[8] R. S. Mulliken. Spectroscopy molecular orbitals and chemical bonding. *Science*, 157(3784):13–&, 1967. 3, 4

[9] G. Horowitz. *Organic Field Effect Transistors(Optical Science and Engineering Series)*. CRC Press, 2007. 4, 5, 14

[10] C. D. Dimitrakopoulos and P. R. L. Malenfant. *AdV. Mater.*, 14:99, 2002. 7

[11] J. Veres, S. Ogier, and D. Lloyd, G.and de Leeuw. *Chem. Mat.*, 16:4543, 2004. 7

[12] A. Facchetti, M. H. Yoon, and T. J. Marks. *AdV. Mater.*, 17:1705, 2005. 7

[13] J. Tate, J. A. Rogers, C. D. W. Jones, B. Vyas, D. W. Murphy, W. J. Li, Z. A. Bao, R. E. Slusher, A. Dodabalapur, and H. E. Katz. *Langmuir*, 16:6054, 2000. 7

[14] T. Kawase, T. Shimoda, C. Newsome, H. Sirringhaus, and R. H. Friend. *Thin Solid Films*, 438:279, 2003. 7

[15] J. Zaumseil and H. Sirringhaus. Electron and ambipolar transport in organic field-effect transistors. *Chemical Reviews*, 107(4):1296–1323, April 2007. doi: 10.1021/cr0501543. 7, 8, 9, 11, 12, 14

[16] M. Ahles. Einfluss der dotierung organischer halbleiter auf den feldeffekt. *PhD. thesis*, 2006. 8

[17] G. Horowitz. Organic thin film transistors: From theory to real devices. *Journal of Materials Research*, 19(7):1946–1962, July 2004. doi: 10.1557/JMR.2004.0266. 8, 14, 15

[18] M. Egginger, S. Bauer, R. Schwodiauer, H. Neugebauer, and N. S. Sariciftci. *Monatsh Chem*, 140:635–750, 2009. 10

[19] G. Horowitz, P. Lang, M. Mottaghi, and H. Aubin. Extracting parameters from the current-voltage characteristics of field-effect transistors. *Advanced Functional Materials*, 14(11):1069–1074, November 2004. doi: 10.1002/adfm.200305122. 11

[20] L. Burgi, T. J. Richards, R. H. Friend, and H. J. Sirringhaus. *Appl.Phys.*, 94:6129, 2003. 13

[21] P. V. Pesavento, R. J. Chesterfield, C. R. Newman, and C. D. J. Frisbie. *Appl. Phys.*, 96:7312, 2004. 13

[22] M. C. J. M. Vissenberg and M. Matters. Theory of the field-effect mobility in amorphous organic transistors. *Physical Review B*, 57(20):12964–12967, May 1998. 15

[23] E. J. Meijer, C. Tanase, P. W. M. Blom, E. van Veenendaal, B. H. Huisman, D. M. de Leeuw, and T. M. Klapwijk. *Appl. Phys. Lett.*, 80:3838, 2002. 15

[24] C. Tanase, E. J. Meijer, P. W. M. Blom, and D. M. de Leeuw. *Org. Electron.*, 4:33, 2003. 15

[25] C. Tanase, E. J. Meijer, P. W. M. Blom, and D. M. de Leeuw. *Phys. ReV. Lett.*, 91: 216601, 2003. 15

[26] O. Ostroverkhova, D. G. Cooke, S. Shcherbyna, R. F. Egerton, F. A. Hegmann, R. R. Tykwinski, and J. E. Anthony. *Phys. ReV. B*, 71:035204, 2005. 15

[27] O. Ostroverkhova, D. G. Cooke, F. A. Hegmann, J. E. Anthony, V. Podzorov, M. E. Gershenson, O. D. Jurchescu, and T. T. Palstra. *M. Appl. Phys. Lett.*, 88:162101, 2006. 15

[28] W. Warta, R. Stehle, and N. Karl. *Appl. Phys. A: Mater. Sci. Process.*, 36:163, 1985. 15

[29] V. Podzorov, E. Menard, A. Borissov, V. Kiryukhin, J.A. Rogers, and M. E. Gershenson. *Phys. ReV. Lett.*, 93:086602, 2004. 15

[30] R. J. Cheng, Y. C.and Silbey, D. A. da Silva, J. P. Calbert, J. Cornil, and J. L. J. Bredas. *Chem. Phys.*, 118:3764, 2003. 15

[31] V. M. Kenkre. *Phys. Lett. A*, 305:443, 2002. 15

[32] P.G. Le Comber and W.E. Spear. Electronic transport in amorphous silicon films. *Phys. Rev. Lett.*, 25:509, 1970. 15

[33] R. Hajlaoui G. Horowitz and P. Delannoy. Temperature dependence of the field-effect mobility of sexithiophene: Determination of the density of traps. *J. Phys. III France*, 5:355, 1995. 15

[34] G. Horowitz and M.E. Hajlaoui. *Synth. Met.*, 122:185, 2001. 16

[35] T. Höfler, T.and Grießer, X. Gstrein, G. Trimmel, G. Jakopic, and W. Kern. *Polymer*, 48:1930, 2007. 16

[36] T. Obermüller. Temperature dependent bias-stress measurements on organic thin film transistors. *Master thesis, Graz University of Technology*, 2010. 18

[37] C. Straka. Automatisierung von tieftemperaturmessungen an organischen feldeffekttransistoren. *Bachelor thesis, Graz University of Technology*, 2010. 20

[38] Golubkov A. W. Temperature dependent characterization of charge transport in organic thin film transistors. *Master thesis, Graz University of Technology*, 2009. 20

[39] Q. Zhong, D. Inniss, K. Kjoller, and V. Elings. Fractured polymer/silica fiber surface studied by tapping mode atomic force microscopy. *Surface Science Letters*, 290:688, 1993. 21

[40] A. Fian. *Private Conversation*. 21

[41] Uppsala University. *http://www.farmfak.uu.se*. 21

[42] H. Kiessig. *Annalen der Physik*, 10:769–787, 1931. 22

[43] A. Neuhold. Private conversation. 2010. 22

[44] Almelo. Win – gixa software and user manual. *Philips Analytical X-Ray, The Netherlands*, 1997. 22

[45] C. Heil, S. Kirnstötter, and H. Brandner. Festkörperphysikpraktikum. 2010. 23

[46] rame-hart instrument co. *http://www.ramehart.com/contactangle.htm*. 23

[47] KRÜSS GmbH. *http://www.kruss.de/kontaktwinkel/zisman.html*, . 24

[48] Imperial College London. *http://www3.imperial.ac.uk/ surfacesandparticleengineeringlab/facilities/wettabilitymeasurement*. 25

[49] P. Pacher. Organic thin film transistors and resistors for armine detection. *PhD thesis, Graz University of Technology*, 2008. 28, 58

[50] J. C. Kuhlmann. Synthese und photolithographische strukturierung photoreaktiver polymere. *Bachelor thesis, Graz University of Technology*, 2007. 31, 32

[51] M. Marchl, A. W. Golubkov, M. Edler, T. Griesser, P. Pacher, A. Haase, B. Stadlober, M. R. Belegratis, G. Trimmel, and E. Zojer. Photochemical control of the carrier mobility in pentacene-based organic thin-film transistors. *Applied Physics Letters*, 96(21):213303, May 2010. doi: 10.1063/1.3432672. 32, 35

[52] M. Edler and A. Kaufmann. Charakterisierung von poly(vbt-costyrene). *Praktikum PCCL*, 2010. 38, 39, 42, 43, 44, 45

[53] J. M. Galvin. 1998. 89-100. 55

[54] J.F. Zhi. Photoelectrochromic properties of a spirobenzopyran derivate. *Journal of Photochemistry and Photobiology*, 92:91–97, 1995. 55, 69

[55] Y. Hirshberg. Reversible formation and eradication of colors by irradiation at low temperatures - a photochemical memory model. *Journal of the American Chemical Society*, 78(10):2304–2312, 1956. 55

[56] J. Andersson. *Journal of the American Chemical Society*, pages 11836–11837, 2008. 58

[57] X. F. Guo, D. Zhang, Y. Gui, M. X. Wax, J. C. Li, Y. Q. Liu, and D. B. Zhu. Reversible photoregulation of the electrical conductivity of spiropyran-doped polyaniline for information recording and nondestructive processing. *Advanced Materials*, 16(7):636–+, April 2004. doi: 10.1002/adma.200305792. 58

[58] V. Podzorov and M. E. Gershenson. Photoinduced charge transfer across the interface between organic molecular crystals and polymers. *PRL*, 95:016602, 2005. 68

[59] S. Dunst. 6,13-bis(triisopropylsilylethinyl)pentazen als halbleitermaterial in organischen feldeffekttransistoren. *Master thesis, Hochschule Fresenius University of Applied Sciences*, 2010. 71, 78, 84

[60] J. E. Anthony, J. S. Brooks, D. L. Eaton, and S. R. Parkin. Functionalized pentacene: Improved electronic properties from control of solid-state order. *J. Am. Chem. Soc.*, 123:9842, 2001. 72

[61] S. K. Park, J. E. Anthony, and T. N. Jackson. Solution-processed tips-pentacene organic thin-film-transistor circuits. *IEEE Electron Device Letters*, 28:10, 2007. 72

[62] J. Smith, R. Hamilton, I. McCulloch, M. Heeney, J.E. Anthony, D. Bradley, and T.D. Anthopoulos. High mobility p-channel organic field effect transistors on flexible substrates using a polymer-small molecule blend. *Synthetic Metals*, 159: 2365–2367, 2009. 72, 92

[63] J. Kwon, S. Shin, K. Kim, M. J. Cho, K. N. Kim, D. H. Choi, and B. Ju. Organic thin film transistors using 6,13-bis(triisopropylsilylethynyl)pentacene embedded into polymer binders. *Appl. Phys. Lett.*, 94:013506, 2009. 72, 92

[64] J. Kim, J. Jeong, Cho H. D., C. Lee, S. O. Kim, Kwon S. K., and Y. Hong. All-solution processed bottom-gate organic thin-film transistor with improved subthreshold behaviour using functionalized pentacene active layer. 74

[65] J. E. Anthony. Organic electronics. *Wiley-VCH Verlag Weinheim*, 2006. 77

[66] MicroChemicals GmbH. *http://www.microchemicals.de/haftvermittler.html*, . 77